Institutionen för vattenbyggnad
Chalmers Tekniska Högskola

Department of Hydraulics
Chalmers University of Technology

Thermal Ice Pressure in Lake Ice Covers

Lars Bergdahl

Report
Series A:2
ISSN 0348-1050 Göteborg 1978

Address: Institutionen för vattenbyggnad
Chalmers Tekniska Högskola
Fack
S-402 20 Göteborg 5, Sweden
Telephone: 031/81 01 00

SUMMARY

The temperature changes of land-fast ice covers will give rise to loads against shores and hydraulic structures. The magnitude and frequency of such thermal ice pressures are important with respect to the design of hydraulic structures.

A numerical model is proposed that calculates the thermal pressure in ice covering a lake for observed ice and snow cover characteristics and observed weather. Other methods are reviewed and compared with the proposed new method.

A complete energy budget is set up for the ice cover, including sensible and latent heat transfer as well as radiation fluxes. The input data are supposed to be the standard weather observations: air temperature, wind speed, cloudiness, and air vapour pressure.

The thermal diffusion in the ice cover is calculated by an implicit difference scheme with the time increment 3600 s and slightly more weight on the later time step because of stability problems at the boundary. The coefficient of diffusion is, on the other hand, set to the rather low constant value of $1.15 \cdot 10^{-6}$ m^2/s.

The following conclusions are drawn concerning the temperature calculations:

- In spring, solar radiation has a great influence on the rate of change of temperature even on the latitudes 60 to 70°N.

- The energy exchange between the ice cover and the atmosphere is too complex to allow the ice surface temperature to be set equal to the air temperature. Such a practice would lead to overestimates of the rate of change of temperature. One should either use some method based on the total energy balance or a method, which takes into account the surface thermal resistance.

- Rather rough methods can be used for the calculations, because the calculation of the pressure does not demand great accuracy of calculated temperature only that the temperatures of the profiles are given at about every 5 cm.

- The choice of values or functions for properties like the coefficients of thermal diffusion, conductivity, heat transfer or wind-speed function etc is less important than the choice between different boundary conditions. If reasonable assumptions are made errors in the rate of change of temperature caused by different choices of properties should not amount to more than 10 %.

The lateral expansion of the ice cover is assumed to be completely restricted, and a constant coefficient of thermal expansion is adopted. For the ice deformation a model composed of a linear elastic element in series with a non-linear creep element is used. The creep rate is set proportional to the stress to a power of 3.65. Both elasticity and creep are functions of temperature. The conclusion is:

- The proposed rheological model is capable of reproducing the course of stress for a given course of deformation or temperature, until accelerated or tertiary creep starts. The model is also rather simple to integrate, although it is non-linear. The resulting accuracy matches the quality of the values on deformation moduli and thermal properties.

For a specified change of air temperature it is shown that the proposed numerical model gives 40 % greater total ice pressure (N/m) that the method proposed by Drouin and Michel (1971). For the doubling of the ice cover thickness from 0.45 to 0.90 m the increase in total pressure is 65 % for the proposed method, 20 % for Drouin and Michel´s method, and 100 % for the Soviet Norm 76-66.

Finally, the calculated highest maximum ice pressures for some lakes in Sweden during 12 or 16 years are listed together with ice cover characteristics and weather observations. At 68.3°N the calculated figure is 437 kN/m and at 57.1°N 189 kN/m.

It is believed that the proposed method gives reasonable estimates of possible thermal ice pressures for given ice covers and weather situations. It gives a correct description of the rate of change of temperature for given ambient conditions, without either grossly understating or overstating the rate of change. On the other hand, it produces pressures that cannot be reached in every ice cover because of crystal orientation and irregularities in the ice cover.

PREFACE

In 1968, the late Professor Lennart Rahm initiated ice engineering research in the Department of Hydraulics. Since 1969 the thermal ice pressure against the walls of reservoirs have been studied. During the winters 69/70 and 70/71 field measurements of the temperature in an ice cover with and without snow were performed. The years 1972 to 1974 some few laboratory experiments were done in order to verify the mechanics of thermal pressures. The field and laboratory experiments are reported in Appendices II and III of this book.

The theoretical studies have been running parallel with the experiments, and seem to be roughly verified by the experiments. Background material is reviewed in the report: "Physics of Ice and Snow as Affects Thermal Ice Pressure" (Bergdahl 1977). In the present report older investigations are reviewed, and a new method is proposed and compared with some of them. The proposed method has been used for calculating hypothetical ice pressures for ice observations and weather records covering 12 or 16 years for five lakes in Sweden. From the calculated pressures the frequency of extreme pressures have been estimated. The result is reported in "Calculated and Expected Thermal Ice Pressures in Five Swedish Lakes" (Bergdahl and Wernersson, 1978).

July 1978

Lars Bergdahl

ACKNOWLEDGMENTS

The studies of thermal ice pressures have, in various ways, been supported by the following organizations:

Chalmers University of Technology, Göteborg
Swedish Council for Building Research, Stockholm
Swedish Natural Science Research Council, Stockholm
Swedish Meteorological and Hydrological Institute, SMHI, Norrköping
AB Tryckrör, Malmö

The following persons have given their advice on parts of the work:

Klas Cederwall, Professor, Royal Institute of Technology, Stockholm
Sven Fremling, Head of the Ice Bureau, SMHI, (Retired)
Rudolf Hiltscher, Dr.-Ing., State Power Board, Stockholm
Bertil Löfquist, Tekn.Dr., Kjessler och Mannerstråle, Stockholm
Anders Sjöberg, Professor, Chalmers University of Technology, Göteborg

Mr Bengt Carlsson and Georg Nilsson have built the experimental equipment. A special thank is directed to the villagers of Ängen who have helped by the field experiments in various ways.

The computer programme used for calculating the temperature and pressure in the ice for the proposed model is made by Mr Lars Wernersson. The programmes for adding the Fourier series of Appendix I were made by Mr Bo Ekelund.

The manuscript has been typed by Mrs Göta Bengtsson, Mrs Ann-Marie Holmdahl, and Miss Annika Dahlqvist. Mrs. Alicja Janiszewska has drawn the figures in the main text, while Mr Jaakko Hämälainen has drawn the figures of the Appendices. The photographs in Appendix III are taken by Mr Per Lindvall.

Finally, I wish to thank my other colleagues in the Department of Hydraulics for all their efforts to support my work.

July 1978

Lars Bergdahl

LIST OF CONTENTS page

1. INTRODUCTION

When a land-fast ice cover has been formed on a lake or on an enclosed part of the sea, stresses will arise in it because of its thermal expansion or contraction caused by the changing weather. The stresses will exert forces against shores, dams or other structures.

It is rather complicated to calculate such forces for design purposes because of the nonlinearity of the deformation of the ice, the irregularity of ice covers, the variation of ice properties, and the difficulty to define probability of extreme situations.

The purpose of this study is to show that a reasonable estimate can be made on thermal ice pressure for a given weather and ice situation. Earlier investigations are briefly reviewed, and some of them are compared with a proposed new method. Finally, a method to estimate return periods of extreme pressures is reported.

The mechanics and physics of ice in general are not discussed in this study, but reference is made to Bergdahl (1977). A detailed account of an attempt to calculate the recurrence of extreme thermal ice pressure on five Swedish lakes is given by Bergdahl and Wernersson (1978).

1.1 The Origin of Thermal Ice Pressure

A very thin sheet of ice has a temperature of close to $0^{o}C$. When such a sheet grows in thickness, the temperature of its surface decreases due to the low air temperature. The upper layers of the ice contract, but since the temperature at the lower boundary still is $0^{o}C$, the contraction causes tension, creep, and cracks in the ice. The growth rate of the ice cover is mostly rather slow, so that, with the exception of the first few centimetres, the ice has time to creep without the formation of tensile cracks, that is, if the ice increases in thickness at a constant temperature of its upper surface.

If, however, at a time when the ice cover already has been formed and has increased in thickness at constant weather conditions, the air temperature suddenly falls considerably, the upper surface of the ice quickly assumes a new temperature of equilibrium, and after some time a new steady state gradient will be established in the ice cover. The upper surface will contract fast, but the lower boundary will keep its length since it is at the constant freezing-point temperature.

Now, the ice is floating on a horizontal water surface, and thus the free bending of the ice cover is restricted. Instead, the effect will be a bending moment in the ice cover, and the stresses will mostly be released in forming deep cracks. (SeeFigure 1.1). If the change of temperature is very slow,the ice may deform viscously without the formation of cracks.

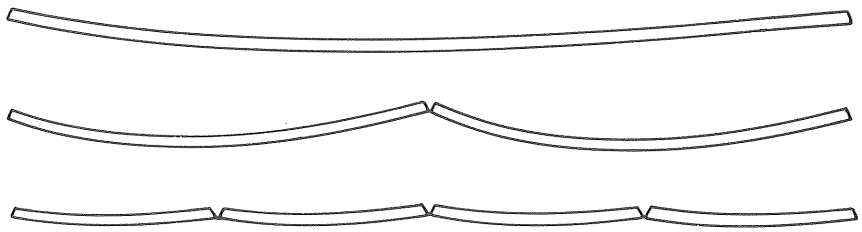

Figure 1.1 The bending and cracking of a floating ice cover due to a fast change of temperature in its upper surface.

The formation of the cracks is often sudden and is followed by a strong wave motion, which is felt if you are standing on the ice. You can also hear the cracks propagating across the ice cover, and it is clearly visible how they are spaced out at intervals of 10 to 20 m. Between these wide parallel cracks, there is a system of thin surface cracks. The cracks will sooner or later be filled by water and drifting snow. Also cracks not extending all through the ice cover will partly be filled by snow and rime. The snow will be packed and recrystallized, and the water will freeze in the crevices. The freezing will sometimes cause pressure in the ice cover because of the increase of volume from water to ice. This pressure is, however, smaller than the extreme thermal pressures.

Later, if the ice cover is warmed due to mild weather or water finding its way on to the ice, the upper layers will again expand. Depending on the steepness of the shores, the thickness of the ice, and the rate of change of temperature, pressure will develop in the ice and may be followed by a shove up onto a beach or folding of the ice cover against banks and in zones of weakness. (See Figure 1.2).

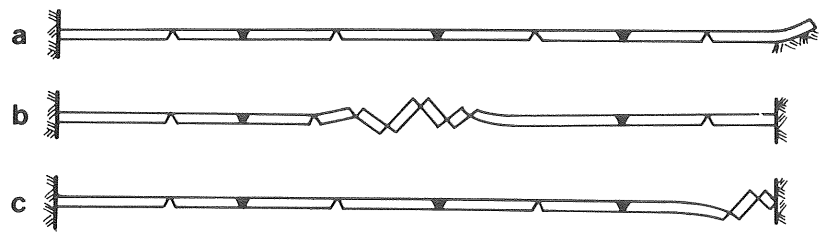

Figure 1.2 Examples of expanding ice covers

a) shoving up onto a beach
b) folding out on a lake
c) folding at a shore

The magnitude of the ice pressure in the ice cover depends on the rate of change of temperature in the ice, the coefficient of thermal expansion, the rheology of ice, the extent to which the cracks have been filled, the thickness of the ice cover, and the degree of restriction from the shores.

Of course, the rate of change of temperature in an ice cover depends on the change of weather conditions such as wind speed, air temperature, solar radiation, and the depth of the snow cover.

Expected magnitudes of ice pressures due to thermal expansion at a certain lake are thus obviously a function not only of ice and snow properties but also of the local climate, ice conditions and lake configuration.

1.2 Partaking Physical Processes

A survey of the different processes considered when calculating ice pressures due to the thermal expansion of an ice cover is given below.

Thermal diffusion

Internal

The equation of thermal diffusion can be used to describe the rate of change of temperature within the ice if appropriate boundary conditions are given.

$$\frac{\partial \theta}{\partial t} = a \frac{\partial^2 \theta}{\partial x^2} + \frac{p(x, t)}{C_p \rho} \qquad \ldots (1.1)$$

where t = time coordinate
x = vertical coordinate
θ = temperature at (x, t)
a = coefficient of thermal diffusion
C_p = specific heat capacity
ρ = bulk density
p = energy source per unit volume and unit time at (x, t).

$$a = \lambda / C_p \rho \qquad \ldots (1.2)$$

where λ = specific heat conductivity

External

Heat is conveyed to the upper surface by the air, which simplified can be written

$$q = A \Delta\theta, \qquad \ldots (1.3)$$

where q = heat flow per unit area
A = coefficient of heat transfer
$\Delta\theta$ = temperature difference between the air and the ice surface

Radiation at the surface and the absorption of short-wave radiation within the ice will add to the external energy exchange. The long-wave radiation absorbed at the surface can simply be included by adding the absorbed radiation to Equation (1.3), whereas the internal short-wave energy absorption must be included in Equation (1.1) by for example,

$$p(x,t) = k\, J(x,t), \qquad \ldots (1.4)$$

where p = energy source per unit volume and unit time at (x, t)
k = absorption coefficient
J = the intensity of penetrating short-wave radiation at (x, t)

A snow cover on the ice will change the external energy flow because of its low thermal conductivity and because of the change in radiation balance and its reflexion of short-wave radiation. Sometimes its weight will cause the ice cover to sink below the water table, that is, the cover will be flooded with water.

Thermal expansion

Thermal expansion of ice is usually written

$$d\varepsilon = \alpha \cdot d\theta, \qquad \ldots (1.5)$$

where $d\varepsilon$ = expansion per unit length caused by $d\theta$
α = linear coefficient of thermal expansion
$d\theta$ = temperature change

Sometimes it is more convenient to use the density as a function of temperature, especially for saline ice, where the expansion coefficient is a discontinuous function because of the crystallization of salts, while the density is a continuous function.

Rheology

The mechanics of ice is very complicated, and there are several ways of constructing mathematical models of the deformation. For each model the coefficients or moduli must then be evaluated from literature or experiments by curve fitting. A possible three-parameter model is for example,

$$\dot{\varepsilon} = \frac{1}{E}\,\dot{\sigma} + KD\,(\sigma)^n \qquad \ldots (1.6)$$

where $\dot{\varepsilon}$ = rate of deformation, $d\varepsilon/dt$
$\dot{\sigma}$ = stress rate, $d\sigma/dt$
E = modulus of elasticity
K, n = coefficients for viscous deformation
D = self diffusion coefficient for the molecules in ice

Nearly all the parameters above are functions of ice type and temperature. The absorption coefficient and radiation balance are also functions of wave length. The coefficient of heat transfer is a function of wind-speed and humidity.

2. PREVIOUS INVESTIGATIONS

Below are some brief summaries of investigations that have been devoted to solving the problem of thermal ice pressure, some of them focusing on the ice rheology, others on the thermal diffusion, and still others trying to span the whole phenomenon. Some aspects on the works are given directly, while more detailed comparisons are made in later chapters treating the separate parts of the problem. Mostly the original systems of units and sign rules are used in this chapter, however confusing they might be.

Investigations that treat some special aspect of the physics of ice without aiming at solving the problem of thermal ice pressure are not included in this chapter even if their results are used in the final design proposal of this work. The physics of ice is treated in another study (Bergdahl 1977).

Literature reviews have been made earlier by Korzhavin (1962), Drouin and Michel (1971), and Kjeldgaard (1977), from which many remarks are quoted.

2.1 Royen (1922)

Royen published a method of calculating thermal ice pressure in 1922. The method was based on deformation experiments with paraffin wax and lake ice. His fundamental deformation equation was

$$\varepsilon = \frac{c \ \sigma \ t^{1/3}}{a + \theta}, \qquad \ldots (2.7)$$

where ε = compressive strain

σ = stress (kp/cm^2)

t = duration of load (hours)

θ = ice temperature (^oC, absolute value)

c and a constants

$$6 \cdot 10^{-4} < c < 9 \cdot 10^{-5} \ {}^oC \ cm^2/(kp \cdot h^{1/3})$$

$$a = 1 \ {}^oC$$

The relation implies that $\varepsilon \propto \sigma$, while later experiments have shown that $\varepsilon \propto \sigma^n$ with n varying from 1 to 5 for different types of ice and strain rates. The strain rate $d\varepsilon/dt \propto t^{-2/3}$ according to Equation (2.7). This is not a good approximation either, because for secondary creep, which is the ordinary design case, $\dot{\varepsilon}$ is constant and for tertiary creep the creep accelerates.

The nonrestricted thermal expansion of ice can be written

$$\frac{d\varepsilon}{dt} = \alpha \frac{d\theta}{dt} . \qquad \ldots (2.8)$$

Royen differentiated (2.7) with respect to t keeping θ and σ constant and equated the result with that of (2.8). This gives

$$\sigma = \frac{3\alpha}{c} (a + \theta)\, t^{2/3} \frac{d\theta}{dt} , \qquad \ldots (2.9)$$

but the act is a violation of the rules of differentiation as both σ and θ are used as functions of time below. Royen justified the approximation by its agreement with experimental values.

Finally, the temperature of the ice is assumed to increase linearly with time,

$$\theta(t) = \theta_i - \dot{\theta} \cdot t, \qquad \ldots (2.10)$$

where $\theta(t)$ = mean temperature of the ice (^{o}C, absolute value)
θ_i = initial mean temperature (^{o}C, absolute value)
$\dot{\theta}$ = the constant mean temperature increase (^{o}C/h)

The substitution of Equation (2.10) into Equation (2.9) and differentiation of σ with respect to time finally gives the maximum stress (kp/cm^2)

$$\sigma_{max} = 0.9772 \frac{\alpha}{c} (a + \theta_i) \sqrt[3]{\dot{\theta} (a + \theta_i)^2} \qquad \ldots (2.11)$$

at the point of time (hours)

$$t_{max} = 5\,\dot{\theta}/(2\,(a+\theta_i)). \qquad \ldots (2.12)$$

With $c = 6 \cdot 10^{-4}$ $^{o}C\ cm^2/(kp\ h^{1/3})$ and $\alpha = 5.5 \cdot 10^{-5}\ ^{o}C^{-1}$ the usual form of Royen´s equation becomes

$$P_{max} = 0.9\ d(\theta_i + a)\ \sqrt[3]{\dot{\theta}\ (\theta_i + a)^2} \qquad \ldots (2.13)$$

P_{max} = force (tonnes/m)

d = ice thickness (m)

For Sweden Royen assumed a minimum temperature of the air to $-40^{o}C$, which was presumed to produce a mean initial temperature of $-12^{o}C$ in the ice. The maximum ice thickness was assumed to be 1.0 m. If the ice temperature should rise linearly to $0^{o}C$ during 100, 170, and 360 h the corresponding values of P_{max} would be 32, 27 and 21 tonnes/m (310, 260 and 200 kN/m). Allowing for some elastic deformation, Royen ended up with a maximum value of 30 tonnes/m for an ice cover biaxially restrained.

Some short-comings of the theory are

that the thermal analysis does not take into account the transient character of the problem, and therefore the maximum force is directly proportional to the thickness of the ice cover.

that the inital temperature is somewhat arbitrary.

that the elasticity of the ice is ignored.

that the creep of ice is not well described by the used equation.

that the difference between uniaxial and biaxial load cases is not discussed.

2.2 USSR Norm SN 76-59 (1959)

The Soviet norm SN (76-59), operative till 1967, was founded on Royen´s theory with some modifications.(See Korzhavin 1962). The initial mean temperature in an ice cover free from snow was set to the empirical value

$$\theta_i = 0.35\,\theta_a , \qquad \ldots (2.14)$$

where θ_a is the mean air temperature during the preceding 48 hours.

The rate of change of temperature is also set to an empirical expression, namely

$$\dot{\theta}_i = 0.35\,\Delta\theta_a/\Delta t , \qquad \ldots (2.15)$$

where $\Delta\theta_a$ is the maximum increase in air temperature during a period of time Δt within the considered period.

The composite coefficient $0.9772\ \alpha\ /c = 1629\,\alpha = 0.09$ of Royen´s expression for σ_{max} is exchanged for an empirical formula $0.78 \cdot |\theta_a|^{-0.88}$. Its origin is not stated. The changes result in the following form of Royen´s equation for the force in tonnes/m.

$$P_{max} = 5.50\,d\,\frac{(0.35|\theta_a| + a)^{5/3}}{|\theta_a|^{0.88}}\,\left(\frac{\Delta\theta_a}{\Delta t}\right)^{1/3} \qquad \ldots (2.16)$$

When there is snow on the ice, with a depth d_s, the value of P_{max} should be multiplied by a factor of

$$r = \frac{d}{d + 9.1\,d_s} \qquad \ldots (2.17)$$

If the extent of the ice cover is more than 50 m, P_{max} should be multiplied by a factor of 0.9 to 0.6.

It is difficult to judge the Soviet norm 76-59 because the reasons for the coefficient $0.78\ |\theta_a|^{-0.88}$ are not well known. (Compare Section 2.3). Fundamentally, the norm is based on the same rheological equation as Royen's original equation, and therefore most of the short-comings remain. The initial temperature is, however, more clearly stated, and the transient might be indirectly taken into account.

2.3 Proskouriakov (1967)

In a paper to the XIIth congress of IAHR in Colorado, Proskouriakov made some comments on the different Soviet norms and Royen's method. He pointed out that the norm 3440-46 was founded on Royen's mistake of using the partial derivative of Equation (2.7) instead of the total derivative (See Peschanskii 1963 or Drouin and Michel 1971). The result is that the final expression for the maximum pressure is divided by three. It may be noted that the coefficient c is empirical.

Regarding the norm SN 76-59 (See Section 2.2) he wrote that it was based on the viscosity of ice under load, and that the coefficients of viscosity are well established by Veinberg (1940). He continued to state that in the norm SN 76-66 this method of calculation is developed and perfected for all types of pressure but concluded by proposing a new formula for the ice viscosity η put up by Voitkovsky

$$\eta = \frac{a + \theta}{K \tau^{n-1}} \qquad \ldots (2.18)$$

where

θ = temperature (absolute value?)

$a = 1^{o}C$ a constant

n and K are unspecified constants

τ = shear stress

Korzhavin (1972) states that Proskouriakov has made the most comprehensive studies. He also lists contributors like Petrunichev, Berdennikov, Pekhovich, Irchenko and Yakunin. Unfortunately, none of these contributions are available in a Western European language.

2.4 Brown and Clarke (1932)

For the purpose of ascertaining the design thermal pressure of the dam at Island Falls on the Churchill River, Brown and Clarke made a series of laboratory experiments.

In the two final experiments,3-inch ice cubes were subjected to an intended linear temperature rise, while two opposite cube faces were loaded as much as needed to counteract the thermal expansion of the ice. The result of the experiments was given as the rate of change of pressure (lb/sqft/h) as a function of the rate of change of temperature (^{o}F/h). The function was originally based on three experimental points, of which two came from the same experimental run. (See Figure 2.1 below.)

The results are few, the experimental equipment was not accurate enough to realize the intended experiment, and finally the test cubes were taken from a large block of river ice supplied by an ice dealer, and therefore the crystal structure or the orientation between load axes and ice growth directions was not under control. The result is not consistent with the notion of creep or viscosity of ice, in which case the rate of deformation for longer load durations must approach a function of the stress itself. When Löfquist (1954) plotted his experimental values in the same diagram, he consequently got a curve with a positive curvature.

When the found relation was applied to the problem of thermal pressure at Island Falls, the temperature of the ice was presumed to vary linearly with the air temperature at the air-ice interface and to be at the freezing point at the ice-water interface. In the calculations the upper half of the ice cover was taking the whole temperature variation and stress as an approximation. The biaxial nature of the problem was acknowledged, but no advice was given as to how to account for it in the calculations.

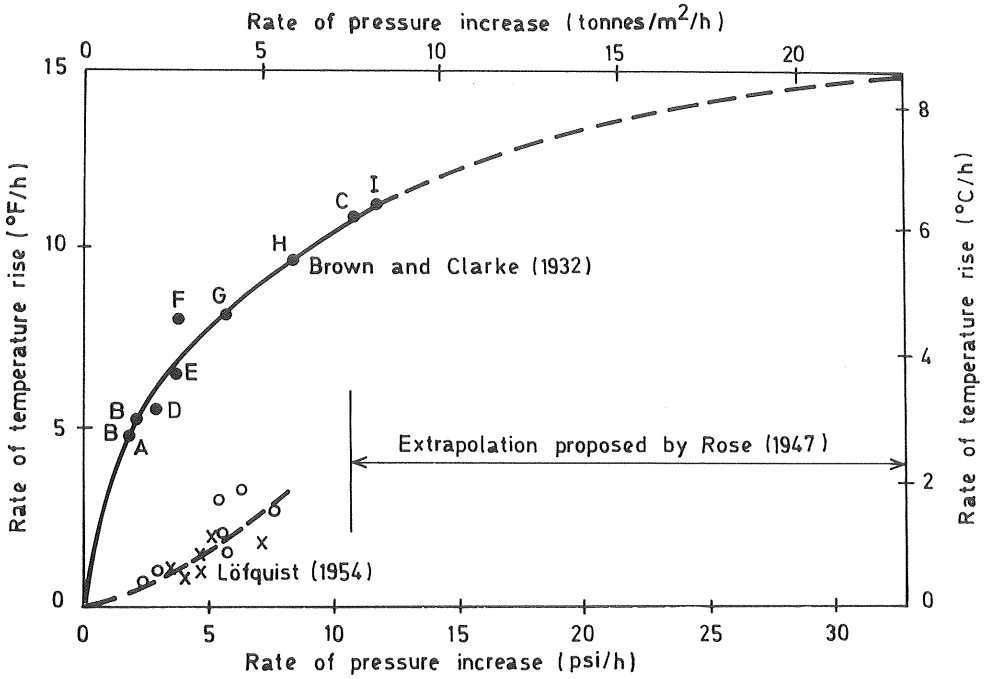

Figure 2.1 The continuous curve is the curve of Brown and Clarke (1932), showing the relation between temperature rise per hour and pressure rise per hour. Filled circles: A-C original points, D-I from shorter parts of the same two experiments. The lower circles, crosses, and dashed curve are from the experiments of Löfquist (1954).

It may be summarized

that the deformation relation found by Brown and Clarke is quite incapable of describing the stress-strain relation of ice. It does not even give the right magnitudes.

that the temperature change is too summarily treated.

2.5 Rose (1947)

Rose improved the work of Brown and Clarke by introducing a correct description of the thermal diffusion in the ice. For pressure, however, he accepted their relationship shown in Figure 2.1 and made an extension of it based on other tests on continuous yielding of ice under sustained load. He also multiplied the result by a factor of $1/(1-\nu)$ to apply it to a completely restricted ice cover with $\nu = 0.365$.

We have already noted that Brown and Clarke´s relation does not give a description of the stresses developing during the thermal expansion of the ice. Consequently, the results of Rose´s method must be as inaccurate, however accurate his treatment of the thermal part of the phenomenon might be.

Rose used the Schmidt difference scheme to describe the variation in ice temperature, and the assumptions of the analysis were as follows

1. Initially a linear thermal gradient with the air temperature (-40^{o}F) at the surface and freezing point temperature ($+32^{o}$F) at the lower surface.
2. Linear rise of air temperature from the initial temperature (-40^{o}F) to the freezing point temperature ($+32^{o}$C) where it remains constant.
3. The surface temperature is set equal to the air temperature.
4. The thickness of the ice sheet remains constant.
5. The diffusivity constant, a, is set to 0.0434 $(ft)^2/h$ $(= 1.12 \cdot 10^{-6}\ m^2/s)$.

The computed solutions are correct and their accuracy is adequate. The profiles are of the same type as displayed in Figure I-5 of Appendix I, and a comparison with the Fourier series solution gives a close concordance. One of Rose´s figures is shown in Figure 2.2.

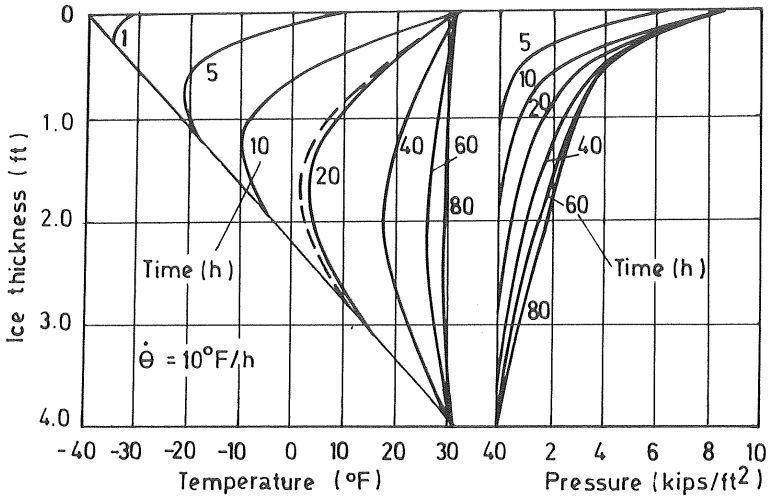

Figure 2.2 Ice temperature curves and resulting pressure curves. After Rose (1947). The dashed line is a solution calculated according to Appendix I-5 for 20 h.

Point 3 is a drawback of the method as it does not take into account the thermal surface resistance or the long-wave radiation balance of the surface. (See Appendices II-6 and III-5 for measured profiles). Point 4 can be shown to have little influence on the problem (See Appendix I-3). As regards point 5, the value of 1.12 m^2/s might be a little too low. 1.15-1.25 m^2/s would be more reasonable. The variation of the diffusivity constant with temperature can be neglected as is also shown in Appendix I-3.

Rose also introduced the solar radiation into the calculations of the rate of change of temperature. In order to do that he put forward some additional assumptions:

6. The latitude is 40°.

7. The time of the vernal equinox is considered.

8. The coefficient of atmospheric transmission to solar radiation is set to 0.9, based on a clear atmosphere of low humidity at a fairly high elevation.

9. A coefficient of heat transfer of 2 BTU/($h^{o}F\ ft^{2}$) is assumed to allow for surface losses of solar energy.

Rose did not specify how these calculations were made. He referred to FW Taylor for different solutions. (See Monfore and Taylor, 1948.) Especially it is difficult to understand the concept of a coefficient of heat transfer for the solar radiation only. According to assumption 3, the surface temperature is equal to the air temperature, and consequently there should be no other losses. In Appendix III-5 a graphical Schmidt-solution is used that takes into account both the heat transfer coefficient and the short wave radiation absorbed in the ice. There the absorbed radiation is included by addition of the absorbed energy in the form of equivalent temperature rises after each time step at the different levels in the ice.

Credit should be given to Rose for treating the thermal part of the problem correctly. His final ice forces are, however, far from satisfactory although they, according to Drouin and Michel (1971),have been widely used in North America.

2.6 Monfore (1947-1954)

In 1947 a major research programme was started at the US Bureau of Reclamation. The programme included theoretical considerations of the thermal response of the ice cover (Monfore and Taylor, 1948), field measurements of temperature and pressures (Monfore 1949), and laboratory investigations of ice deformation properties (Monfore 1951). A summary of the results is given by Monfore in an ASCE symposium on ice pressures against dams 1954.

In the first mentioned contribution Monfore and Taylor (1948) gives the course of temperature in the ice cover as expansions in characteristic functions of a type presented in Appendix I-8. The given solutions are probably correct although they are difficult to survey. (The heat transfer coefficient is incorrectly named emissivity). The solu-

tions take into account the transfer of energy from the air, absorption of part of the solar energy at the upper surface, and absorption of part of that portion of solar energy transmitted through the ice. Because of the modern development of high-speed computors and less complex difference methods the solutions have probably lost in importance.

The most important contribution by Monfore has proved to be the laboratory investigation of the ice properties.(Monfore 1951). The experiments were based on the same concept of nil expansion as the ones by Brown and Clarke, but the equipment was better. Small cylindrical specimens 4 x 4 inches were used, taken from two reservoirs with approximately 45 cm thick ice covers, and cut with the axes horizontally oriented in the ice cover. The strain rate was measured with gauges in direct contact with the specimens. The temperature of the specimens was controlled by an air circulation system, and the temperature was measured in both the periphery and the center of the specimens.

Before the start of each experiment the specimen was kept at constant initial temperature for some time. Then the temperature of the ice was made to increase at the predetermined rate. The load was first ajusted to give zero total deformation every 5 minutes, but after half an hour every 15 minutes only.

The initial temperatures were -30, -20, -10, 0, 10 and 20^{O}F. The rates of change of temperature were 2, 5, 10 and 15^{O}F/h. The results of the experiments were curves over the necessary stress for nil deformation as a function of time. The curves have approximately the same shape, with first a nearly linear increase of stress,then curved to a maximum, and decreased. See Figure 2.3.

Check tests were run on several specimens to determine the reproducibility of the technique. The average deviation of the maximum pressures for duplicate tests on a given specimen was 6 %.

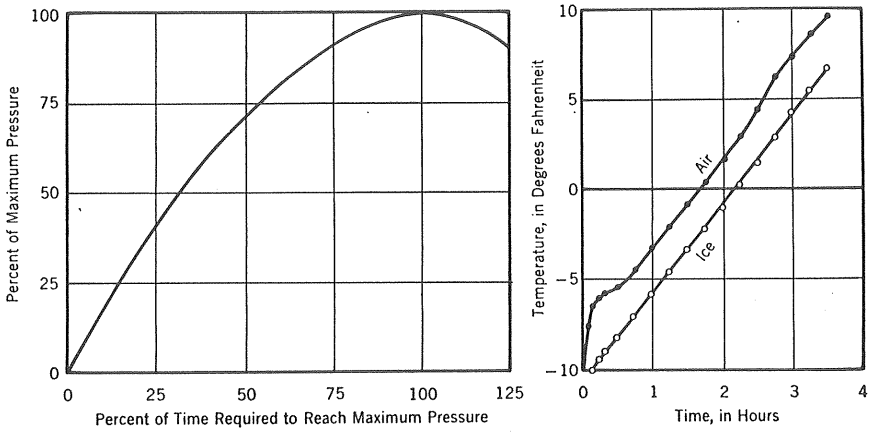

Figure 2.3 a) Average pressure-time curve.
b) Air and ice temperature for typical laboratory test.
After Monfore (1954).

Much larger variations, an average of 25 %, were found in the maximum pressures reached by different ice specimens tested under the same conditions.

The small scatter in the duplicate tests can be taken as a measure of the quality of the test technique. The scatter between values from tests with different specimens can be caused by variations of the crystal structure of the ice, which was also confirmed by Monfore.

The results of the experiments were summarized in two diagrams Figures 2.4 a and b showing the maximum pressure and the time to reach the maximum as functions of the rate of change of ice temperature for different initial temperatures.

The steps in computing thrusts from ice temperatures is as follows. For each level in the ice the rate of change of temperature to be used is decided. From Figure 2.4a the maximum pressure is read and from Figure 2.4b the available time is checked. The maximum pressures from the different levels are then added to a total ice thrust.

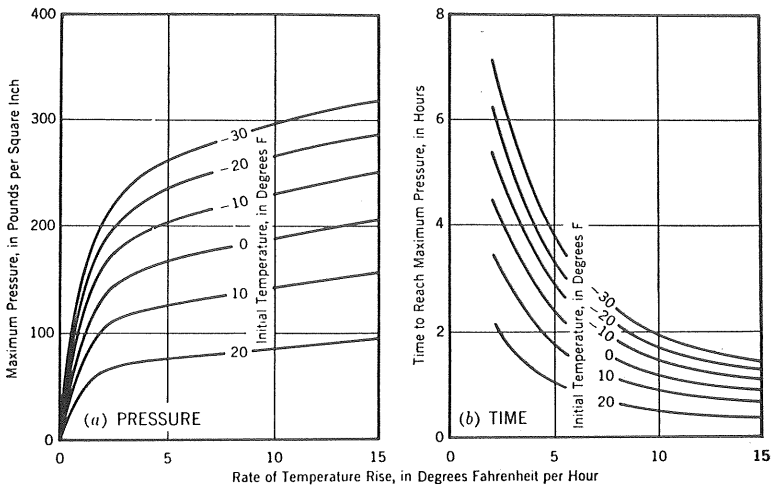

Figure 2.4 Maximum ice pressure (a) and time of temperature rise (b) related to rate of ice temperature rise. (Monfore, 1954).

The weaknesses of Monfores method are

that uniaxial tests are used for biaxially restricted ice covers

that the crystal structure was not considered as a parameter when evaluating the tests

that the phase lag of temperature (or stress) at different levels are not included in the method (although the diffusion problem was solved in principle).

In spite of these remarks Monfore´s experiments brought the understanding of ice rheology a great step forward. Later will be shown that the form of Monfore´s experimental curves can be rather well described by the rheological model recommended in this report.

2.7 Löfquist (1954)

Löfquist (1954) introduced a new concept for studying thermal ice pressure. He reproduced a part of an ice cover in a cylindrical concrete basin diameter 50 cm with an insulated wall. The experiment was of the same type as described in Appendix III, with temperature and pressure gauges embedded in the ice.

During the experiments the ice was allowed to grow to some thickness, whereafter the temperature of the room was raised. In the first two experiments the cracks that developed in the ice when growing was too narrow or shallow to be filled by water welling up. In the final experiment a double cylindrical skirt was placed in the basin, so that the ice could contract freely without adhering to the wall. Before raising the temperature, the gap in between the steel skirts was carefully filled with water that froze to ice. This procedure is important, and the experiments described in Appendix III or Drouin and Michel´s similar experiments became partly failures because the filling of cracks was not controlled.

When the temperature of the room was raised, the temperature of the ice surface was rising approximately exponentially from -30° to 0°C during 15 hours. The course of temperature in the ice is shown in Figure 2.5 as given by Löfquist.

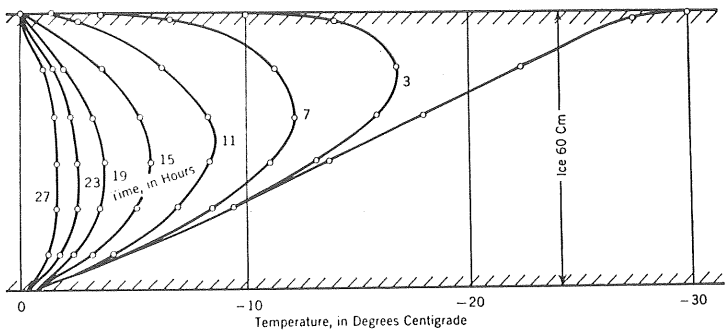

Figure 2.5 Temperature distributions in test No 4.
After Löfquist (1954).

The measured pressure profiles at 10, 14 and 17 hours are shown in Figure 2.6. As the temperature increase penetrated through the ice,the stress profile developed into the shape of a half pear,with a maximum moving down through the ice some hours delayed with respect to the minimum of the temperature curve. The maximum total ice thrust was measured to 20 tonnes/m at about 14 hours after the start of the temperature increase.

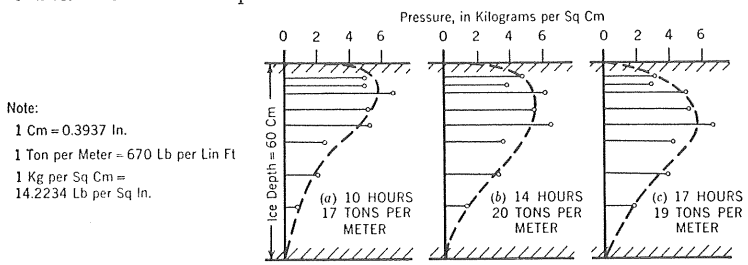

Figure 2.6 Pressure distribution in a cross section of the ice. (Löfquist, 1954).

In the paper describing his experiment, Löfquist also sketched a method to calculate an upper bound for the pressure caused by plastic buckling. He introduced a bulk stiffness modulus, F, which included both the lateral restraint, plastic and elastic deformation. The bulk modulus should replace $E/(1-\nu^2)$ in the buckling formula (Equation 4.9). F was set proportional to negative ice temperature $-\theta$ and inversely proportional to the third root of the load duration t. $(1/F = 1/E + C\, t^{1/3}/(1^{o}C-\theta))$.

Löfquist remarked that the measured pressure was reduced by the facts

that the concrete basin must have been deformed by the load from the ice cover.

that the concrete itself has a linear coefficient of thermal expansion approximately 25 % of the value for the ice itself

that there were some cracks in the uppermost part of the ice cover.

2.8 Assur (1959)

Assur proposed some steps towards a solution of the problem of thermal ice pressure at the eighth Congress of IAHR in Montreal 1959. He started off with a quasi-linear model for the rheology, later used in another form by Lindgren (1968), completed this model with a temperature and stress dependent creep law, later used by Ramseier (1971), Drouin and Michel (1971), and Ramseier and Dickins (1972). Assur solved the equation for constant rate of change of temperature, and finally he formulated a differential equation for the elastic buckling of the ice cover when not loaded symmetrically. Plastic buckling was discussed by Löfquist (1954).

Although his presentation is somewhat sketchy, its basic concepts will be referred below, because they are reflected later in the works of others. The creep deformation of ice under a load was approximately described by a rheological model with a Maxwell and a Kelvin unit in series. (See Bergdahl 1977.) A solution for a constant load is

$$\varepsilon = \frac{\sigma}{E_1} + \frac{\sigma}{m S}\left[\frac{t_o}{\eta_2}\left(1 - e^{-t/t_o}\right) + \frac{t}{\eta_1}\right] \qquad \ldots (2.19)$$

where
- σ is compressive stress
- t time from the load application
- $t_o = E_2/\eta_2$ relaxation time for elastic lag
- E_1 and E_2 elastic moduli
- η_1 and η_2 viscosity moduli
- m a factor depending on the load case
- S a function of temperature and stress
- 1 and 2 indices for the Maxwell and Kelvin unit respectively.

For the uniaxial case $m = 2(1 + \nu)$, and for the biaxial case $m = 2/\nu$, where $\nu = 0.5$ for the case of viscous flow.

$$S = \exp(Q_c/RT)\ \frac{\tau/\tau_o}{\sinh\ \tau/\tau_o} \qquad \ldots (2.20)$$

where
- Q_c is the activation energy for creep
- R the universal gas constant
- T the absolute temperature
- $\tau = \sigma/m$
- $\tau_o = cT$
- c is a constant

The differential equation for $\sigma = f(t)$ was given as, neglecting the elastic lag (the first term within the brackets of Equation 2.19):

$$\dot{\sigma} + \frac{E_1 \sigma}{m \eta_o S} = \alpha E_1 \dot{\theta}, \qquad \ldots (2.21)$$

which actually is very equal to Equation (1.6) for the rate of deformation $\dot{\varepsilon} = \alpha \dot{\theta}$.

The maximum ice pressure σ_{max} was calculated from Equation (2.21) for $\dot{\sigma} = 0$.

$$\sigma_{max} = \alpha m \eta_o \exp(Q_c/RT) S_1 \dot{\theta}, \qquad \ldots (2.22)$$

where $S_1 = (\sigma_{max}/mcT)\sinh(\sigma_{max}/mcT)$
is unit for low stresses
α the linear coefficient of thermal expansion
$\dot{\theta}$ the rate of warming

Assur gave values equivalent to $\eta_o = 0.4172 \cdot 10^{-10}$ (tonnes h/m^2), $Q_c = 81$ kJ/mol, $R = 8,31$ J/(mol · K), $c = 0.154$ tonnes/(m^2 K), $\alpha = 51.5 \cdot 10^{-6}\ ^oC^{-1}$ and $E_1 = 0.65 \cdot 10^6$ tonnes/m^2.

Assur also gave a nondimensional solution of the complete function $\sigma = f(t)$ for a constant rate of change of temperature $\dot{\theta}$ by linearizing Equation (2.21).

An empirical Equation for maximum pressure σ_{max} was found by searching unknown functions with an electronic computor

$$\sigma_{max} = -a\theta_o(1 - b\theta_o)(\dot{\theta} + \dot{\theta}_1) \qquad \ldots (2.23)$$

where θ_o is the initial temperature
a, b and $\dot{\theta}_1$ constants

with $a = 0.33964$ tonnes/(m^2 ^oC), $b = 0.010137\ ^oC^{-1}$ and $\dot{\theta}_1 = 21.1\ ^oC/h$. The agreement with test results given by Monfore was

said to be excellent with a correlation coefficient of 0.9986 for $\dot{\theta} \geq 2.5^{o}C/h$.

Assur pointed out that the total lateral force to a considerable degree depends on the depth of penetration of the warming wave and is limited by the buckling,if the ice cover is thin. He criticized the use of the assumption of an axial load at half the depth of the ice cover, and he proposed a corrected equation probably based on an assumed unfavourable stress distribution.

As will be seen later most of Assur´s concepts are still acceptable. One may regret that he has not published his ideas in a more pedagogical and precise form. The drawbacks are further

> that he only discussed constant rates of change of temperature of the ice.
>
> that he did not follow up the rheological study by calculating the integrated pressure for some case.
>
> that he did not explicitely solve the buckling load or discussed viscoelastic buckling.

2.9 Lindgren (1968)

Lindgren (1968, 1970) made laboratory experiments to determine the rheological properties of ice under both uniaxial and biaxial load. He also utilized his results in a method to calculate the thermal ice pressure in an ice cover for a prescribed air-temperature variation.

The uniaxial tests were performed with ice prisms 7 x 7 x 20 cm, that were loaded with constant weights, at $-10^{o}C$ equivalent to 2, 6, 8, 10 and 14 kp/cm^2, and at -0.5, -5 and $-20^{o}C$ equivalent to 6 kp/cm^2. The deformation as a function of time was measured.

A diagram from his uniaxial experiments is shown in Figure 2.7.

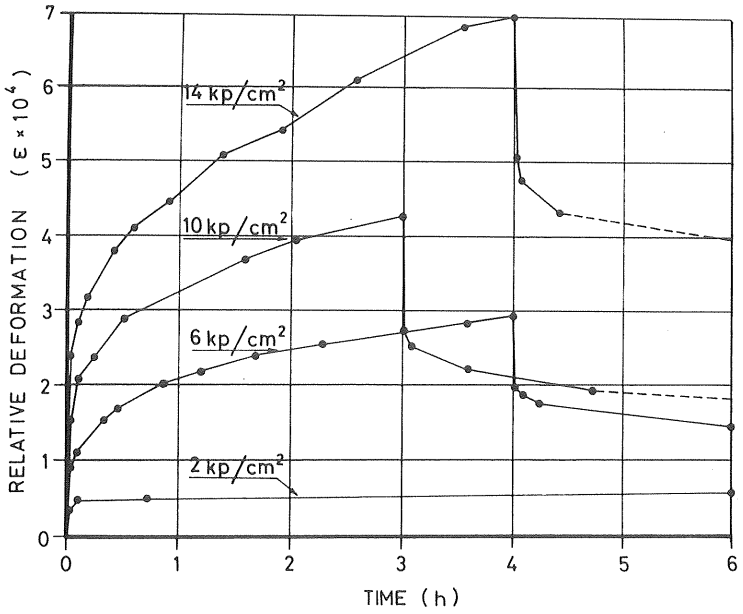

Figure 2.7 Uniaxial creep tests. Experiment No 6. Deformation as a function of time for different stress levels. Specimens unloaded after 3 or 4 hours. (Lindgren, 1968).

Biaxial experiments with restricted thermal expansion were also made with circular ice-plates, diameter 80 cm, thickness 7 cm, that were placed in a steel ring, where the small space between the ice and ring was filled by water. Starting from a low temperature the temperature was raised at different rates. The temperature and the force in the ring were measured with thermocouples and strain gauges respectively as functions of time. The relative deformation of the ice was calculated from the ring force and thermal expansion of the steel ring and ice plate. The expansion coefficients were set to $\alpha_{ice} = 52.0 \cdot 10^{-6}\ {}^{o}C^{-1}$ and $\alpha_{steel} = 12 \cdot 10^{-6}\ {}^{o}C^{-1}$. A result from his biaxial experiments is given in Figure 2.8.

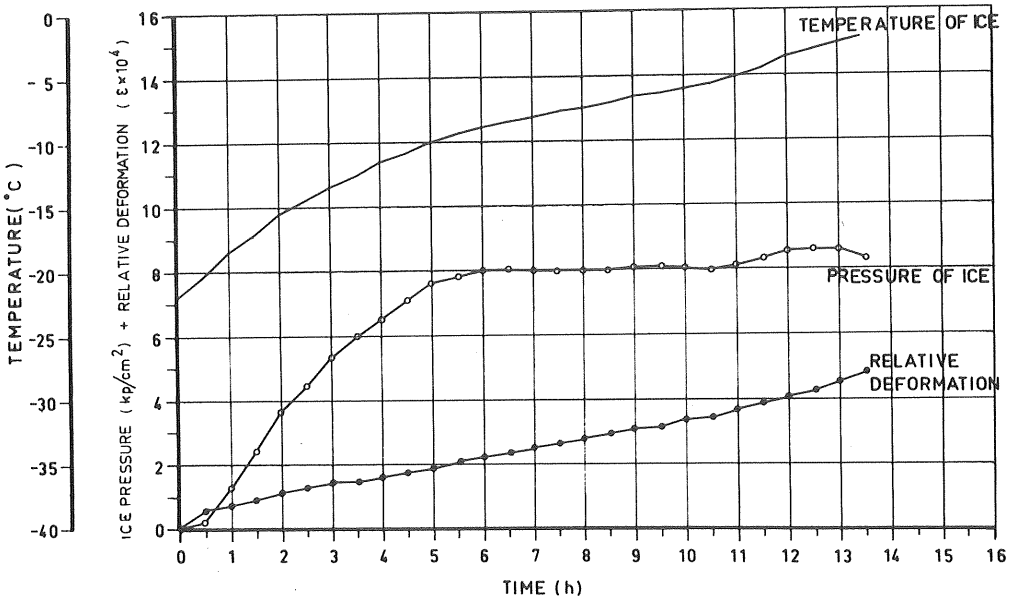

Figure 2.8 Biaxial thermal pressure test. Experiment No 7. Ice temperature, ice pressure and the relative deformation between the ice plate and the steel ring as functions of time. (Lindgren 1968).

Lindgren used a linear visco-elastic model with a Maxwell and a Kelvin unit in series to evaluate the test results. Its differential equation is given by e.g. Bergdahl (1977 p. 103) and a solution for the case of constant-load tests is

$$\varepsilon = \frac{\sigma}{E_1} + \frac{\sigma}{E_2}\left(1 - \exp\left(-\frac{E_2 t}{\eta_2}\right)\right) + \frac{\sigma\, t}{\eta_1} \qquad \ldots (2.24)$$

Compare Equation (2.19).

Here E_1 and E_2 are elastic moduli
η_1 and η_2 are viscosity moduli
ε strain
σ stress

1	index for the Maxwell unit
2	index for the Kelvin unit

Lindgren remarked that Equation (2.24) is not a good description for ice, which does not behave linearly. To make up for that, he investigated the dependence on stress and time of the moduli, and thus violated the assumption of the solution (2.24) that the moduli are constant.

Lindgren gave the following values from his experiments

$$\begin{aligned} E_1 &= 66000\,(1 - 0.012\,\theta)\ \text{kp/cm}^2 \\ E_2 &= 70000\ \text{kp/cm}^2 \\ \eta_1 &= 18.5\ \sigma^{-1}\,(0.20 - 0.08\,\theta)\,\left(\frac{t}{3600}\right)^{0.5} \cdot 10^8\ \text{kps/cm}^2 \\ \eta_2 &= 1.1 \cdot 10^8\ \text{kps/cm}^2 \end{aligned} \quad \ldots\ (2.25)$$

The fact that η_1 is a function of stress does not interfere with the validity of (2.24), for the tests, because σ is constant for each test, but the dependence on time t is a violation.

From the biaxial tests Lindgren estimated the same values of E_1 and E_2 as for the uniaxial tests with the assumption that Poisson's modulus was 0.36. The value of η_2 was assumed to be the same while a new equation was put up for η_1.

$$\eta_1 = 31 \cdot \sigma^{-1}\,(0.30 - 0.07\,\theta)\left(\frac{t}{3600}\right)^{0.25} \cdot 10^8\ \text{kps/cm}^2 \ldots\ (2.26)$$

on condition that Poisson's modulus was 0.5 for the viscous deformation (last part of experiment).

In his thermal analysis Lindgren established that the influence of the growing of the ice cover on the thermal gradient can be disregarded. Compare Appendix I-3. For the calculation of the temperature profile in the ice for arbitrary changes of air temperature he used a graphical variant of the Schmidt difference scheme, which also included the thermal resistance at the surface neglected by most other authors (except by the Soviet norm SN 76-66). Examples of such calculations can be seen in Figures III-7 and III-8 of Appendix III.

For the found relationship of $\eta \propto \sigma^{-1}$ the used model is no longer linear and the solution of σ for a given rate of deformation must be solved by numerical integration. The creep element of the model gives the rate of creep to $\dot{\varepsilon} \propto \sigma^2$ Lindgren's Equation (2.26) was set up for $0.5 < \sigma < 1.6$ MPa,for the range of which it does not give rates that deviates much from the model proposed by the author or from Drouin and Michel's experiments (1971).

Criticism of Lindgren's work can be based on the fact that the experimental results are very scattered. Lindgren's own comment is: ".... calculations of the values of maximum ice pressure are somewhat unreliable. With this in mind, rough estimates can be used to assess maximum ice pressure".

2.10 Reeh (1970)

Reeh published a paper on the thermal stress in a visco-elastic plate of simple extension in 1970. The first part of the paper dealt with the temperature response of a plate subjected to a linear temperature change at one of its surfaces, while the temperature of the other surface was kept constant. Approximate solutions were given for the dimensionless time $ta/h^2 \leqslant 0.3$. (See Figure I-2 Appendix I.) The solutions were based on a solution for the semi-infinite space, but a correction term was added. (Compare Drouin and Michel, Section 2.11.)

The second part dealt with the stress response of a plate in simple extension to the temperature response deduced in the first section, assuming the plate to consist of a linear Maxwell material.

The temperature profile solution did not shed much new light on the understanding of the problem, and as the rheological model was far too simplified,the paper was more of an elegant display of mathematics than a contribution to the solving of the problem of thermal ice pressure.

2.11 Drouin and Michel (1971)

Drouin and Michel (1971, Drouin 1972) made a great contribution to the solving of the problem of thermal ice pressure. Their work spanned over the whole problem from the weather fluctuations to the ice thrust.

They made exhaustive and critical reviews of former works on the problem. They gave a thorough treatment of the thermal diffusion problem in the ice cover for both transient and stationary conditions, including the effect of snow insulation, but neglecting the question of thermal surface resistance. The air temperature variations in the Quebec area were studied statistically as to the rate of change of temperature and the shape of the curves of temperature increases.

The most valuable part of their work is the study of uniaxial deformation of ice and biaxially restricted expansion tests of the same type as made by Lindgren (1968) but with better controlled conditions. They also tried to make an improved experiment of the same type as Löfquist (1954) but did not succeed because of difficulties with their sophisticated equipment.

Some aspects of Drouin and Michel´s work will be taken up below. The thermal properties of ice and snow is not discussed here but it is referred to Bergdahl (1977), where also the mechanical properties of ice are discussed more fundamentally.

Drouin and Michel derived the deviation of the temperature from the linear gradient because of the variation of conductivity with temperature. They concluded that the temperature in the ice is a little higher than is given by the linear gradient. This conclusion must be wrong as is shown in Appendix I-3. The thermal conductivity of ice increases with decreasing temperature, which means that the thermal gradient close to the upper surface of the ice must not be as steep as deeper in the ice to drive the same heat flux. The equally small deviation caused by the growth of the ice cover was not discussed. See Appendix I-3 Eq(I-28).

The variation of temperature in an ice cover more than 40 cm thick due to a cyclic temperature variation at the surface was approximated by the Fourier -solution for a semi-infinite space. This gives satisfactory solutions for the said cyclic variation, but Drouin and Michel used the result for a single sinusoidal rise from one constant temperature to another (Appendix I-7), which is not acceptable. It will be shown in

Chapter 3 that this gives underestimates of both the rate of change of temperature and the total temperature rise of the ice cover. The approximation, as used, was probably the cause to the peculiar fact that the faster the temperature rise is the smaller the thermal thrust, which is true only for a cyclic variation.

The uniaxial tests were performed as constant strain rate tests. Examples of graphs from such tests are shown in Figure 2.9. Tests were performed with artificial snow ice, with ice monocrystals taken from an ice cover with mostly vertical c-axes (Ice S1), and with nucleated columnar ice of preferentially small-diameter crystals with horizontal c-axes (Ice S2).

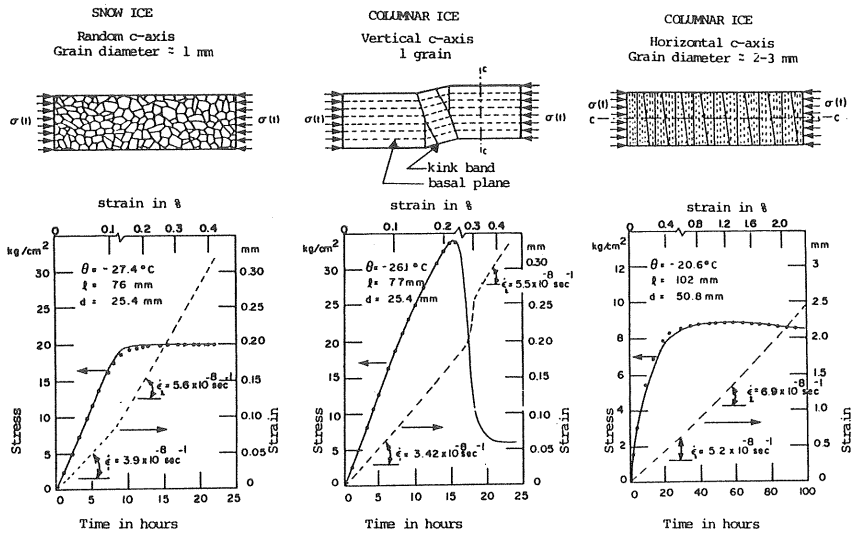

Figure 2.9 Stress-time and strain-time curves obtained by acting on ice specimens with a constant-speed crosshead testing machine. Continuous and dashed lines are experimental curves. The points are values calculated with the model Eq. (2.27). From Drouin (1972).

The test specimens were made as circular cylinders length 7.62 diameter 2.54 cm and loaded axially at constant temperature. They were cut with their axes horizontally in respective ice cover. The test results from the tests on the snow ice and the mononcrystals (S1) showed comparitively little scatter when evaluated by the composite mechanical model used by Drouin and Michel. The specimens of the S2 ice were, however, too small compared to the grain size why the test result became too dubious. Only two tests with bigger specimens were performed.

The typical curves of Figure 2.7 show a nearly constant rate of increase of stress during the first period of time. Then the slope diminishes and a maximum is reached. For the monocrystals (S1) the decrease is rather abrupt, for the snow ice and S2-ice only gradually decreasing.

The rheological equation used by Drouin and Michel for evaluating the tests is

$$\frac{d\sigma}{dt} = \dot{\varepsilon} E_a - 2b\beta E_a \left(\left(\frac{n_o}{\beta} + \dot{\varepsilon}t\right) - \frac{\sigma(t)}{E_a}\right)\left(\frac{\sigma(t)}{2p}\right)^m \quad \ldots \quad (2.27)$$

where
- σ is stress
- $\dot{\varepsilon}$ strain rate
- t time
- E_a apparent elastic modulus
- n_o initial number of dislocations
- β rate of multiplication of dislocations
- b Burgers´s vector
- p a constant
- m a constant

The complex Equation (2.27) is capable of reproducing the decrease of stress after the maximum is reached for snow ice and S2-ice because of the inclusion of $\dot{\varepsilon}t$. For the monocrystals the equation is valid only slightly beyond the maximum pressure. A simpler model can reproduce the most interesting case of an S-1 ice cover equally well.

The tests are probably the best ones performed and they are made within a relevant range of deformation rates.

Biaxial experiments were also conducted in approximately the same way as was done by Lindgren (1968). The ice specimens were discs of ice, diameter 15 or 30 cm, thickness 5 cm. They were placed in rings of invar instead of steel. In the tests the temperature was raised from different initial values to $0^{\circ}C$ so that the rate of relative deformation became approximately constant.

Five tests were performed with snow ice, eight each with ice types S1 and S2. For each case the Equation (2.27) was used to calculate the stress that would have developed in uniaxial cases with the same histories of strain and temperature as the discs. The maximum calculated and measured stresses were compared by the ratio between experimental and calculated stresses.

For snow ice:

$$\frac{\sigma\,(\text{max, biaxial, measured})}{\sigma\,(\text{max, uniaxial, calculated})}$$

The ratios were 1.81, 1.51, 1.83, 1.72, 1.56, which gives the Poisson moduli 0.45, 0.34, 0.45, 0.42, and 0.36. For plastic deformation $\nu = 0.50$ and for isotropic elastic materials usually around 0.30. Mean and standard deviation of the ratios were 1.69 and 0.15.

For S1 ice

$$\frac{\sigma(\text{max, biaxial, measured})}{\sigma(\text{max, uniaxial, calculated})}$$

The ratios ranged from 1.00 to 1.97, mean 1.33 standard deviation 0.35. The great variation was probably caused by the variation of the direction of the optical axes in the biaxial case. The uniaxial tests were performed with monocrystals, while the discs of the biaxial tests consisted of several crystals. For tests with high ratios the crystal axes were found to be more perfectly vertically oriented, while larger deviations were found for tests with a low ratio.

Nine of the twelve biaxial experiments by Lindgren (1968) were compared in the same way by Drouin and Michel. The ratios ranged from 0.92 to 1.07, mean 0.95 standard deviation 0.10. The diameter of Lindgren's discs were 80 cm and, their thickness 7 cm, and consequently they were 7 and 28 times bigger than the ones used by Drouin and Michel. The number of crystals with inclined axes is therefore greater.

The following conclusion was drawn: In nature, it is not possible that all crystals in an ice cover have a vertical orientation. For this reason, the determination of thermal ice pressure in ordinary (not seeded) columnar ice covers for a biaxially restricted case might be based on the results of maximum pressures obtained for uniaxially restricted specimens (monocrystals) deformed perpendicular to their optical axes.

For S2 ice

Too few (two) results from uniaxial tests were received to make a basis for comparison. Therefore the following ratio was formed

$$\frac{\sigma\,(\text{max, biaxial, S2, measured})}{\sigma\,(\text{max, uniaxial, S1, calculated})}$$

The value of this ratio ranged from 0.83 to 1.16, mean 1.02 and standard deviation 0.11 (one test excluded). A conclusion is that the seeded columnar ice (S2) cannot attain higher values of thermal stress than an ice cover with preferentially vertical c-axes (S1).

On the basis of the tests, and using the results of uniaxial (S1) tests directly, Drouin and Michel presents graphs over the maximum of total thermal ice pressure of an ice cover as functions of cover thickness, with initial surface (or air) temperature and time for the increase (half period of the sinusoidal variation) as parameters. See Figure 2.10. Note, that the longer the time for the increase the greater the pressures. This was explained by the term $\dot{\varepsilon} t$ of Eq. (2.27) by Drouin and Michel.

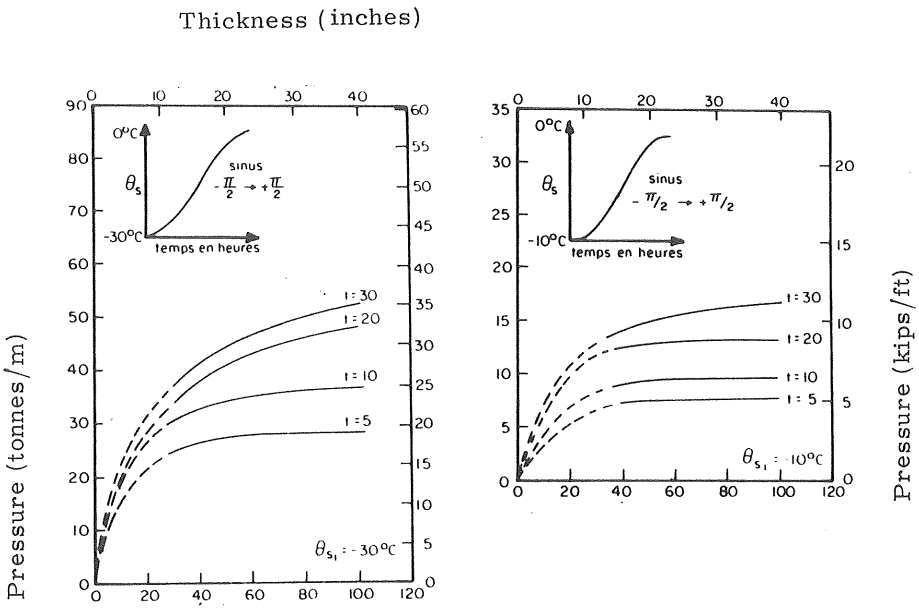

θ_s surface temperature

t time for temperature rise

Figure 2.10 Thermal ice pressure as function of ice cover thickness for different initial surface temperatures θ_s and times t for the increase to 0°C. (Drouin and Michel, 1971).

The deformation tests of Drouin and Michel seem to make an excellent foundation for the calculation of thermal ice pressure, and their test results are used for the creep element in the mathematical model proposed in this work. The work of Drouin and Michel may be criticized by the facts

that the thermal boundary layer at the ice surface is completely neglected.

that the rheological Equation (2.27) is unnecessarily complicated. This is a drawback when calculating continuous records.

that the given model parameters seem to depend on the method of integration and the length of its time increments.

that the error in the thermal calculations gives rise to a very weird dependence of time (See Figure 2.8) with lower pressure for faster rates of change of temperature of the upper surface.

2.12 Jumppanen (1973)

Jumppanen (1973) made a study on thermal ice pressure for the Saima Canal. He tried to find the compliance function J(t) directly from creep tests by fitting curves to the test results. Then he used the compliance function in a folding integral to calculate the pressure. See e.g. Flügge (1975).

Cylindrical specimens, diameter 9 cm length 15 cm, were loaded axially at the stress levels 3, 7 and 12 kp/cm^2 at -2, -5, -12 and -25°C. The specimens were cut with their axes horizontal and parallel to the c-axes of the grains. (The ice cover ought then to have been of type S2 with ordered crystals or very big crystals). The specimens were taken from artificial ice covers produced from tap water, density 870-910 kg/m^3 and from an ice cover in the Saima Canal, ρ=920 kg/m^3.

For a linear material the creep compliance J(t) is a monotonously increasing function for $t \geq 0$, and for $t < 0$ $J(t) \equiv 0$. For a constant stress σ_o applied to a material obeying the same differential equation as the one used by Lindgren (1968), the deformation ε as a function of time t can be written

$$\varepsilon = \sigma_o J(t) = \sigma_o \left[\frac{1}{E_1} + \frac{1}{E_2} (1 - e^{-t/t_o}) + \frac{t}{\eta_1} \right] \qquad \ldots (2.28)$$

Here E_1, E_2, t_o and η_1 are constant. Compare Equation (2.19) or (2.24). The compliance function found by Jumppanen in the tests was

$$J(t) = a + b\, t^n \qquad \ldots (2.29)$$

with t in hours

$$a(\Delta\theta) = (1.17 + 0.036\,\Delta\theta) \cdot 10^{-5}\ cm^2/kp$$

$$b(\Delta\theta) = (24.5 + 0.5\,\Delta\theta) \cdot 10^{-5}\ cm^2/kp, \text{artificial ice.}$$

$$b(\Delta\theta) = (12 + 0.25\,\Delta\theta)\ 10^{-5}\ cm^2/kp, \text{Saima Canal ice.}$$

$$n = 0.3$$

$$\Delta\theta = \theta + 25^oC \qquad -25^oC \leqslant \theta \leqslant 0^oC$$

Creep curves for artificial ice are shown in Figure 2.11.

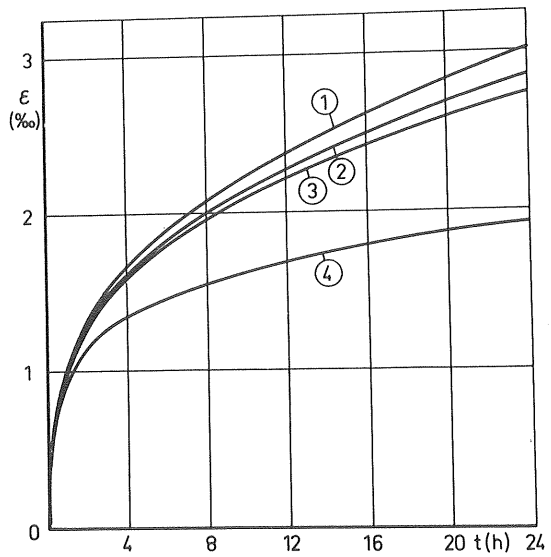

Figure 2.11 Creep curves for artificial ice at different temperatures at the stress level 0.3 MPa

1	$\theta = -2^oC$	$\sigma = 3.08\ kp/cm^2$
2	-5	3.21
3	-12	3.16
4	-25	3.2

The instantaneous elastic deformation is according to (2.29) $\sigma_o \cdot a$ which implicates that $a \approx 1/E_i$. For $\theta = -25^oC$ thus $E_i = 8.55$ GPa which is in the usual range of values given for ice. (See Bergdahl, 1977). Note that the exponent $n = 0.3$ is close to the 1/3 used by Royen (1922), Equation (2.7).

The value of $b(\Delta\theta)$ was quite different for the artificial ice and the Saima Canal ice. This was according to Jumppanen probably caused by the air content of the artificial ice, and by the fact that the canal ice had earlier been loaded by temperature changes of the ice cover.

The compliance function was finally used for calculating the expansion of a circular ice plate, a square ice plate, and an ice plate in a long trough. The solution did not involve the calculation of temperatures in an ice cover. The plates were supposed to be warmed linearly from some initial temperature to $0^{o}C$. For the biaxial calculations Poisson´s modulus is set to $\nu(\theta) = 0.4 + 0.004\,\theta$.

During the winter 1972/73 some measurements were done in the Saima Canal. An example and comparison with theory at the depth 8 cm in the ice is given in Figure 2.12.

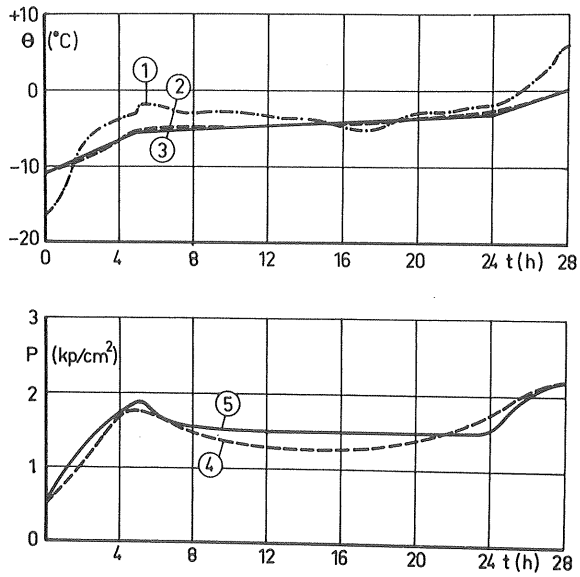

Figure 2.12 Values of ice pressure at the Saima Canal: 1 air temperature, 2 ice temperature at the depth 8 cm, 3 approximated ice temperature for the calculations, 4 measured ice pressure at the same depth, 5 calculated ice pressure. (Jumppanen 1973).

The short-comings of Jumppanen´s theory are

that the tests showed weak nonlinearity at 0.7 MPa and strong nonlinearity at 1.2 MPa. Thus the method cannot be used for compressive stresses greater than around 1 MPa which is quite ordinary for design pressure.

that his tests are quite few, and there seems to be some mistake as concerns ice types and crystal directions.

3. CALCULATION OF ICE TEMPERATURES

The basis for the calculation of the stress in the ice is a rheological equation like Equation (1.6), where the rate of strain, $\dot{\varepsilon}$, is given as a function of stress, σ, and rate of change of stress, $\dot{\sigma}$. The rate of strain is a function of the rate of change of ice temperature $\dot{\theta}$, Eq. (1.5). For a completely restricted ice cover

$$\alpha\dot{\theta} = \dot{\varepsilon} = \frac{1}{E}\dot{\sigma} + KD\sigma^n \qquad \ldots (3.1)$$

A first step towards the estimation of thermal ice pressure is thus to calculate the ice temperature or its time derivative.

This chapter is devoted to the calculation of the rate of change of temperature in the ice by accounting for the energy balance of and the thermal diffusion in the ice cover. Physical constants for ice and snow are not discussed in general but it is referred to Bergdahl (1977). A complete solution is given and comparisons between this and simplified solutions are performed as well as comparisons with some of the solutions given by the scientists reviewed in Chapter 2.

3.1 Energy Balance of an Ice Cover

The energy balance of ice or snow covers have mostly been studied in order to evaluate their growth or decay. Although such studies have often been performed with sophisticated methods, they work with daily, weekly or monthly mean values, why they can seldom be used directly for the calculation of the fast temperature fluctuations that are responsible for thermal ice pressure.

Studies aiming at thermal ice pressures tend, however, to oversimplify the energy balance of the surface by simply setting the surface temperature equal to the air temperature or only calculating advective heat transfer. On one hand, the omission of the thermal surface resistance means overestimation of the rate of change of temperature. On the other hand, the omission of radiation fluxes means underestimation, because the short-wave radiation increases the rate of change of temperature in the mornings,

especially at clear weather, and because the long-wave back radiation can cause a considerable depression of the ice surface temperature, which is especially noticeable in clear mornings.

Below follows a list on the terms of the energy flux to the ice or snow surface. The energy flux from underneath is commented in Paragraph 3.4. The terms taken up here are the fluxes of

- net solar radiation (+) (irradiation-reflexion)
- long-wave radiation from the atmosphere (+)
- emitted long-wave radiation (-)
- heat transfer because of different temperature in the air and on the surface (sensible heat) (+ or -)
- heat transfer due to vapour transport in the air and condensation (+) or sublimation (-) on the surface (latent heat)

The different terms are only given not evaluated below. For evaluations of heat balance functions it is referred to Paily et al (1974) or Sweers (1976), and for a discussion of the balance of ice or snow fields to Pounder (1965), Liljequist (1962) or Bengtsson (1976). Coefficients and equations are mostly taken from Paily et al (1974), and the given expressions are assumed to give the best available descriptions of the energy balance.

3.2 Heat Transfer

Latent Heat Transfer

The convective heat transfer from the air to the surface consists of sensible heat, because of the temperature difference between the air and the surface, and latent heat, because of the vapour transport to the surface and condensation on it. The latent heat transfer is often written

$$q_e = f(u)\,(e_a - e) \qquad \ldots (3.2)$$

where

e_a is the vapour pressure of the air 2 m above the surface

e the saturation vapour pressure at the ice surface

The saturation vapour pressure over an ice surface is a function of the surface temperature and is in this study approximated by a linear function

$$e = a(1 + b\theta) \quad -32^{o}C \leqslant \theta \leqslant 0 \qquad \ldots (3.3)$$

where $a = 610$ Pa

$b = (32^{o}C)^{-1} = 0.031^{o}C^{-1}$

θ = the ice surface temperature

A wind function recommended by Paily et al (1974) is the Rymsha-Donchenko function

$$f(u) = \rho L_s a (1 + bu + c(\theta - \theta a)) \qquad \ldots (3.4)$$

where $a = 2.42 \cdot 10^{-11}$ m /(s Pa)

$b = 0.49$ s/m

$c = 4.36 \cdot 10^{-2}\ ^{o}C^{-1}$

$\rho = 1000$ kg/m^3 the density of water

$L_s = 2.82 \cdot 10^6$ J/kg the specific heat of sublimation (condensation + fusion)

u the wind speed at 2 m above the surface

θ the surface temperature

θ_a the air temperature at 2 m

Sensible Heat Transfer

The sensible heat transfer and the latent heat transfer are usually considered proportional to each other. The ratio between the two types of heat transfer is called Bowen's ratio

$$B = \gamma (\theta_a - \theta) / (e_a - e) \qquad \ldots (3.5)$$

where $\gamma \approx 61$ Pa/^{o}C is the psycrometric "constant".

The sensible heat transfer can then be written

$$q_S = B\, q_e = f(u)\, \gamma (\theta_a - \theta) \qquad \ldots (3.6)$$

where q_e is given by Equation (3.2)

B -"- (3.5)

$f(u)$ -"- (3.4)

Finally, the total convective heat transfer to the surface is

$$q_c = q_e + q_S = f(u) [(e_a - e) + \gamma (\theta_a - \theta)] \qquad \ldots (3.7)$$

3.3 Radiation Fluxes

Emitted Long-Wave Radiation

The emitted long-wave radiation from the ice surface can be calculated by the Stefan-Boltzmann law of radiation with due respect to the emissivity of the ice or snow surface

$$q_b = \varepsilon \sigma T^4 \qquad \ldots (3.8)$$

where $\sigma = 5.6697 \cdot 10^{-8}$ W/m^2 K^4 is the Stefan Boltzmann constant

T the absolute temperature of the ice surface

ε the emissivity of the surface

In many temperature calculations it is convenient to linearize Equation (3.8). In implicit difference schemes it is necessary. The fourth-order binomial expansion of (3.8) for $T = T_o + \theta$ gives, if two terms are considered:

$$q_b = \varepsilon\sigma(T_o^4 + 4\ T_o^3\theta) \qquad \ldots (3.9)$$

where $T_o = 273.15$ K

θ = the temperature of the ice surface in ^oC

Absorbed Long-Wave Radiation

The atmosphere can also be considered a gray body that emits radiation at the rate

$$q_{\ell a} = \varepsilon_a\ \sigma\ T_a^4 \qquad \ldots (3.10)$$

where ε_a is the emissivity of the atmosphere

σ the Stefan-Boltzmann constant

T_a the absolute temperature of the atmosphere

While the emission of the surface, Equation (3.8) is rather well defined by the temperature and emissivity of the surface, these quantities are not as easily established for the atmosphere. The air temperature and humidity, which governs the emissivity, are mostly measured 2 m above the ground, but as the air is rather transparent to the considered radiation ($\lambda \approx 10$ µm) the incoming radiation originates from higher altitudes at least at clear weather. By clear, calm and cold weather the

difference in air temperature between the ground level and 5 or 10 m level can be 10 to 20°C or more. At Maudheim (71°S) midnight, July 2, 1950 the temperature at 10 m was measured to -30°C but at ground level to -44°C. This was not unusual. If such a strong inversion was broken up by a strong wind the temperature often rose 10°C and sometimes 20°C (Liljequist, 1962).

Another problem is to approximate the emissivity of the atmosphere, which is mainly a function of its content of water vapour and water, that is, humidity and cloud cover. A relation for the emissivity of the Ångström type is

$$\varepsilon_a = a - b \exp (- c\, e_a) \qquad \ldots (3.11)$$

where

$a = 0.806$

$b = 0.236$

$c = 1.15 \cdot 10^{-3}\ \mathrm{Pa}^{-1}$

e_a is the water vapour pressure at 2 m above ground

The influence from the cloud cover can be taken into account by

$$q_{\ell c} = q_{\ell a} (1 + kC^2) \qquad \ldots (3.12)$$

where $k = 0.0027$

C = the cloud cover in eights

The absorbed long-wave radiation flux from the atmosphere is finally

$$q_\ell = \varepsilon\, \varepsilon_a\, \sigma (1 + k\, C^2)\, T_a^{\,4} \qquad \ldots (3.13)$$

where ε is the emissivity of the ice or snow surface.

The emissivity of ice and snow can be set to $\varepsilon = 0.97$.
See Bergdahl 1977.

Absorbed Solar Radiation

The incoming short-wave radiation is composed of the direct solar irradiation, 0.9 kW/m^2, calculated on an area normal to the sun's rays, and diffuse sky radiation 0.1 kW/m^2. The flux through a horizontal surface from a clear sky can then be approximately written

$$q_{CL} = (a \cdot \sin \alpha + b) \quad \ldots (3.14)$$

where $a = 0.9\ kW/m^2$

$b = 0.1\ kW/m^2$

α is the altitude of the sun

The altitude of the sun can be approximated by

$$\alpha = \arcsin (\sin\varphi \cdot \sin \delta + \cos\varphi \cos\delta \cos h) \quad \ldots (3.15)$$

where δ is the declination of the sun

φ the latitude

h the local solar angle of the sun

The declination is written

$$\delta = 0.409 \cos ((172-D)\ 2\pi/365) \text{ rad} \quad \ldots (3.16)$$

where D is the number of the day in a year with D = 1 for January 1.

The local solar angle of the sun

$$h = (H - a)\ \pi/a \text{ rad} \quad \ldots (3.17)$$

where $a = 12\ h$

H is the solar time of the day $0 \leqslant H < 24$ h

If the sun is below the horizon ($\sin\alpha < 0$), the short-wave radiation is set to zero, $q_{CL} = 0$.

The solar radiation is reduced by cloud covers. Approximately this is written

$$q_C = q_{CL}\ (0.35 + 0.65\ (1-C/8)) \quad \ldots (3.18)$$

where q_{CL} is the radiation from a clear sky, Eq. (3.14)

C is the cloud cover in eighths.

The Equation (3.18) is probably correct only for the mean value over a day, while the short term fluctuations are much greater when clouds intermittently pass the sun.

The incoming short-wave radiation is approximately contained in different wave-length bands so that 50 % of the energy flux lies between 350-700 nm, 25 % between 700-1200 nm, and 25 % between 1200 and 4000 nm (Lyons and Stoiber, 1959, Pounder 1965).

Some of the incident light is reflected from the snow or ice cover. The absorbed radiation is for an optically rough surface (snow, snow ice, candled ice etc) calculated according to

$$q_s = (1-r)\, q_c \qquad \ldots (3.19)$$

where q_c is the incident radiation, Eq (3.18)
r the reflexion coefficient or albedo

In Table 3.1 below are rough values given for the coefficients of reflexion. More details are given by Bergdahl (1977).

Table 3.1 Proposed coefficients of reflexion for ice and snow surfaces

Wave-length bands (nm)	Snow	Snow Ice
350 - 700	0.9	0.05
700 - 1200	0.7	0.05
1200 - 4000	0.6	0.05

For clear ice the direct light can be calculated as reflected against a polished surface. If the angle of incidence is α_1 and the angle of reflexion is β, the coefficient of reflexion is calculated as

$$r = \frac{1}{2}\left[\frac{\sin^2(\alpha_1-\beta)}{\sin^2(\alpha_1+\beta)} + \frac{\tan^2(\alpha_1-\beta)}{\tan^2(\alpha_1+\beta)}\right] \qquad \ldots (3.20)$$

where $\sin \alpha_1 = 1.31 \sin \beta$

$0 \leqslant \beta \leqslant \alpha_1$

$\alpha_1 = \pi/2 - \alpha$

α is the altitude of the sun. For notations, see sketch Figure 3.1.

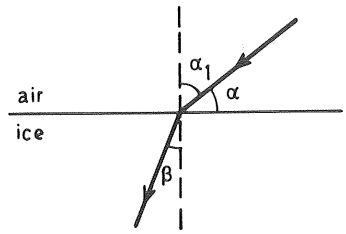

Figure 3.1 Definition sketch of angles.

For the diffuse light the coefficient is set to 0.02, and consequently the absorbed radiation flux for a clear-ice surface can be written

$$q_s = ((1-r)\ a \sin\alpha + 0.98\ b)\cdot(0.35+0.65(1-C/8)) \quad \ldots (3.21)$$

where $a = 0.9\ kW/m^2$
$b = 0.1\ kW/m^2$
C = the cloud cover in eighths
r = the reflexion coefficient according to Eq. (3.20)

3.4 Approximations of the Energy Balance

For stationary conditions the energy balance equation can approximately be written

$$q_m = q_c + q_\ell - q_b + q_s \quad \ldots (3.22)$$

where q_m is energy flux used to melting
q_c the total convective heat transfer Eq (3.7)
q_ℓ atmospheric long-wave radiation flux, Eq (3.13)
q_b long-wave back radiation flux, Eq (3.8)
q_s net short-wave radiation flux, Eq (3.21) or (3.19)

When the surface temperature of the ice is below the freezing point, the melting term q_m only consists of the freezing at the lower boundary of the ice, where the temperature is 0^oC. Then the melting term can approximately be written

$$q_m = - \lambda \theta / h \qquad \ldots (3.23)$$

where λ is the conductivity of the ice
θ the surface temperature (^oC)
h the depth of the ice cover

The assumption is approximately true if the growth of the ice cover is not too fast. In the discussion in this paragraph we will further disregard the solar radiation flux q_s.

In Figures 3.2 solutions for the temperature profiles in ice covers of different thickness are shown for two slightly different stationary weather situations. Only the cloudiness is different between the situations a) and b).

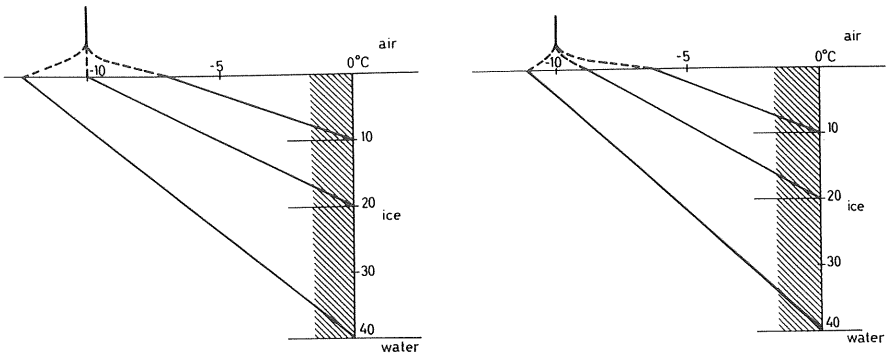

Figure 3.2 Temperatures in ice covers free from snow:

air temperature	a)	-10^oC	b)	-10^oC
wind speed		2 m/s		2 m/s
vapour pressure		300 Pa		300 Pa
cloudiness in octas		0/8		8/8
short-wave radiation (night conditions)		0		0

Depth of the ice covers 0.10, 0.20 and 0.40 m.

Now, there are mainly three different approximations proposed for the calculations of ice pressures let aside the short wave radiation:

1. Equal surface and air temperature for example Drouin and Michel (1971), Rose (1947), Brown and Clarke (1932).

2. A heat exchange coefficient defined by the simple relation (1.3) $q = A \cdot \Delta\theta$ or possibly with A as a function of wind speed, for example Lindgren (1968).

3. Some initial mean temperature at semi-stationary conditions before the sudden rise of air temperature: Sovietic norm SN 76-59. (1959) $\theta_i = 0.35\ \theta_a$.

Approximation 1 $\theta = \theta_a$

For the stationary cases considered in this paragraph it is seen that the approximation 1 means underestimates of the temperature in the ice for three out of the six cases in Figure 3.2, and overestimates in two cases. Only one case is properly represented. For two of the cases the potential for temperature rises is thus underestimated and this coincides with the thickest ice covers 0.40 m. The approximation 1 also causes overestimation of the rate of change of temperature, why the suitability of the approximation for thermal ice pressure cannot be evaluated from this stationary case.

Approximation 2 $q = A(\theta_a - \theta)$

If the value of the heat-exchange coefficient in the approximation 2 is evaluated by Equation (3.24) below, its value will vary considerably for the same wind speed and air temperature. See Table 3.2. On the other hand, if the surface temperatures are solved from Equation (3.24) with A according to Equation (3.25a) (u = 2 m/s), the temperatures would be overestimated for all the cases. See Table 3.3. The potential for temperature rises is thus underestimated, which would result in too small figures of ice pressure.

If the thermal gradient in the ice is considered linear, Approximation 2 gives

$$-\lambda\,\theta/h + A(\theta_a - \theta) = 0 \qquad \ldots (3.24)$$

Here $\lambda = 2.24$ W/m ^{o}C thermal conductivity of ice

h = ice thickness

θ = ice surface temperature
θ_a = air temperature
A = heat exchange coefficient

Table 3.2 The heat exchange coefficient A in Eq. (3.24) evaluated for the six hypothetical cases of Figure 3.2.

Ice thickness (m)	Cloudiness	Coefficient A ($W/m^2\ ^oC$)
0.10	0/8	50.9
	8/8	35.7
0.20	0/8	∞
	8/8	100.8
0.40	0/8	-28.7
	8/8	-60.0

Table 3.3 Surface temperatures of the ice cover for the three different ice thicknesses calculated with A according to Eq. (3.25), with q according to Eq.(3.26), and with the total energy balance.

		Surface temperature (^oC)		
h	Cloudiness	Eq. (3.25)	Eq. (3.26)	Energy balance
0.10	0/8	b) -6.0	-6.7	-6.9
	8/8	a) -5.5	---	-6.1
0.20	0/8	b) -7.5	-8.4	-10.0
	8/8	a) -7.1	---	-9.0
0.40	0/8	b) -8.5	-9.6	-12.4
	8/8	a) -8.3	---	-11.0

The method might not be as insecure as indicated by the hypothetical example above. Field measurements by the author reported in Appendix II gave A = 9.8 $W/(m^2\ ^oC)$ with the standard deviation $\pm$ 2.9 $W/(m^2\ ^oC)$ for no wind. Field measurements by Wold (1957) evaluated in the same way by the author gave A = 12.0 $\pm$ 5.2 $W/(m^2\ ^oC)$. Extensive measurements on wet surfaces of heated roads at negative air temperatures by

Magnusson (1977) gave total values for wet surfaces of

a) $A = 16.0\ (1+0.34\ u)\ W/(m^2\ ^oC)$ overcast

b) $A = 22.5\ (1+0.24u)\ W/(m^2\ ^oC)$ clear sky

$u < 4.5$ m/s at elevation 2 m. ... (3.25)

The coefficient of u has been recalculated for the elevation 2 m by the author. See Table 3.3 for estimated surface temperatures. The heat flow was found to be well estimated at overcast sky, but the deviation was great for clear sky for the case of which the radiation is important even if the temperature difference is small. For this latter case a better approximation was found by using an expression of the type

$$q = a\ (1 + bu)\ (\theta_a - \theta) - q_o \qquad \ldots (3.26)$$

with

$a = 22.5\ W/(m^2\ ^oC)$

$b = 0.24$ s/m

$q_o = 40\ W/m^2$

The result of calculations of the surface temperature using Eq. (3.26) is also shown in Table 3.3. The estimate is better with a clear difference between clear sky and overcast.

Approximation 3 $\theta_i = 0.35\ \theta_a$

The approximation that the mean initial temperature is $0.35\ \theta_a$ means that with a linear gradient the surface temperature is $\theta = 0.7\ \theta_a$. For all the cases in Figure 3.2 then the surface temperature would be $-7\ ^oC$ which accordingly lies in a probable range but does not account for extreme situations.

3.5 Equilibrium Temperature

If the solar radiation is excluded and the expressions (3.7), (3.13) and (3.8) for the total convective heat transfer, long-wave sky radiation, and the long-wave back radiation respectively are inserted, Equation (3.22) gives

$$q_m = f(u)\left[(e_a - e) + \gamma(\theta_a - \theta)\right]$$
$$+\varepsilon\varepsilon_a \sigma T_a^4 (1 + kC^2) - \varepsilon \sigma T^4 \qquad \ldots (3.27)$$

Further the linearization (3.9) is performed:

$$q_m = f(u)\left[(e_a - e) + \gamma(\theta_a - \theta)\right] +$$
$$+\varepsilon\sigma 4T_o^3\left[\varepsilon_a(1+k C^2)\, T_o/4 + \theta_a) - (T_o/4+\theta)\right] \qquad \ldots (3.28)$$

Finally, the saturation vapour pressure is approximated by Eq (3.3) which gives q_m as a linear function of the surface temperature and the weather variables: wind speed, air vapour pressure, air temperature atmospheric emissivity, cloudiness.

Now, it is possible to define an equilibrium temperature of the ice for which there is no net energy transport, that is, at zero gradient in the ice cover,

$$0 = f(u)\left[e_a - a\ (1+b\theta_e) + \gamma(\theta_a - \theta_e)\right] +$$
$$+\varepsilon\sigma\, 4T_o^3\left[\varepsilon_a(1+k\, C^2)\ (T_o/4+\theta_a) - T_o/4+\theta_e)\right] \qquad \ldots (3.29)$$

And thus $\theta_e = f(u, e_a, \theta_a, \varepsilon_a, C)$. The subtraction of 0 from q_m now gives

$$q_m = f(u)\left[ab(\theta_e - \theta) + \gamma(\theta_e - \theta)\right] + \varepsilon\sigma 4T_o^3 (\theta_e - \theta) =$$
$$= (\theta_e - \theta)\left[f(u)\ (ab+\gamma) + \varepsilon\sigma\, 4\, T_o^3\right] \qquad \ldots (3.30)$$

The expression within the parentheses is a kind of coefficient of heat transfer, but through the introduction of the equilibrium temperature it does not involve any rough approximations as does $q_m = A(\theta_a - \theta)$. The coefficient of Eq. (3.30) can be reached alternatively by derivating Eq. (3.28) with respect to θ. Its value is, for the functions given here and if the wind-speed function is supposed to be independent of the ice temperature:

$$\partial q_m / \partial \theta = A_e = a(1 + bu) \qquad \ldots (3.31)$$

where

$a = 10.1\ W/(m^2\ ^oC)$

$b = 0.26\ s/m$

The use of the energy balance equation in the form of Equation (3.30) or $q_m = A_e (\theta_e - \theta)$ is, of course, equivalent to using the original expression. The heat exchange coefficients A and A_e must not be mixed up.

3.6 Calculation of Non-Stationary Temperature Distributions

The non-stationary temperature distributions or the rate of change of temperature in the ice cover at different depths can be calculated by several methods.

a) Analytical solutions expressed in Fourier series can for example be used for the case of a prescribed surface temperature which is demonstrated in Appendix I-4 to I-8. Such a solution was applied by Drouin and Michel (1971).

b) Other types of expansions in characteristic functions can be used for special cases, like the calculations performed by Monfore and Taylor (1948) for an application with a constant heat transfer coefficient. See Appendix I-8.

c) Explicit difference methods are mostly more convenient to use. One method is the Schmidt method used by Rose (1947) and by Lindgren (1968) which is rather conveniently calculated by hand or graphically. For calculations of long series, however, explicit difference methods are rather expensive to use if one wishes to have good resolution near the surface, as the methods demand time steps proportional to the geometrical differences squared in order to retain numerical stability and sufficient accuracy. Different types of boundary conditions and internal heating by penetrating solar radiation are easily incorporated in the computer based schemes.

d) By using an implicit difference scheme like for example Crank-Nicholson's scheme the problem of stability is overcome as such a scheme is unconditionally stable for internal points. The length of time and length differences can be chosen with respect only to the needed accuracy of the result. Boundary conditions can cause instability, which must be observed for every new application.

Below the equation of thermal diffusion along with initial temperatures and boundary conditions are presented. Then follows a short description of the implicit method used by the author.

Equation of Thermal Diffusion

The equation of thermal diffusion is used to describe the rate of change of temperature within the ice.

$$\frac{\partial \theta}{\partial t} = a \frac{\partial^2 \theta}{\partial x^2} + \frac{p(x,t)}{C_p \rho} \qquad \ldots (3.32)$$

where

t is the time
x the vertical coordinate
θ the temperature at (x, t)
a coefficient of thermal diffusion
C_p = 2120 J/kgK the specific heat capacity
ρ the bulk density
p the effect source per unit volume at (x, t)

$$a = \lambda / C_p \rho \qquad \ldots (3.33)$$

where λ is the specific thermal conductivity.

The bulk density ρ is given the following values

snow	250 kg/m^3
snow ice	890 kg/m^3
columnar ice	916.8 kg/m^3

The thermal conductivity is set to the following constant values for the three used materials

snow	0.3 W/mK
snow ice	2.14 W/mK
columnar ice	2.24 W/mK

The long-wave radiation and the heat transfer at the upper surface of the ice are included in the source term p. The short wave radiation must be separately considered as it is absorbed not only in the upper surface of the ice but throughout the thickness of the ice cover.

For an internal layer at the depth x from the upper surface of the ice the quantity p(x, t) is absorbed

$$p(x,t) = q_s k e^{-kx} \qquad \ldots (3.34)$$

where q_s is the solar radiation that penetrates into the ice, equation (3.19) or (3.21). q_s is a function of time.

t the time

x depth in the ice cover

k absorption coefficient

The used absorption coefficients for the three different materials and the three wave-length bands are given in the table below.

Table 3.4 Absorption coefficients $k(m^{-1})$ given for different wave-length bands

wave length (nm)	350-700	700-1200	1200-4000
snow	120	200	10 000
snow ice	30	50	10 000
columnar ice	0.2	2	5 000

For the uppermost layer of the ice the source term is now written

$$p(0,t)\,dx = q_\ell - q_b + q_c + q_s k e^{-kx}\,dx \qquad \ldots (3.35)$$

where q_ℓ is the absorbed long wave radiation from the atmosphere, Equation (3.13)

q_c the total convective heat transfer to the surface, Equation (3.7)

q_b emitted long-wave radiation, Equation (3.8)

At the lower boundary of the ice heat is supposed to be taken only from the freezing of water. The heat diffusion in the underlying water is thus neglected, and the source term at the lower boundary is written

$$p(h,t)\,dx = q_s\, k\, e^{-kx}\, dx + L\,\rho\,\frac{dh}{dt} \qquad \ldots (3.36)$$

where h is the thickness of the ice cover
$L = 3.34 \cdot 10^5$ J/kg is the specific heat of fusion
$\rho = 916.8$ kg/m^3 the density of ice

The equation of thermal diffusion is solved numerically with the help of the implicit difference scheme described below.

Difference Scheme

The temperatures in the ice cover are calculated by the help of an implicit difference scheme (Crank-Nicholson). The implicit scheme was chosen so as to be able to make a rather free internal division into intervals, as this scheme gives unconditionally stable calculations for the internal points. The boundary conditions at the upper surface introduced instability, however, which was overcome by giving more weight to the later timestep. The weight given is $\beta = 0.6$.

The equation of diffusion

$$\frac{\partial\theta}{\partial t} = a\,\frac{\partial^2\theta}{\partial x^2} \qquad \ldots (3.37)$$

is fundamentally approximated by the difference equation

$$\theta(x, t+\Delta t) = \theta(x,t)$$

$$+ a\,\frac{\Delta t}{\Delta x^2}\,\big[(1-\beta)\{\theta(x+\Delta x,t) - 2\theta(x,t) + \theta(x-\Delta x,t)\}$$

$$+ \beta\{\theta(x+\Delta x, t+\Delta t) - 2\theta(x,t+\Delta t) + \theta(x-\Delta x, t+\Delta t)\}\big] \ldots (3.38)$$

where the searched temperature $\theta(x, t+\Delta t)$ is a function of known temperatures at the point of time, t, and of unknown temperatures in the neighbour points, $x + \Delta x$ and $x-\Delta x$, at $t+\Delta t$. The equation (10.2) must thus be solved for all points in the ice simultaneously and this is done by a double sweep method (Gauss elimination).

If the weight $\beta = 0$ is given to the later time step Equation (3.38) will give an explicit scheme where the searched temperature is given by known temperatures directly:

$$\theta(x, t + \Delta t) = \theta(x, t) +$$

$$+ a \frac{\Delta t}{\Delta x^2} \{\theta(x+\Delta x, t) - 2\theta(x, t) + \theta(x-\Delta x, t)\} \quad \ldots (3.39)$$

If further $a\Delta t/\Delta x^2 = 1/2$ the Schmidt method will emerge:

$$\theta(x, t+\Delta t) = \frac{1}{2}\{\theta(x+\Delta x, t) + \theta(x - \Delta x, t)\} \quad \ldots (3.40)$$

In this last method the searched temperature is simply given by the arithmetic mean of the temperatures in the neighbour points at the previous time step.

The diffusion equation has not the simple form (3.37) but contains also the source term, p, due to absorption of short-wave radiation in internal points (Eq. 3.34), as well as the energy input to the uppermost element (Eq. 3.35) and the heat of fusion at the lower boundary (Eq. 3.38). A detailed description of how these source terms can be incorporated into the implicit difference scheme is given by Bergdahl and Wernersson (1978), and shall not be repeated here.

System of Equations

The system of equations that develops, when all difference expressions for the elements are gathered, is of the type

$$A T_2 = B T_1 + D \quad \ldots (3.41)$$

where A and B are tridiagonal matrices

T_2 the column vector of new (unknown) temperatures $\theta_i(t+\Delta t)$, i=1,2....

T_1 the column vector of old (known) temperatures $\theta_i(t)$, i = 1,2 ....

D vector of terms that do not depend on ice temperatures but on the weather conditions only.

The right hand side of Equation (3.41) consists of known quantities only why $C = BT_1 + D$ can be calculated and finally the double sweep method gives the solution:

$$T_2 = A^{-1} C \qquad \ldots (3.42)$$

Notes on Accuracy and Stability

The accuracy of the used scheme can for internal points be estimated by expansion in Taylor series. If first β is neglected it is found that the difference approximation of the right hand side of the equation of thermal diffusion (10.1) has a truncation error of

$$\Delta x^2/12 \cdot \partial^4\theta/\partial x^4 + O(\Delta x^4) \qquad \ldots (3.43)$$

and the approximation of the left hand side has a truncation error of

$$\Delta t/2 \cdot \partial^2\theta/\partial x^2 + O(\Delta t^2) \qquad \ldots (3.44)$$

The errors due to $\beta \approx 0.5$ is also of the same order as (3.44).

It can be shown by the von Neuman criterion that the used implicit scheme is unconditionally stable for all choices of length and time intervals. It proved, however, to be necessary to put slightly more weight ($\beta = 0.6$) on the later time step, because of problems introduced at the upper boundary.

3.7 Comparisons between Some Solutions

Complete case without and with solar radiation. In Figure 3.3 solutions for two cases without and with solar radiation are compared. The initial air temperature is -30°C and rises as a single cosine half wave to 0°C in 5 h. The ice thickness is 0.4 m. The wind speed is constant u = 2 m/s, the sky is clear C = 0, and the vapour pressure is 80 % of the saturation vapour pressure of the air. The first case, continuous curves, is for night condition starting at 18.00 Dec. 21. The second case, dashed curves, takes solar radiation into account, for which the latitute is set to 60°N and the time is the vernal equinox. This latter case starts at 6.00 March 21.

The difference between the two cases is remarkable and the faster rate of change of temperature for the spring day is reflected in the calculated pressures. The maximum pressure is reached at 13.00 (7 h after start) and amounts to 435 kN/m. The maximum pressure of the winter night is calculated to 374 kN/m and is reached 4.00 (9 h after start).

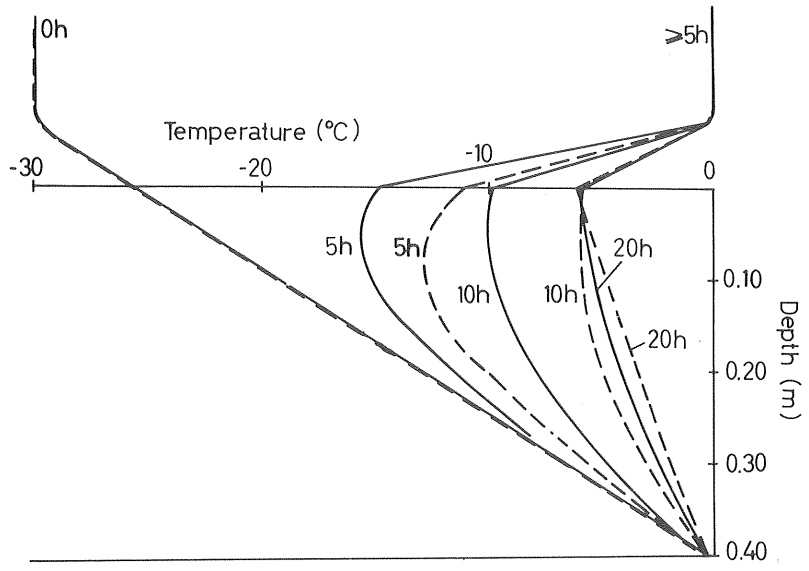

Figure 3.3a Temperature profiles in an ice cover for a case without solar radiation, continuous curves, and for a case with solar radiation, dashed curves. The same course of air temperature, air vapour pressure and wind speed.
$a = 1.15 \cdot 10^{-6}$ m^2/s.

Snow cover

In Figure 3.3b temperature profiles are shown for an ice cover covered with 0.20 m of snow. The temperature again varies along a half cosine wave from -30°C to 0°C in 5 h. The starting time of the example is 06.00 March 21 conditions as before: clear sky, wind 2 m/s and vapour pressure 80 % of saturation vapour pressure. It is well illustrated that the temperature change in the ice is much smaller than in the cases with ice covers free from snow, in spite of the fact that the coefficient of thermal diffusion of the snow is assumed rather high $0.57 \cdot 10^{-6}$ m^2/s. The total maximum pressure amounts to 142 kN/m and is not reached until 35 h after the start of increase of temperature, that is at 17.00 the next day. In reality it is very likely that the night temperature in between is a little lower, especially at the considered clear and rather calm weather.

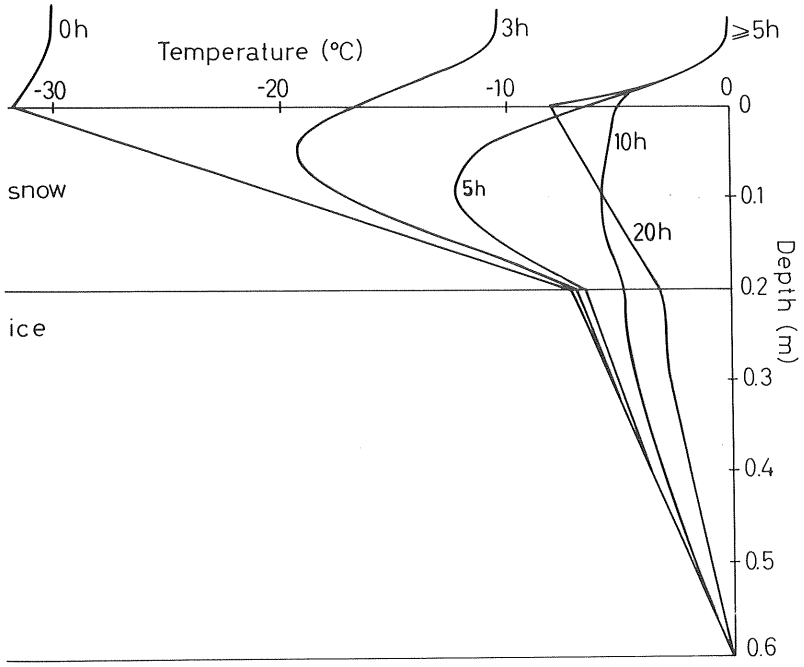

Figure 3.3b Temperature profiles in a snowcovered ice cover for a case with solar radiation. The same ambient conditions as for the dashed curves of Figure 3.3a.

Different boundary conditions

In Figure 3.4 temperature profiles for the complete case above without solar radiation, continuous curves, are compared to profiles received with a coefficient of heat transfer A, dashed curves, and with the air temperature equal to the surface temperature, dotted curves.
A = 33.3 W/m^2 according to Equation (3.25) for u = 2 m/s.

It is clearly seen how exaggerated the assumption is, that the temperature of the ice surface should be equal to the temperature of the air. The use of a heat exchange coefficient is better. Coincidentally its initial steady state profile is equal to the one of the complete case. The increase and the rate of increase is however greater. This is partly caused by the fact that the final linear profile of the complete case has an ice-surface temperature of -6°C, while it is 0°C for the other two methods. If the final air temperature is +4°C or the weather turns windy this difference will partly vanish.

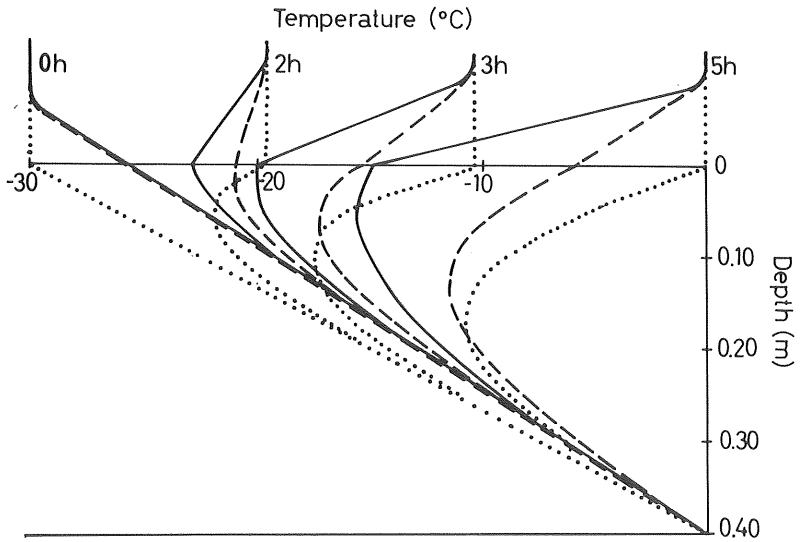

Figure 3.4 Temperature profiles in an ice cover for the complete case of Fig. 3.3, continuous line, for a case with A = 33.3 W/m^2 °C, dashed line, and for a case with air and ice surface temperature equal, dotted line.
a = 1.15 · 10^{-6} m^2/s.

Different methods of calculation

In Figure 3.5 temperature profiles are shown that are calculated in three different ways for the case with the ice surface temperature rising from $-30^{o}C$ to 0^{o} along a half cosine wave. The different methods are the Fourier series solution Equation (I-47) and (I-48) (Appendix I), continuous line, the Schmidt scheme, dash-dot line, and the expression of Drouin and Michel, dashed line.

If one compares the profiles for the same points of time, it is seen that the Schmidt scheme and the Fourier series solution give practically the same results, while Drouin and Michel´s expression lags behind. The Fourier series gives the most accurate profiles.

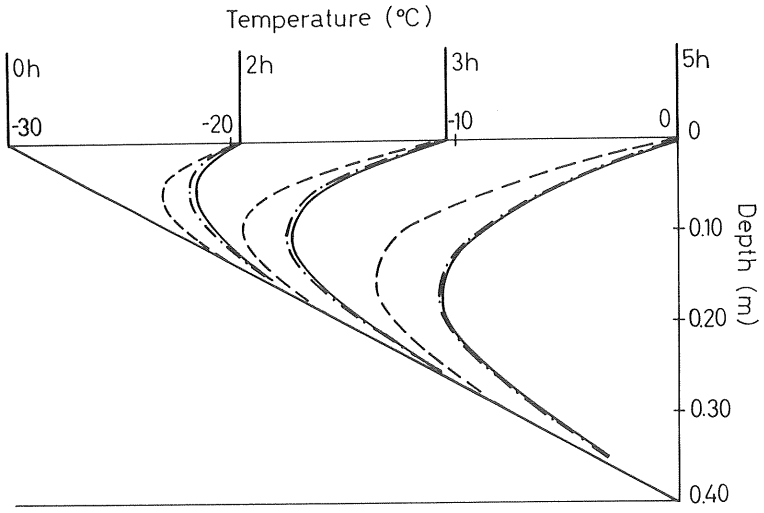

Figure 3.5 Temperature profiles calculated in three different ways for the same boundary condition, ice surface temperature equal to air temperature. Continuous line: Fourier series solution. Dash-dot line: Schmidt scheme. Dashed line: Drouin and Michel´s expression. $a = 1.15 \cdot 10^{-6}$ m^2/s.

The approximation used by Drouin and Michel is constructed by adding the solution for a periodic fluctuation in an infinitely thick ice cover (Eq. I-41) to the initial linear gradient:

$$\theta(x,t) = \theta_o(1-x/h) + A\, e^{-kx}\,(1 - \cos(\omega t - kx)) \qquad \ldots (3.45)$$

$$\theta(x,t) = \theta_o(1-x/h) \quad \text{for} \quad t < kx/\omega$$

there θ_o is the initial ice surface temperature
x the vertical distance from the ice surface
h the ice thickness
k the attenuation factor $k = (\omega/2a)^{1/2}$
ω the angular frequency
a the coefficient of thermal diffusion
A the amplitude of the surface variation

The equation is a good approximation for cyclic changes of the ice surface temperature if the ice cover thickness is greater than 0.4 m for periods up to around 24 h. For cases where the temperature rises from θ_o to $\theta_o + 2A$ along a half cosine wave and stays there (Appendix I-7), it gives far too low estimates of both the magnitude and the rate of change of temperature in the ice cover.

The total increase of temperature is given as 2A exp (-kx) while it asymptotically attains 2A (1- x/h). For cycles of 5 h, 10h and 24 h this means 9, 34 and 50 % respectively of the correct value. At the end of the 5 h shown in Figure 3.5 the temperature increase according to Equation (3.45) is 78 % of the correct value at x = 0.25 h and 51 % at x = 0.5 h.

The used expression is probably the reason why the ice pressure per unit length as calculated by Drouin and Michel is inversely proportional to the

time of increase (T/2). (See Figure 2.10). The attenuation with depth

$$\exp(-kx) = \exp(-\sqrt{\pi/aT}\cdot x) \qquad \ldots (3.46)$$

is namely relatively more pronounced for shorter periods why the underestimation is most severe for fast changes.

One of Rose's (1947) solutions has also been checked by the Fourier series solution. See Figure 2.2. The agreement is excellent. The graphical method proposed by Lindgren (1968) takes the surface thermal resistance into account, and should be preferred because of that. In Figure 3.6 below, a comparison is made with an explicit difference solution. The difference between the solutions is negligible.

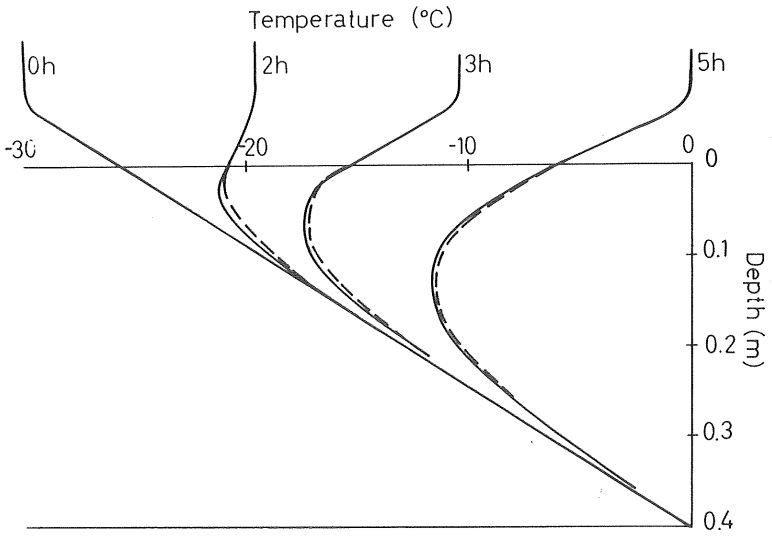

Figure 3.6 Temperature profiles calculated by the graphical method proposed by Lindgren (1968) $2a\Delta t = \Delta x^2$, continuous line, and with a numerical difference solution $6a\Delta t = \Delta x^2$, dashed line. $\Delta x \approx 0.05$ m. $A = 33.3$ W/m^2 °C. $a = 1.15 \cdot 10^{-6}$ m^2/s.

3.8 Different Values of the Coefficient of Thermal Diffusion

In Figure 3.7 temperature profiles are shown for a case calculated with the coefficient $a = 1.15 \cdot 10^{-6}$ m^2/s and with $a = 1.36 \cdot 10^{-6}$ m^2/s. The former value has been used by Bergdahl and Wernersson (1978) and the latter value by Drouin and Michel (1971). The value $1.15 \cdot 10^{-6}$ m^2/s corresponds to the diffusivity at $0^{\circ}C$ and $1.36 \cdot 10^{-6}$ m^2/s to the diffusivity at $-20^{\circ}C$. For the rather extreme case the difference of temperature change is a maximum of 16 % at x = 0.5 h at the end of the rise (5 h). The average difference over the depth is approximately only a half of the maximum. An averaged coefficient of $1.25 \cdot 10^{-6}$ m^2/s might be close to the truth. It might then be concluded that the fault amounts to around 5 % if either of the two values 1.15 or 1.36 m^2/s is used.

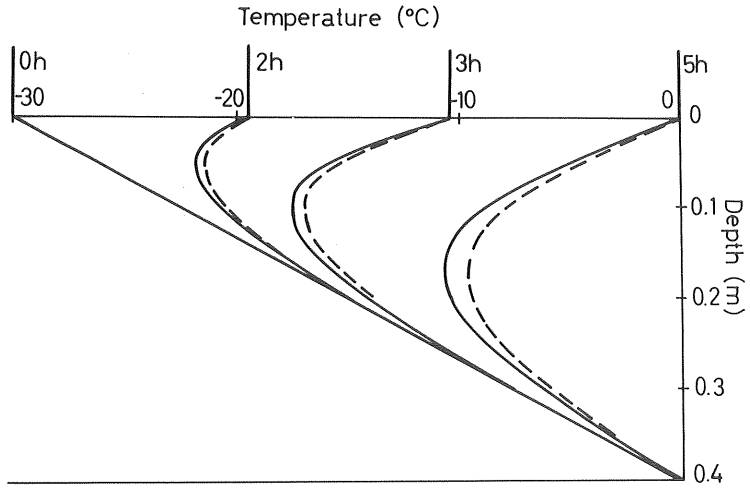

Figure 3.7 Temperature profiles for a case calculated with two different thermal diffusivities $a = 1.15 \cdot 10^{-6}$ m^2/s, continuous line, and $a = 1.36 \cdot 10^{-6}$ m^2/s, dashed line.

3.9 Comparisons with Measurements

In Appendix II comparisons are made between measured temperatures in a lake ice cover and temperatures calculated with an explicit difference method. The heat transfer coefficient was set to $A = 10.4\ (1 + 0.40\ u)\ W/(m^2\ ^oC)$ for $u < 5$ m/s, which gave reasonably good agreement.

In Appendix III comparisons are performed for profiles measured in a laboratory experiment for which it proved necessary to use $A = 14\ W/(m^2\ ^oC)$ in order to get good agreement between measurements and calculations.

3.10 Conclusions

The most important conclusions to be drawn from this chapter are as follows.

In spring solar radiation has a great influence on the rate of change of temperature even on the latitudes 60 to 70°N.

The energy balance of an ice cover is too complicated to allow the ice surface temperature to be set equal to the air temperature. Such a practice would lead to overestimates of the rate of change of temperature. One should either use some method based on the total energy balance or a method, which takes into account the surface thermal resistance.

Any correct analytical, numerical or graphical method may be used for the calculations. The calculation of the pressure does not demand great accuracy, only that the temperatures of the profiles are given for around every 5 cm.

The choice of values or functions for properties like the coefficients of thermal diffusion, conductivity, heat transfer or wind-speed function etc. is less important than the choice between different boundary conditions. If reasonable assumptions are made faults in the rate of change of temperature caused by different choices of properties may not amount to more than 10 %.

4. STRESS-STRAIN RELATIONSHIPS

It has been acknowledged by inter alii Glen and Stephens (1958), Drouin and Michel (1971), Ramseier (1971), and Jumppanen (1973) that linear visco-elastic models give an unsatisfactory description of the stress-strain relationship of ice. Some fundamentals on the deformation behaviour of ice is given by Bergdahl (1977).

4.1 The Proposed Model

Here a rather simple model is proposed,and it has been used for the calculation of design ice pressure by Bergdahl and Wernersson (1978). The model is composed of a linear spring in series with a nonlinear dashpot. See Figure 9.4.

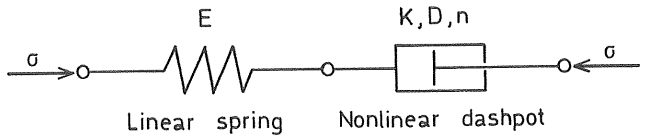

Figure 4.1 The used nonlinear rheological model. E is the elasticity modulus. K, D and n is defined by Equations (4.1) and (4.3).

The differential equation of the model is

$$\dot{\varepsilon} = \frac{1}{E}\dot{\sigma} + KD\ \sigma^n \qquad \ldots (4.1)$$

where K and n are functions of strain rate and temperature and E and D functions of temperature.

The modulus of elasticity is based on the results by Lindgren (1968) and Gold (1958) whose results are in reasonable agreement.

$$E = (1 - c\theta) \cdot 6.1 \text{ GPa} \qquad \ldots (4.2)$$

where $c = 0.012\ ^{o}C^{-1}$

The thermal activity in ice is reflected by the diffusion of whole water molecules within the solid. The diffusion coefficient D, which is used as a parameter in Equation (4.1), is written

$$D = D_o \exp(-Q_s/RT) \qquad \ldots (4.3)$$

where $D_o = (9.13 \pm 0.57) \cdot 10^{-4}\ m^2/s$

Q_s = 59.8 kJ/mol, the activation energy for self diffusion
R = 8.31 J/(mol · K), the universal gas constant
T = the absolute temperature

The values of D_o and Q_s are taken from Ramseier (1967 a, b) and seem to be very firmly based.

The basis for the values of K and n is the experiments by Drouin and Michel (1971) on ice monocrystals loaded parallel to the basal planes. The constant strain rate tests have been evaluated for the maximum stress when $\dot{\sigma} = 0$ of Equation (4.1). The result is

$$K = 4.40 \cdot 10^{-16}\ (m^{-2}\ Pa^{-n})$$

$$n = 3.651$$

for the temperature compensated creep rate range

$$2 \cdot 10^{7} < \dot{\varepsilon}/D < 8 \cdot 10^{9}\ m^{-2}$$

In the calculations the coefficients are used even below this range. For sixteen years and five Swedish lakes the upper limit was not exceeded once (Bergdahl and Wernersson, 1978).

The proposed model is rather close to the one used by Drouin and Michel (1971). This latter model can be written

$$\dot{\varepsilon} = \frac{\dot{\sigma}}{E_a} + 2b\left(n_o + \beta\left(\varepsilon - \frac{\sigma}{E_a}\right)\right)\left(\frac{\sigma}{p}\right)^{m} \qquad \ldots (4.4)$$

where b, β , n_o, m are constants, p is a function of temperature and strain rate. Obviously E_a corresponds to E, $2b(n_o + \beta(\varepsilon - \sigma/E_a))$ to K, and p to D.

The most apparent difference is that the creep rate is proportional to the viscous deformation $(\varepsilon - \sigma/E_a)$, which should be avoided in order not to make the use of the model too difficult. See further Bergdahl (1977). Another difficulty is that the apparent modulus of elasticity is given as

$$E_a = \text{const} \cdot \dot{\varepsilon}^{0.079} \exp(1335/T) \qquad \ldots (4.5)$$

which makes it impossible to calculate the pressure for cases where $\dot{\varepsilon} = 0$, which must be very common when the temperature in the upper part of the ice cover has reached the melting point temperature. Some extra condition must be added for this case.

Both models must be integrated numerically, and because of the unlinearities the result depends on the chosen time steps, but the complex model Equation (4.4) is more sensitive. Its parameters are by Michel and Drouin given for a numerical time increment of 3 minutes. The correctness of a calculation with the simpler model can easily be checked for the maximum pressure, for which $\dot{\sigma} = 0$ and $\sigma_{max} = (\dot{\varepsilon}/KD)^{1/n}$.

The advantages of using the simpler model seem great, and the experimental basis as concerns biaxial thermal pressure in an ice cover is not broad enough to justify the use of the more complicated one. Remember the basis for using the same constants for a biaxial pressure in an ice cover as for ice monocrystals in uniaxial compression. The maximum pressures were compared between uniaxial and biaxial experiments performed by Lindgren (1968) and Drouin and Michel (1971). See Paragraph 2.11. The conclusion was:

In nature it is not possible that all crystals in an ice cover have a vertical orientation. For this reason, the determination of thermal ice pressure in ordinary (not seeded) columnar ice covers for a biaxially restricted case might be based on the results of maximum pressures obtained for uniaxially restricted specimens (monocrystals) deformed perpendicular to their optical axes. For seeded ice covers or columnar ice covers with horizontal optical axes (S2) the pressure was found not to exceed the pressure in ordinary (S1) ice covers.

4.2 Pressure Calculations

The calculated temperature profile can be used to calculate the thermal ice pressure for each depth interval separately. The pressures are then integrated over the depth of the ice which gives the total ice pressure (N/m).

The rate of deformation is the coefficient of linear thermal expansion times the rate of change of temperature

$$\varepsilon = \frac{d\varepsilon}{dt} = \alpha \frac{d\theta}{dt} = \alpha \theta \qquad \ldots (4.6)$$

which with Equation (4.1) gives

$$\alpha \, d\theta = d\varepsilon = (d\sigma/dt \, E + KD\sigma^{n}) \, dt \qquad \ldots (4.7)$$

This is written on difference form as

$$\sigma_{k+1} = \sigma_k + E_m \left\{ \Delta\varepsilon - (D_k K \sigma_k^{n} + D_{k+1} \sigma_{k+1}^{n}) \frac{\Delta t}{2} \right\} \qquad \ldots (4.8)$$

where σ_k is the stress at the point of time $t = k\Delta t$

σ_{k+1} is the stress at $t+\Delta t = (k+1)\,\Delta t$

$\sigma_{k+1} - \sigma_k = \Delta\sigma$

E_m elasticity of the ice for $\theta = (\theta(t) + \theta(t+\Delta t))/2$

D_k is the self diffusion for $\theta(t)$

D_{k+1} -"- $\theta(t+\Delta t)$

The equation is of the n:th degree of the unknown σ_{k+1}, and because of this unlinearity, a special iterative procedure is used to solve it. The procedure is described by Bergdahl and Wernersson (1978). The coefficient of thermal expansion is set to $\alpha = 4.83 \cdot 10^{-5}\ ^{o}C^{-1}$ in the calculations.

The stresses are integrated over the depth of the ice cover, and if the integrated ice pressure is greater than an elastic buckling load, the thermal ice pressure is set to that lower value. The limiting load is set to

$$P_b = 2\sqrt{\rho_w g E h^3/12\,(1-\nu^2)} \qquad \ldots (4.9)$$

where

ρ_w is the density of water
g the earth acceleration
E the elastic modulus of of ice at the mean depth of the ice cover, Eq. (4.2)
h the thickness of the cover
$\nu = 0$ Poisson´s modulus

Equation (4.9) may be criticized because it does not take into account the excentric loading (Assur, 1959),and the buckling should be calculated as viscous or plastic (Löfquist, 1954).

For the extreme cases calculated by Bergdahl and Wernersson (1978) the ice covers were too strong to buckle according to Equation (4.9). Note, however, that there always are zones of weakness in an ice cover, or that pressure ridges can develop along cracks where the equation is not valid.

4.3 Comparisons between Some Models

Below comparisons are made between some models described in Chapter 2 and the proposed model. The comparisons are made for

a) deformation at constant load
b) stress at constant strain rate
c) stress at constant rate of change of temperature

Deformation as a function of time

In Figures 4.2a and b the deformation as a function of time for constant load is drawn for Royen´s (1922), Assur´s (1959), Lindgren´s (1968), and Jumppanen´s (1973) models and for Equation (4.1). The constant stresses are 1.0 and 2.0 MPa respectively. It is seen that for $\sigma = 1$ MPa Royen´s and Jumppanen´s models give much greater deformation than Assur´s and Lindgren´s models, while Eq. (4.1) describes a much stiffer behaviour.

For $\sigma = 2$ MPa the picture is quite different with the yield according to Equation (4.1) a little greater than according to Lindgren. Assur´s model is now the stiffest while Royen´s and Jumppanen´s still show

the greatest yield. The stiff or order is caused by the fact that the creep element in Equation (4.1) is proportional to σ^4, in Lindgren´s model to σ^2 and in Assur´s to σ.

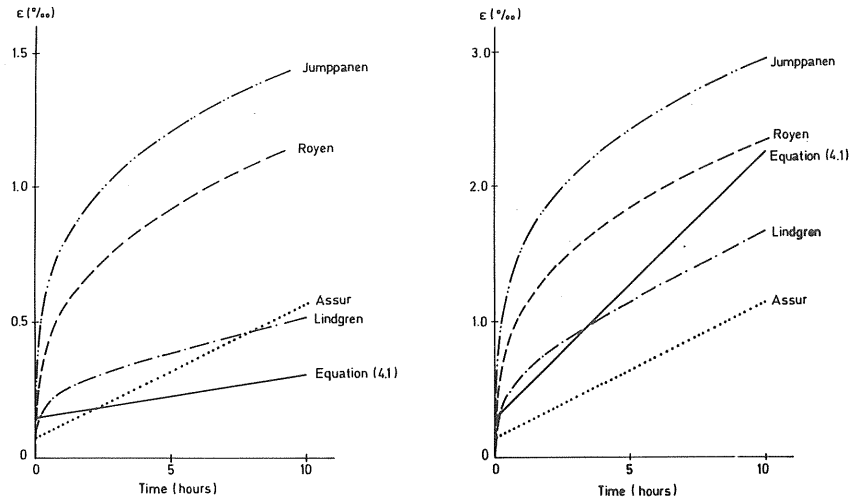

Figure 4.2 Deformation as a function of time for the constant stresses
a) σ = 1 MPa and b) 2 MPa.
Ice temperature - 10°C and two-axial deformation.

Stress for Constant Strain Rate

In Figure 4.3 the stress as a function of time for the constant strain rate $1.45 \cdot 10^{-8}$ s^{-1} is drawn for the temperatures -10°C and -20°C. Only the proposed model and Drouin and Michel´s model are compared in this figure. It is seen that Drouin and Michel´s model has a much smaller slope at the origin which depends on the low modulus of elasticity used by them. See further below. The same magnitude of pressure is, however, reached after 20 hours of deformation.

Another interesting property is that Drouin and Michel´s model gives a decreasing pressure after the maximum is reached. The proposed model reaches rather fast a constant pressure which is

maintained indefinitely long. So does the model proposed by Assur (1959), while Lindgren's model gives a slowly increasing pressure with time, because the viscosity modulus increases with $t^{0.25}$.

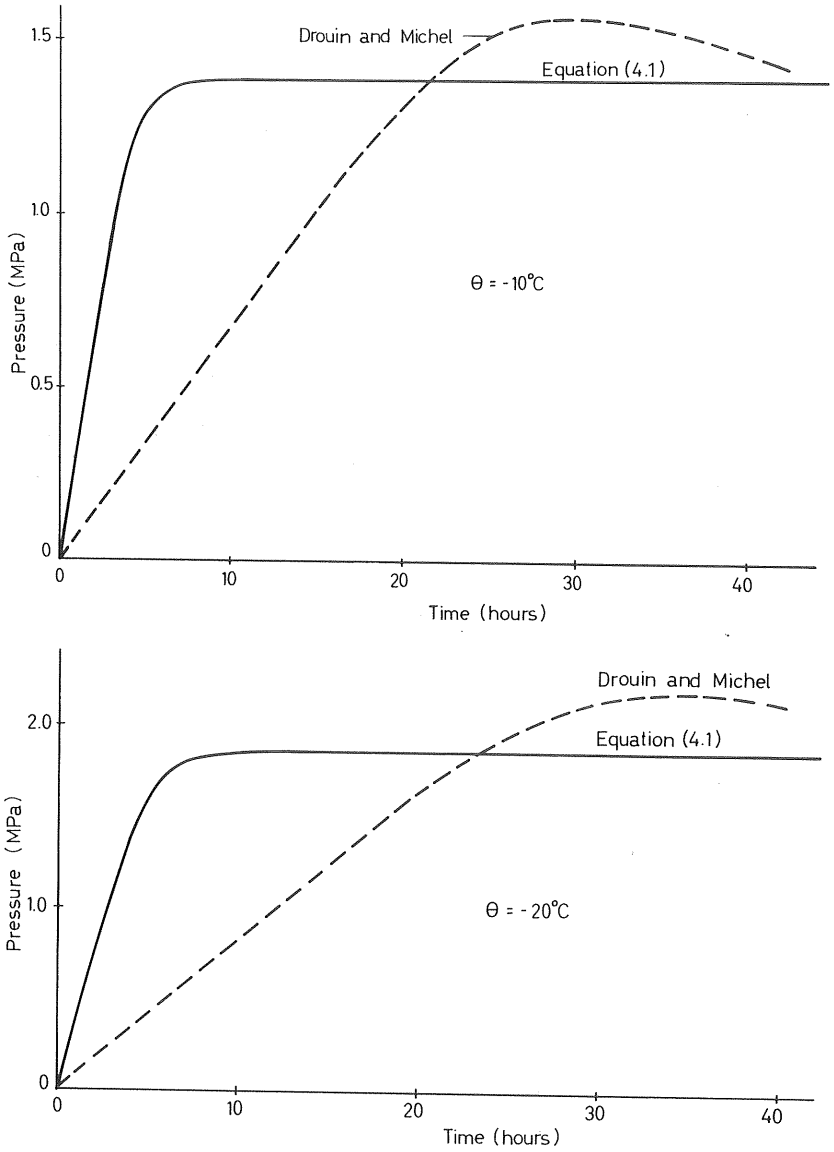

Figure 4.3 Stress as a function of time for constant rate of strain $\dot{\varepsilon} = 1.45 \cdot 10^{-8}\ s^{-1}$.
a) at $-10^{o}C$, b) at $-20^{o}C$.

Stress for Constant Rate of Change of Temperature.

In Figure 4.4 the stress in an ice plate subjected to different constant rates of increase of temperature is shown as a function of time according to Monfore´s, Drouin and Michel´s, and Lindgren´s models, and according to Equation (4.1). The ice plate is completely restricted in its plane and the rates of change of temperature are 1, 2 and 2.5 ^{o}C/h in Figures a, b and c respectively. The initial temperatures are chosen so as to get the final temperature 0^{o}C.

The most apparent feature is that Monfore´s original method gives much smaller pressures than Lindgren´s or the proposed model. This depends primarily on the fact that his method is based on uniaxial pressure. If Poisson´s modulus is assumed to be 0.36 his method would give the shown "corrected" curves.

Also here, it is evident that Drouin and Michel´s model gives quite another slope at the origin. This is again caused by the fact that they use an apparent modulus of elasticity that is nearly one order of magnitude smaller than what is ordinarily expected for ice. For -10^{o}C it is given to 1.5 GPa, while for example Equation (4.2) gives 6.8 GPa. The pressures in the experiments of Appendix III cannot be explained if the lower value is used.

It should also be pointed out that Monfore´s and Drouin´s curves end after a certain time. Monfore´s curve ends because he did not sketch it longer than 1.25 times the time from the start to maximum stress. Drouin´s curve ends, because Equation (4.5) gives E_a=0 when the temperature has become constant 0^{o}C. Lindgren´s model or the proposed model have no such limitation.

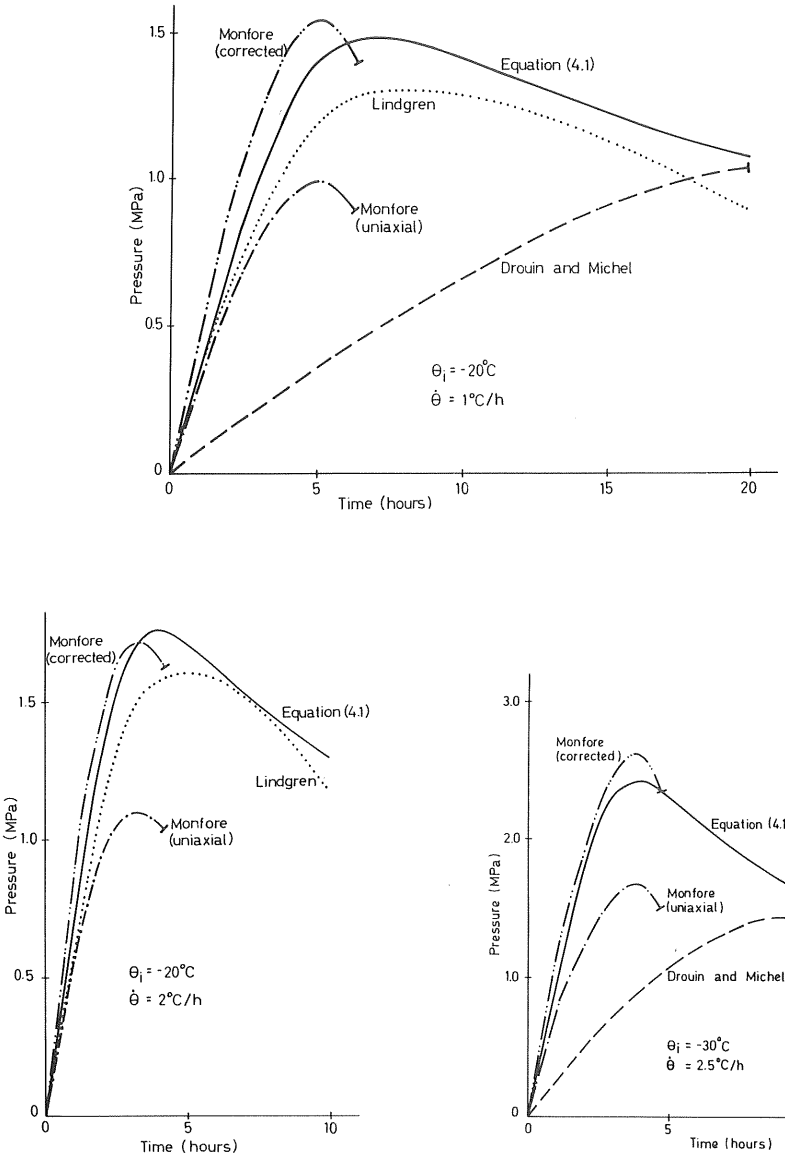

Figure 4.4 Stress as a function of time for constant rates of change of temperature θ. Final temperature $0^{o}C$.

a) $\dot{\theta} = 1^{o}C/h$. Initial temperature $\theta_i = -10^{o}C$

b) $\dot{\theta} = 2^{o}C/h$. $\theta_i = -20^{o}C$

c) $\dot{\theta} = 2.5^{o}C/h$. $\theta_i = -30^{o}C$

4.4 Comparisons with Experiments

In Appendix III the stresses from two biaxial experiments conducted by the author are compared to stresses calculated with Equation (4.8). Here comparisons are made for two arbitrary experiments from Drouin and Michel (1971) and for two of Lindgren´s experiments (1968).

The author´s own experiments give the same order of magnitude as the proposed model Equation (4.1). See Figures III-11 and 12. The experiments are, however, not of very good quality.

The fit to the first shown experiment Figure 4.5a by Drouin and Michel is very good until the ice plate fails to sustain the load from the confining ring. If the corresponding deformation was forced on an intact plate the stress must amount to 1.7 MPa. In Figure 4.5b the calculated curve gives a higher stress level right through the experiment. The slope at the origin is still in good agreement why at least the elasticity of the ice is accurately given.

The experiment shown in Figure 4.6a performed by Lindgren gives a nearly perfect agreement with the calculated pressure, while again the theory gives too high stress level in the experiment shown in Figure 4.6b.

The proposed model Equation (4.1) seems to give an upper bound for the thermal pressure reached in the plate experiments. In a thick ice cover such high pressure levels could be reached more often, but in in a vast ice cover there ought to be other factors that limit the pressures.

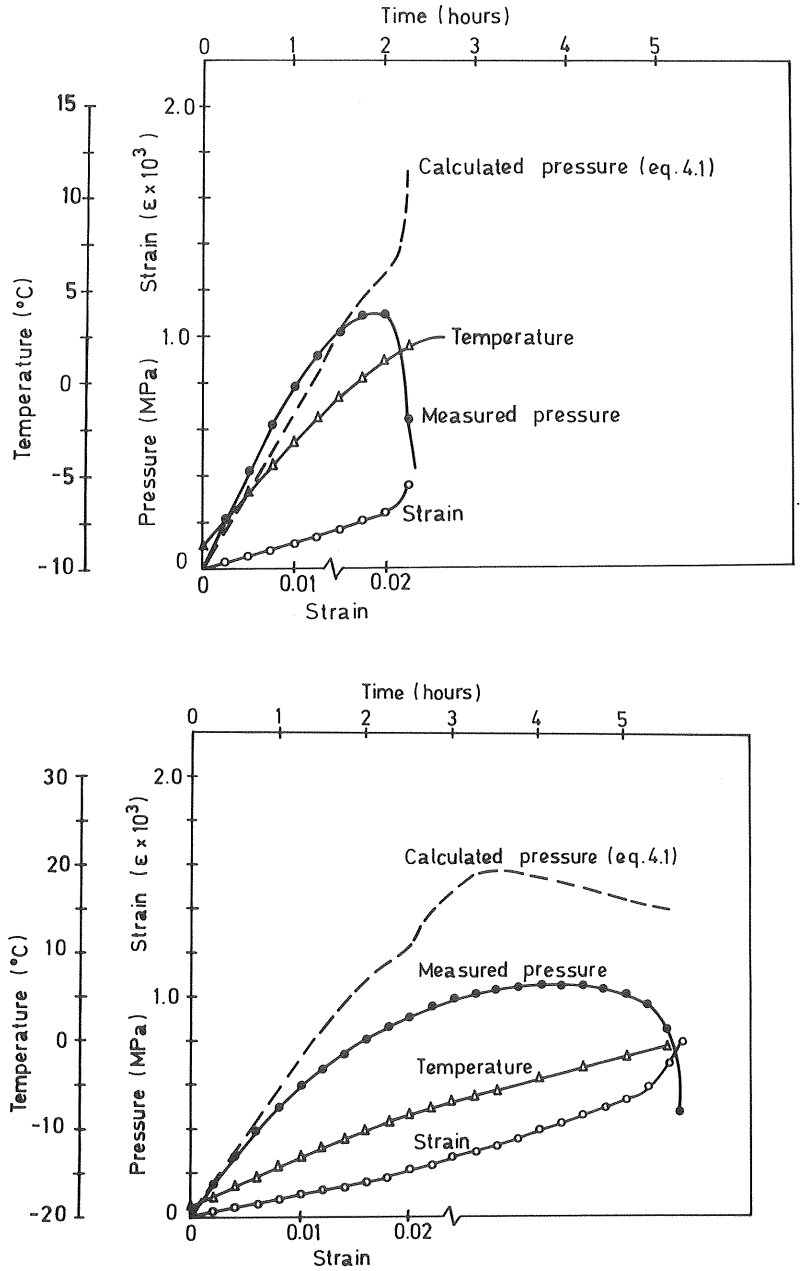

Figure 4.5 Comparison between measured ice pressure and ice pressure calculated on basis of Equation (4.1) and shown deformations. Experimental curves from Drouin and Michel (1971).

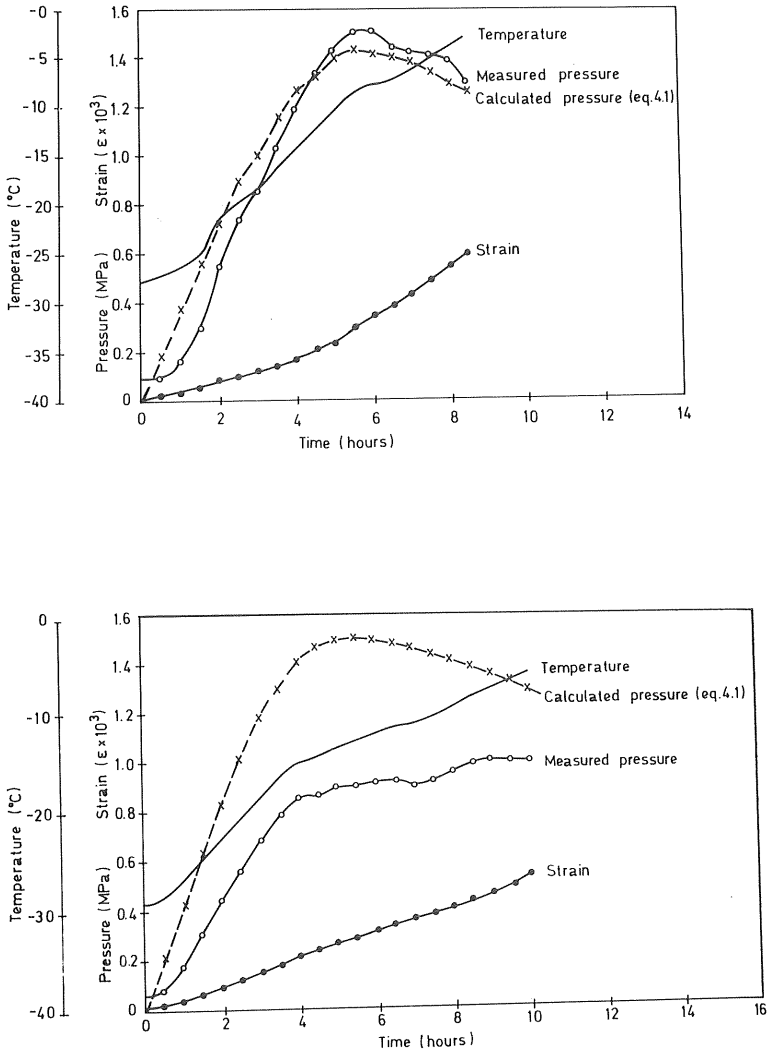

Figure 4.6 Comparison between measured ice pressure and ice pressure calculated on basis of Equation (4.1) and shown deformations. Experimental curves from Lindgren (1968).

4.5 Conclusion

The proposed rheological model is capable of reproducing the course of stress for a given course of deformation or temperature, until accelerated or tertiary creep starts. The model is also rather simple to integrate although it is unlinear, if the approximate expression Equation (4.8) is used. The resulting accuracy matches the quality of the values on deformation moduli, and thermal properties.

5. CALCULATION OF ICE PRESSURE

5.1 Simplifying Assumptions

Below some examples will be given on thermal ice pressure, but first some simplifying assumptions will be pointed out.

When the ice cover is contracted because of low air temperatures it is supposed to crack up till it becomes free from tension. The cracks are assumed to be completely filled with water that freezes to ice before the temperature rises again in the ice cover. The assumptions are conservative, because a great many cracks will be dry and do not extend to the underside of the ice cover. There may also be some tension left in the ice cover. On the other hand, the water that freezes in the slots can cause pressure that could partly compensate for the tension and dry surface cracks.

When the ice cover expands it is supposed that there is complete restriction from the shores. This is true only for steep shores. Often the ice is seen to shove up on beaches or gently sloping rubble shores. The pressure may also not be able to rise to its maximum because of buckling or local defects in the ice cover. In the used program elastic buckling is considered. This is much too conservative but is supposed not to interfere with values on the greatest pressures at ice thicknesses from a half to one meter. Leads and old cracks are not considered at all.

The named simplifications are used in most methods for calculating ice pressures. The proposed method includes, however, a complete energy balance and takes insulation by snow into account. The rheological model and temperature calculations are combined into one numerical model that calculates continuous records of ice temperature and pressure, if ice and snow thickness and weather information are fed into it.

5.2 Stress Profiles for Three Cases

In Figure 5.1a and b calculated stress profiles are shown for the same cases whose temperature profiles are illustrated in Figure 3.3a. For

both cases the air temperature rises from -30°C to 0°C along a half cosine curve during 5 hours, the wind speed is 2 m/s,and the air vapour pressure is 80 % of the saturation vapour pressure. In case 5.1a, a midwinter evening there is no solar radiation, but case 5.1b starts at 06.00 March 21,a clear day. It is seen how the pressure profiles penetrates faster in the ice cover subjected to solar radiation. The maximum pressure in the ice cover subjected to solar radiation is reached 7h after the start of rise of temperature and it is 435 kN/m while the corresponding figures for the other case are 9h and 374 kN/m. The pressure is 16 % greater for the spring day than for the winter night.

In Figure 5.2 stress profiles are shown for the spring day in an ice cover covered by 0.20 m of snow. The pressure that in this case only amounts to 142 kN/m reaches its maximum 35 hours after start. The stresses are only one third of the stresses in the corresponding uncovered ice cover.

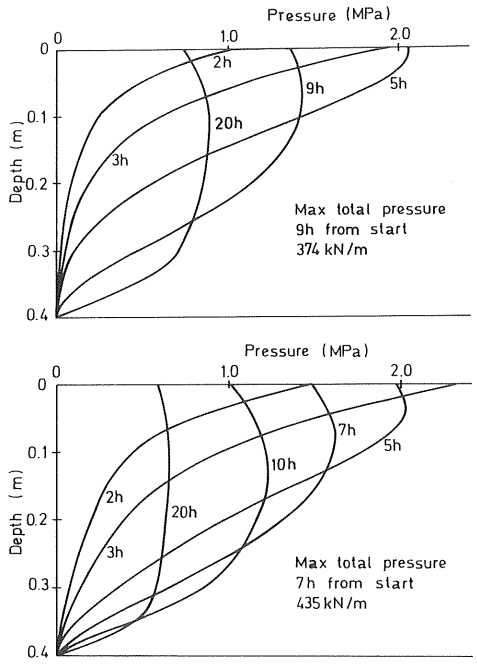

Figure 5.1 Stress profiles for ice covers subjected to the temperature changes shown in Figure 3.3. Figure a) is for an ice cover not subjected to solar radiation and Figure b) for one subjected to solar radiation.

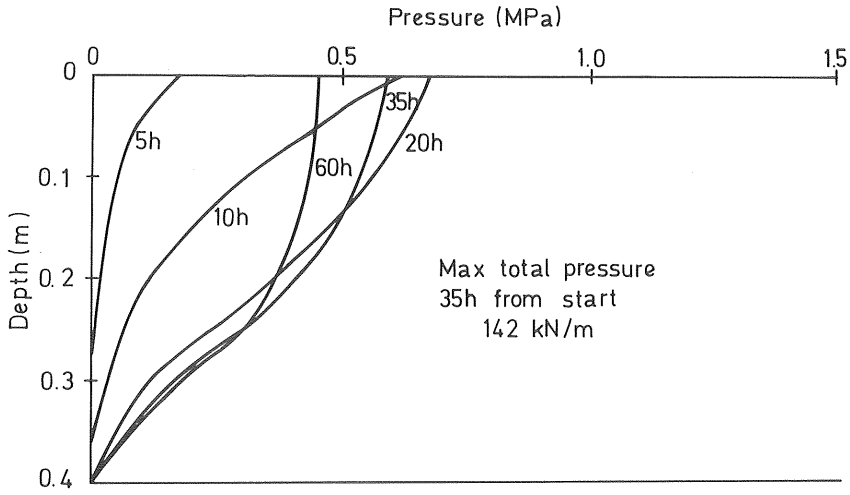

Figure 5.2 Stress profiles in a snow covered ice cover subjected to the same ambient conditions as the ice cover of Figure 5.1b. Its temperature profiles are shown in Figure 3.3b.

5.3 Maximum Pressure, Comparison between Methods

In his paper "State of research on ice thermal thrust" Drouin (1970) makes a comparison between some methods of calculating thermal ice pressure for two hypothetical cases: one with the ice cover thickness 0.45 m, and the other with the thickness 0.90 m, both subjected to the same ambient conditions:

The initial air temperature is set to -40°C and is made to rise 2.8°C/h to 0°C. No solar energy is absorbed.

Drouin calculates the pressure with Rose´s theory, Monfore´s experimental result and the USSR norm SN 76-59. Kjeldgaard (1977) went on calculating the pressures according to Drouin and Michel´s (1971) results for S1 and snow ice, and according to the latest USSR norm SN 76-66.

The author has extended the calculations with pressure figures according to the method proposed in this work.

It should be noticed that all calculations are performed for a linear rise of temperature, while Drouin and Michel´s original graphs are given for a sinusoidal rise. For Rose´s, Monfore´s and Drouin and Michel´s methods the surface temperature is supposed to be equal to the air temperature. The temperatures in both Monfore´s and Drouin and Michel´s method are calculated according to Drouin´s method. The norm SN 76-59 is calculated according to Paragraph 2.2, while the norm SN 76-66 incorporates some wind-speed function for the thermal transfer. The proposed method is calculated with the complete energy balance assuming clear sky, no solar radiation, and vapour pressure 80 % of the saturation vapour pressure of the air.

In Table 5.1 below the results are listed. Notice that Rose´s, Monfore´s, and Drouin and Michel´s values are founded on uniaxial cases. The values for S1 ice (monocrystals) are recommended for biaxially restricted ordinary ice. The USSR norms and the proposed method are supposed to be valid for biaxially restricted ice covers.

Table 5.1 Ice pressures for ice covers of two thicknesses for the hypothetical conditions stated in the text. A comparison between different methods.

		Values of thermal pressure kN/m	
Ice thickness		0.45 m	0.90 m
Method	Origin		
Rose (1947)	Drouin (1970)	47	86
Monfore (1954)	-"-	222	232
SN 76-59 (1959)	-"-	128	255
Drouin and Michel (1971):			
S1 ice	Kjeldgaard (1977)	330	390
Snow ice	-"-	220	270
SN 76-66 0 m/s	-"-	30	60
-"- 5 "	-"-	310	440
-"- 20 "	-"-	410	580
Proposed method:			
0 m/s		459	752
5 m/s		502	830
20 m/s		531	829

It is immediately noted that the method proposed in this work gives much higher pressures than the others. At no wind and 0.45 m ice cover it gives 40 % greater pressure than Drouin and Michel´s method. If a correct method were to be used for calculating the temperature in Drouin and Michel´s case, their pressure would probably be a little higher. For the thicker ice cover this is still more pronounced.

For their cases the total pressure is only 20 % greater in the thicker ice cover, while the difference is 65 % according to the proposed method. The Soviet norms give 100 % difference. Monfore´s method as used by Drouin also show very little difference. Probably the difference would be greater if correct temperatures were used.

Concerning the dependence on wind speed, it can be noted that the Soviet norm SN-76-66 gives a very great difference between no wind and a rather moderate wind of 5 m/s. This is not the case with the proposed method, although the calculated total pressures are greater. The cases are calculated for constant wind speed during the whole course of temperature change. The rate of change of temperature in the ice would be greater if the wind speed increased during the temperature rise, as this would increase the change of energy flux. In the tables of Appendix IV it is seen that combinations of air temperature rise, wind increase, and increase of cloudiness have produced the most severe conditions for thermal ice pressure during the 12 or 16 years considered for five lakes in Sweden.

5.4 Conclusion

It is believed that the proposed method gives reasonable estimates of maximum possible thermal ice pressures for a certain case. It gives a correct description of the rate of change of temperature for given ambient conditions, without either grossly understating or overstating the rate of change. On the other hand, it produces pressures that cannot be reached in every ice cover because of crystal orientation and irregularities in the ice cover. In Chapter 4 it was shown that for some small ice plates such high pressures are reached. It might be reasonable to reduce the values of the highest pressures, because in vast ice covers the conditions may be less favourable for high pressures.

6. DESIGN THERMAL PRESSURE

The occurrence of thermal ice pressure in a lake depends on ice and snow properties, ice and snow cover thickness, and weather fluctuations. The level of maximum pressure depends on some special combination of ice cover configuration and change of weather.

A rational way of calculating the recurrence of extreme pressures ought then to be to calculate time series of possible ice pressure for combinations of recorded ice cover characteristics and weather observations. This has been done by Bergdahl and Wernersson (1978) for five Swedish lakes between 68.3°N and 57.1°N.

From the calculated time series of maximum pressures annual-maximum series and peaks over a threshold series were formed for the lakes. Different distributions were fitted to the series, and reasonable estimates of the expected pressures with the return periods 100, 500 and 1000 years were finally found as given in Table 6.1 below for the five lakes.

In Appendix IV the weather conditions, and ice and snow thicknesses are given for the calculated highest maximum pressure for each lake during the treated 12 or 16 years. From north to south these pressures were 437, 357, 236, 161 and 189 kN/m. For further information see Bergdahl and Wernersson (1978).

Table 6.1 Expected thermal ice pressures in kN/m for some return periods of annual maxima.

		Return Period (years)		
Lake	Position	100	500	1000
Torne träsk	68.3°N 19.5°E	507	550	569
Stora Bygdeträsket	64.3°N 20.5°E	453	532	568
Runn	60.6°N 15.6°E	410	475	500
Glan	58.6°N 16.0°E	419	507	543
Vidöstern	57.1°N 14.0°E	330	380	400

APPENDIX I

ANALYTICAL SOLUTIONS OF TEMPERATURE PROFILES IN AN ICE COVER.

CONTENTS OF APPENDIX I

I-1 The Equation of Thermal Diffusion

The mathematics of the conduction of heat in solids has long been studied by mathematicians, and therefore a great many tools exist for the solution of thermal diffusion problems. This appendix will not give anything like a complete review of these tools, but some analytical solutions will be given that are relevant to the conduction of heat in an ice cover. For basic mathematics it is referred to Hildebrand: Advanced Calculus for Applications (1962) and for specialized solutions to Carslaw and Jaeger: Conduction of Heat in Solids (1959).

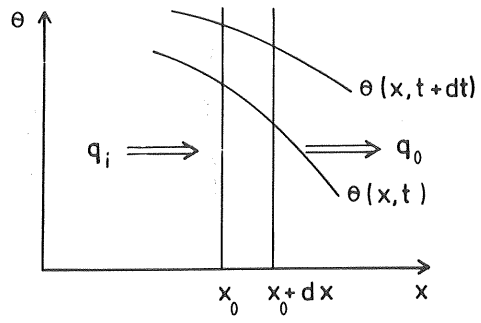

Figure I-1. Thermal diffusion through a thin layer dx of a solid, whose temperature distribution is changing from θ(x,t) to θ(x,t+dt) during the time interval dt because of the difference in incoming and outgoing energy flux $q_i - q_o$.

Considering the heat budget of a thin layer of a solid, shown in Figure I-1, the equation of thermal diffusion can be established. The heat flux into the layer at x is

$$q_i = - \lambda \frac{\partial \theta}{\partial x} \qquad \ldots (I\text{-}1)$$

where λ is the thermal conductivity and θ the temperature.

The flux out of the layer at x+dx is

$$q_o = - \lambda \frac{\partial}{\partial x} \left(\theta + \frac{\partial \theta}{\partial x} dx \right) \qquad \ldots (I\text{-}2)$$

provided the thermal conductivity is constant.

The difference in incoming and outgoing heat flux gives rise to an increase of temperature in the layer per unit time, and thus

$$C_p \rho \, \partial\theta/\partial t = q_i - q_o = \lambda \frac{\partial^2 \theta}{\partial x^2} \qquad \ldots (I-3)$$

where C_p is the specific heat capacity and ρ the density.

If heat is produced within the layer for example by the absorption of radiation a productive term must be added to the right hand side of Equation (I-3), and the equation that appears is

$$\partial\theta/\partial t = a \, \partial^2\theta/\partial x^2 + p(x) \qquad \ldots (I-4)$$

where $a = \lambda/C_p\rho$ is the thermal diffusivity
and $p(x)$ produced energy per unit volume and unit time divided by $C_p\rho$.

If the density, thermal conductivity and specific heat capacity cannot be considered constant, Equation (I-3) must be written

$$C_p \rho \partial\theta/\partial t = \partial/\partial x \, (\lambda \partial\theta/\partial x) \qquad \ldots (I-5)$$

I-2 Boundary and Initial Conditions

Interface Ice-Water

At an interface between ice and water, for example at the lower boundary of an ice cover, it can be stated that the temperature should remain at the freezing point of water throughout the course of temperature change. If h is the ice thichness, and x denotes the vertical coordinate and is defined positive downwards with its origin in the upper surface of the ice cover, the condition can be written

$$\begin{cases} \theta = 0^{\circ}C \\ x = h \end{cases} \qquad \ldots (I-6)$$

The heat flux at the boundary is thus only bounded by the temperature gradient which is permissible as the thermal resistance at the interface is small.

The heat flow to the interface must be compensated by a heat flow down through the underlying water or by melting at the boundary

$$\begin{cases} -\lambda(\partial\theta/\partial x)^{-} + L\,\rho\,dh/dt = -\lambda_W\,(\partial\theta/\partial x)^{+} \\ x = h \end{cases} \qquad \ldots (I\text{-}7)$$

where +/- is just below/above the interface

λ the thermal conductivity of ice

λ_W the thermal conductivity of water

θ the temperature

L the latent heat of fusion

ρ the density of the ice

h the thichness of the ice cover

x vertical coordinate

t time

The interface will thus move vertically at the rate dh/dt.

$$dh/dt = \left[\lambda(\partial\theta/\partial x)^{-} - \lambda_W(\partial\theta/\partial x)^{+}\right]/L\,\rho \qquad \ldots (I\text{-}8)$$

Mostly this growth of the ice cover will be disregarded below, as it is unimportant when deciding the fast temperature fluctuations, see paragraph I-3 below.

Interface Ice - Air

At the interface between ice or snow and air, that is, at the upper boundary, conditions are a little more complicated. The heat rate through the boundary is a result of several processes, namely: convection by wind, sun and sky radiation, black body back radiation, and sublimation.

If we only consider convection a simple boundary condition can be formed

$$\begin{cases} -\lambda(\partial\theta/\partial x)^{+} = -A\,(\theta-\theta_a) \\ x = 0 \end{cases} \qquad \ldots (I\text{-}9)$$

Here A is the transfer coefficient of heat. It can be considered to be a function of windspeed, or windspeed and air stability. θ_a is the temperature of the air.

Analytical solutions of the equation of thermal diffusion Eq. I-4 with the boundary conditions (I-6) and (I-9) are given by Carslaw and Jaeger (1959) in the form of Fourier series and hereditary integrals which must be evaluated numerically. For a complete case with varying air temperature and solar radiation it is therefore more convenient to solve the equation directly by means of difference methods. For speical cases, however, analytical solutions can offer good illustrations of the course of temperature and probably may give a better understanding of the involved processes.

In most illustrations below the hypothetical boundary condition of a prescribed surface temperature is used. That is

$$\begin{cases} \theta = \theta\ (t) \\ x = 0 \end{cases} \qquad \ldots\ (I\text{-}10)$$

Initial Conditions

It is important to state the initial conditions for the solutions of the equation of thermal diffusion. That is, the temperature preceding a fast rise in air temperature must be clearly stated and the found solution, $\theta(x,t)$, has to satisfy the conditions, $\theta(x,0)$. Otherwise the calculated pressures can be misleading.

It is usually assumed that the greatest thermal ice pressures arise when the air temperature increases suddenly after a long cold period. At the beginning of the increase of air temperature the distribution of the temperature in the ice can then be considered stationary, with the equilibrium temperature at the upper surface and zero temperature at the lower interface. In the next paragraph it is shown that the distribution can be considered linear as well.

I-3 Initial Temperature Distributions

Steady State Solutions

As an initial condition for the analytical solutions of the different cases in the following paragraphs, a linear temperature distribution will be used. Such a condition is, however, only an approximation of the true steady state condition because partly the conductivity is a function of temperature and partly the ice cover grows in thickness. The magnitudes of these approximations are estimated below.

Steady state and constant conductivity give the problem, (Equations (I-3), (I-6) and (I-10))

$$\begin{cases} \partial\theta/\partial t = a\ \partial^2\theta/\partial x^2 = 0 \\ \theta\ (0,t) = \theta_s \\ \theta\ (h,t) = 0 \end{cases} \qquad \ldots\ (I\text{-}11)$$

which by integrating twice gives the idealized solution:

$$\theta\ (x,t) = \theta_s\ \ (1 - x/h) \qquad \ldots\ (I\text{-}12)$$

If the variation of the conductivity with temperature is considered, Equation (I-5) has to be used. Letting $\lambda(\theta) = \lambda_o(1+\alpha\theta)$ will give the problem

$$\begin{cases} C_p\rho\ \partial\theta/\partial t = \partial/\partial x(\lambda_o(1+\alpha\theta)\partial\theta/\partial x) = 0 \\ \theta\ (0,t)=\theta_s \\ \theta\ (h,t)= 0^oC \end{cases} \qquad \ldots\ (I\text{-}13)$$

which also by integration gives the solution

$$\theta(2+\alpha\theta) = \theta_s\ (2+\alpha\theta_s)(1-x/h) \qquad \ldots\ (I\text{-}14)$$

The thermal conductivity of ice increases linearly with decreasing temperature and the constant can be approximated by $\alpha = -4.8\cdot10^{-3}/^oC$. This means that the thermal gradient $\partial\theta/\partial x$ close to the cold upper surface of the ice is smaller than at the ice-water interface, and consequently the mean temperature of the ice is a little lower than

that given by a linear gradient, Eg. (I-12). A comparison at half the depth, x/h = 1/2, at the extreme surface temperature $\theta_s = -30^oC$, gives

Eq. (12) $\theta\ (x = h/2) = -15.0^oC$
Eq. (14) $\theta\ (x = h/2) = -15.5^oC$

The difference is thus only 3% and the mean difference over the depth is approximately 2%. This difference is without any practical importance.

The Growth of an Ice Cover

The growth or melting of the ice cover at the ice-water interface also distorts the linear temperature profile, although when growing this causes the ice temperature to be higher than is given by the linear profile.

The problem can be formulated by the following set of equations; if the initial conditions are, a very thin layer of ice and a water temperature 0^oC throughout.

Initial condition:

$$\begin{cases} h = 0 \\ t = 0 \end{cases} \qquad \ldots (I-15\ a)$$

Diffusion in the ice: Eq. (I-4)

$$\partial\theta/\partial t = a\ \partial^2\theta/\partial x^2 \qquad \ldots (b)$$

Boundary conditions: Eq. (I-6) and (I-10)

air-ice $\theta(0,t) = \theta_s$ ... (c)
ice-water $\theta(h,t) = \theta_i = 0^oC$ ... (d)

Growth condition Eq. (I-7)

$$\begin{cases} L\rho\ dh/dt = \lambda(\partial\theta/\partial x) \\ x = h^- \end{cases} \qquad \ldots (e)$$

As the temperature in the water is assumed to be $0^{o}C$ the temperature gradient and heat flux in the water are also identically zero.

Solutions for this set of equations are presented by Carslaw and Jaeger (1959) and have been used by Janson (1963) to calculate frost depth in soils. The solutions are expressed with the aid of the error function.

$$\text{erf}\ (x) = \frac{2}{\sqrt{\pi}} \int_{o}^{x} e^{-\zeta^2}\, d\zeta \qquad \ldots \text{(I-16)}$$

This integral is tabulated in Abramowitz and Stegun (1972), and it is of fundamental interest for the solution of diffusion problems.

Two key values are erf (0) = 0 and erf (∞) = 1, and an important property is that

$$\text{erf}\ (-x) = -\text{erf}\ (x) \qquad \ldots \text{(I-17)}$$

Sometimes it is also convenient to use the notation

$$\text{erfc}\ (x) = 1 - \text{erf}\ (x) \qquad \ldots \text{(I-18)}$$

A particular solution of Eq. (I-15 b) can now be written

$$\theta = A + B\ \text{erf}\ (x/\sqrt{4at}) \qquad \ldots \text{(I-19)}$$

The boundary condition (I-15 c) gives $A = \theta_s$ and thus the interface condition (I-15 d) yields

$$\theta_i = \theta_s + B\ \text{erf}\ (h/\sqrt{4at}) \qquad \ldots \text{(I-20)}$$

Since B, θ_s and θ_i are constants, also erf $(h/\sqrt{4at})$ must be a constant if Eq. (I-20) should be valid, that is

$$h = m\, t^{1/2} \qquad \ldots \text{(I-21)}$$

where m is a proportionality factor.

The value of B can be solved out of Eq. (I-20) as a function of m.

$$B = \frac{\theta_i - \theta_s}{\text{erf } (m/\sqrt{4\ a})} \qquad \ldots \text{(I-22)}$$

Finally, for $\theta_i = 0^oC$ the temperature distribution in the ice is given by the equation

$$\theta = \theta_s \left\{ 1 - \text{erf } (x/\sqrt{4at})/\text{erf } (m/\sqrt{4a}) \right\} \qquad \ldots \text{(I-23)}$$

The factor m must be solved from the remaining condition (I-15), with (I-21) and (I-23) substituted. From (I-21)

$$dh/dt = 1/2\ m\ t^{-1/2} \qquad \ldots \text{(I-24)}$$

and from (I-23)

$$(\partial\theta/\partial x)_{x=h} = -2\theta_s/\sqrt{\pi\ 4at} \cdot \exp\ (-h^2/4at)/\text{erf}(m/\sqrt{4a}) \qquad \ldots \text{(I-25)}$$

The substitution in (I-15) gives

$$L\rho\ m\sqrt{\pi\ a}\ \ \text{erf}\ (m/\sqrt{4a}) = -2\lambda\theta_s\ \ \exp\ (-m^2/4a) \qquad \ldots \text{(I-26)}$$

which can be written

$$\mu \cdot e^{\mu^2}\ \text{erf}\ \mu = -\ C_p\theta_s/L\sqrt{\pi} \qquad \ldots \text{(I-27)}$$

where μ stands for $m/\sqrt{4a}$.

It is seen by the equation that m is a function of the surface temperature θ_s and material properties only. Solving for the following values on these properties μ was found to be 0.297 and $m = 6.37 \cdot 10^{-4}\ ms^{-1/2}$.

$\theta_s = -\ 30^oC$
$C_p = 2.12 \cdot 10^3$ J/kg K
$L = 3.34 \cdot 10^5$ J/kg
$a = 1.15 \cdot 10^{-6}\ m^2/s$

Furthermore, at any point of time, $t > 0$, the temperature at half the depth of the ice cover, $x/h = 1/2$, will be given by the Equations (I-23) and (I-21) to

$$\theta(x = h/2) = \theta_s(1 - \text{erf}\,\frac{\mu}{2}/\text{erf}\,\mu) \qquad \ldots \text{(I-28)}$$

Thus for $\theta_s = -30^{\circ}C$ and $\mu = 0.297$

$$\theta\ (x = h/2) = -\ 14.7^{\circ}C$$

and the deviation from a linear gradient is consequently very small. Taking into account both the growth of the ice cover and the variation of the conductivity with temperature the deviation will be still smaller as the two approximations give errors that counteract each other.

I-4 The Answer to a Step Rise of Surface Temperature

After having settled that a linear temperature profile is a fairly good approximation for the temperature in an ice cover after an enduring period of cold, the rate of change of temperature in the ice shall be described for a varying surface temperature.

The temperature in the ice cover in the unsteady state can be described by a superposition integral, using the fundamental solution for the case where the temperature is initially zero throughout the ice cover but whose surface temperature, $\theta\ (0,t)$ is raised by a unit step at the point of time $t = 0$. See Hildebrand (1962) or Carslaw and Jaeger (1959).

This fundamental solution for an ice cover with the thickness h, where the lower surface is kept at 0, can be written

$$F(x,t) = 1 - x/h - \sum_{n=1}^{\infty} \frac{2}{n\pi} \sin \frac{n\pi x}{h}\, e^{-n^2\pi^2 at/h^2};\ t \geqslant 0 \qquad \ldots \text{(I-29)}$$

The first two terms of Equation (I-29) are the asymptotic steady state gradient while the last term is a transient that gradually vanishes as $t \to \infty$. The problem and solution (I-29) is illustrated in Figure I-2.

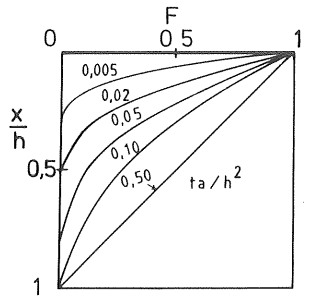

Figure I-2. The "temperature", F, in an ice cover initially at zero temperature when the temperature of the upper surface is raised by a unit step at the point of time t = 0. The parameter is the dimensionless time $t\,a/h^2$.

Thus if the surface temperature is raised by the step A at the point of time $t = \tau$, the temperature is given by

$$\begin{cases} \theta\ (x,t) = 0 & t < \tau \\ \theta\ (x,t) = A\ F\ (x,t-\tau) & t \geqslant \tau \end{cases} \qquad \ldots\ (I\text{-}30)$$

Equation (I-29) gives us the possibility to estimate how long the surface temperature must be constant in order that we can regard the temperature gradient as steady. For an ice cover 0.5 m thick the deviation is negligible after 30 h ($ta/h^2 = 0.50$). For 0.25 m thickness the corresponding time is 7.5 h and so on.

I-5 The Folding Integral for Variations of Surface Temperature

It can be shown, see for example Hildebrand (1962), that for any prescribed variation of the surface temperature $\theta(0,t)$ the solution to the internal temperature can be calculated by the help of Eq. (I-30) by the folding or superposition integral

$$\theta(x,t) = \int_0^t \theta(0,\tau)\ \frac{\partial F(x,t-\tau)}{\partial t}\ d\tau \qquad \ldots\ (I\text{-}31)$$

The initial temperature is accounted for by adding the solution to the problem.

$$\begin{cases} \partial\theta/\partial t = a\ \partial^2\theta/\partial x^2 \\ \theta(0,t) = 0 \\ \theta(h,t) = 0 \\ \theta(x,0) = f\ (x) \qquad 0 \leqslant x \leqslant h \end{cases} \qquad \ldots \text{(I-32)}$$

where f (x) is the initial distribution. The solution to (I-32) can be written

$$\theta(x,t) = \sum_{n=1}^{\infty} A_n \sin \frac{n\pi x}{h}\ e^{-an^2\pi^2 t/h^2} \qquad \ldots \text{(I-33)}$$

where the Fourier coefficients A_n are given by

$$A_n = \frac{2}{h} \int_o^h f(x) \sin \frac{n\pi x}{h}\, dx \qquad \ldots \text{(I-34)}$$

With the aid of the equations (I-29) through (I-33) it is possible to describe the course of temperature in an ice cover, initially with a linear temperature distribution f(x) and exposed to a sudden rise, A, of the surface temperature. The problem can be formulated as

$$\begin{cases} \partial\theta/\partial t = a\partial^2\theta/\partial x^2 \\ \theta(0,t) = \theta_o + A;\ t \geqslant 0 \\ \theta\ (h,t) = 0 \\ \theta\ (x,0) = f\ (x) = (1 - x/h)\ \theta_o \end{cases} \qquad \ldots \text{(I-35)}$$

The corresponding A_n is given by Eq. (I-34) as

$$A_n = \frac{2}{h} \int_o^h (1 - x/h)\ \theta_o \sin \frac{n\pi x}{h}\, dx = \frac{2\theta_o}{n\pi} \qquad \ldots \text{(I-36)}$$

and the entire solution is by virtue of (I-29), (I-31) and (I-33)

$$\theta(x,t) = (\theta_o + A)(1 - x/h) - \sum_{n=1}^{\infty} \frac{2A}{n\pi} \sin \frac{n\pi x}{h}\ e^{-n^2\pi^2 at/h^2} \qquad t \geqslant 0 \quad \ldots \text{(I-37)}$$

Also in this equation the solution is thus composed of a steady state solution for the final temperature profile and a transient part that is gradually vanishing with the lapse of time. The solution (I-37) is illustrated in Figure 3 below for $\theta_o = -30^oC$, $A = 20^oC$

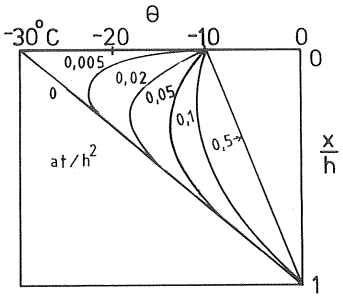

Figure I-3. The temperature θ in an ice cover with an initially linear temperature profile at a rise of surface temperature from $-30^{o}C$ to $-10^{o}C$ at t = 0. The parameter ta/h^2 is dimensionless time. If h = 0.5 m, at/h^2 = 0.0166 corresponds to 1h for ice with a = 1.15 m^2/s. The figure corresponds to Eq. (I-37).

I-6 Linear Growth of Surface Temperature

Of course, the temperature of the ice surface does not rise instantaneously from one constant temperature to another, but the rise takes its time. Drouin and Michel (1971) have, for example, found that air temperature rises in the area of Quebec, Canada, can be described by linear or sinusoidal functions of time. The growth of ice surface temperature should approximately follow functions of the same shape but with different amplitudes. Drouin and Michel assumed that ice surface temperatures and air temperatures are equal.

A linear growth of the surface temperature of an ice cover from one constant surface temperature θ_o to another constant temperature $\theta_o + bT$ during the space of time T is illustrated in Figure I-4.

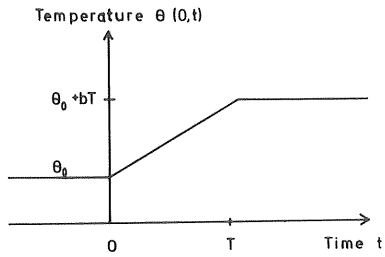

Figure I-4. Linear growth of the ice surface temperature from one constant temperature to another. Compare Equation (I-38).

The internal temperature of the ice cover is given by the solution to the following problem.

$$\begin{cases} \partial\theta/\partial t = a\partial^2\theta/\partial x^2 \\ \Theta(0.t) = \theta_o + bt \qquad 0 \leqslant t \leqslant T \\ \theta(0,t) = \theta_o + bT \qquad t > T \\ \theta(h,t) = 0 \\ \theta(z,0) = (1 - x/h)\theta_o \qquad t < 0 \end{cases} \qquad \ldots \text{(I-38)}$$

The solution is for $t \leqslant T$

$$\theta(x,t) = (1 - x/h)(\theta_o + bt) + \sum_{n=1}^{\infty} \frac{2}{n\pi} \frac{bh^2}{n^2\pi^2 a} (e^{-n^2\pi^2 at/h^2} - 1)\sin n\pi x/h \qquad \ldots \text{(I-39)}$$

For $t > T$ the temperature is given by

$$\theta(x,t) = (1 - x/h)(\theta_o + bT) + \sum_{n=1}^{\infty} \frac{2}{n\pi} \frac{bh^2}{n^2\pi^2 a} e^{-n^2\pi^2 at/h^2} \cdot (1 - e^{n^2\pi^2 aT/h^2}) \sin n\pi x/h \qquad \ldots \text{(I-40)}$$

The solution (I-39, I-40) is illustrated in Figure I-5 for θ_o = = -30°C b = 6°C/h and T = 5h.

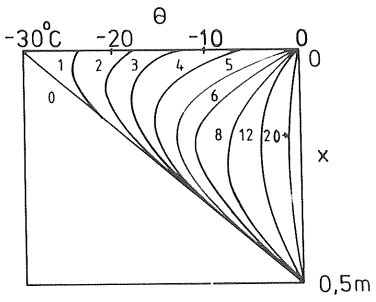

Figure I-5. Temperature profiles in an ice cover at different points of time for the initial surface temperature $\theta_o = -30^oC$ and rate of change $b = 6^oC/h$ during T = = 5h. (Five hours correspond to the dimensionless time 0.083).

I-7 Sinusoidally Varying Surface Temperature

If the surface temperature follows a periodic function, the temperature in the ice will exhibit the same period but there will be a phase lag at some depth in the ice cover. After the initial temperature has lost its influence, the solution will be given by a steady periodic solution. For a very thick ice cover this periodic solution is for example given by

$$\theta(x,t) = \theta_o + A\, e^{-kx} \cos(\omega t - kx) \qquad \ldots (I\text{-}41)$$

when the surface temperature is given by

$$\theta(0,t) = \theta_o + A \cos \omega t \qquad \ldots (I\text{-}42)$$

where ω is the angular frequency
$k = (\frac{\omega}{2a})^{1/2}$ the attenuation factor
kx the phase lag at depth x
a the thermal diffusivity

The amplitude of the temperature variation thus decreases with depth. In an ice cover of finite thickness h this decrease is even more pronounced. For the same surface temperature as above the solution will be given by

$$\theta(x,t) = \theta_o\ (1 - x/h) + AB \cos\ (\omega t + \varphi) \qquad \ldots\ (I\text{-}43)$$

Here

$$B = \left[\frac{\cosh\ 2k(h - x) - \cos\ 2k(h - x)}{\cosh\ 2kh - \cos\ 2kh} \right]^{1/2} \qquad \ldots\ (I\text{-}44)$$

and the phase lag

$$\tan\ \varphi = \frac{\tanh\ kh\ \tan\ k(h - x) - \tan\ kh\ \tanh\ k(h - x)}{\tanh\ kh\ \tanh\ (h - x) - \tan\ kh\ \tan\ k(h - x)} \qquad \ldots\ (I\text{-}45)$$

The solution (I-43) is most conveniently found by the use of complex numbers, i e by seeking solutions of the type C exp (rx - iωt). See Carslaw and Jaeger (1959).

The solution can be used in order to estimate the influence of daily temperature variations in an ice cover. For an ice cover 0.5 m thick the temperature amplitude and phase lag as a function of depth is illustrated in Figur I-6.

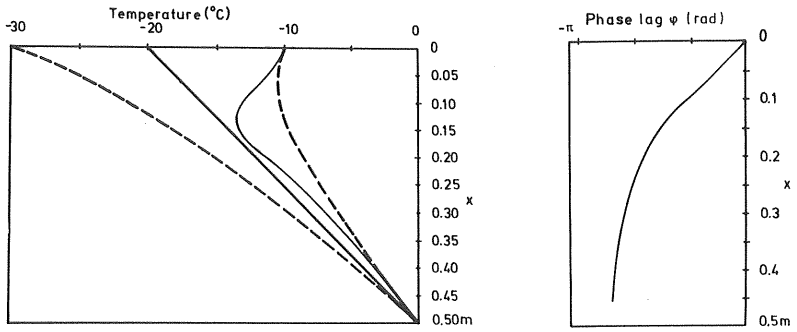

Figure I-6. Temperature for ωt=2nπ (solid line), temperature amplitude (dash line) and phase lag as a function of depth for a 0.5 m thick ice cover, when the surface temperature varies as $(-20+10 \cos \omega t)^{o}C$ with the period 24 h.

For the case when the surface temperature increases from a constant surface temperature θ_o to another constant temperature $\theta_o + 2A$ along a half sinewave, the temperature variations can be calculated with the same technique as before. In Figure I-7 the surface temperature is sketched.

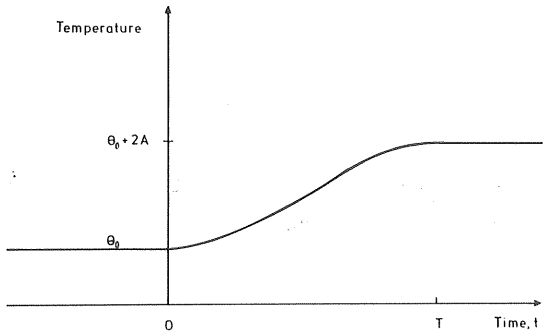

Figure I-7. Sinusoidal growth of the ice surface temperature from one constant temperature to another.

The problem can be formulated by the following set of conditions.

$$\begin{cases} \partial\theta/\partial t = a\ \partial^2\theta/\partial x^2 & \\ \theta(0,t) = \theta_o + A(1-\cos\omega t) & 0 \leqslant t \leqslant \frac{\pi}{\omega} = T \\ \theta(0,t) = \theta_o + 2A & t > T \\ \theta(h,t) = 0 & \\ \theta(z,0) = (1 - x/h)\theta_o & t < 0 \end{cases} \quad \ldots \text{(I-46)}$$

For points of time $t < T$ the solution is given by

$$\theta(x,t) = (\theta_o + A)(1 - x/h)$$

$$- \sum_{n=1}^{\infty} \frac{2A}{n\pi} \frac{\alpha_n^2}{\alpha_n^2+\omega^2} (\cos\omega t + \frac{\omega}{\alpha_n} \sin\omega t) \sin\frac{n\pi x}{h}$$

$$- \sum_{n=1}^{\infty} \frac{2A}{n\pi} \frac{\omega^2}{\alpha_n^2+\omega^2} e^{-\alpha_n t} \sin\frac{n\pi x}{h} \quad \ldots \text{(I-47)}$$

where $\alpha_n = n^2\pi^2 a/h^2$

For points of time $t > T$

$$\theta(x,t) = (\theta_o + 2A)(1 - x/h)$$

$$- \sum_{n=1}^{\infty} \frac{2A}{n\pi} \left[1 + \frac{\alpha_n^2}{\alpha_n^2+\omega^2} (\cos\omega T + \frac{\omega}{\alpha_n} \sin\omega T)\right] e^{\alpha_n(T-t)} \sin\frac{n\pi x}{h}$$

$$- \sum_{n=1}^{\infty} \frac{2A}{n\pi} \frac{\omega^2}{\alpha_n^2+\omega^2} e^{-\alpha_n t} \sin\frac{n\pi x}{h} \quad \ldots \text{(I-48)}$$

In Figur I-8 the temperature profiles in an ice cover subject to the sinusoidal rise of temperature of the surface from $-30^{o}C$ to $-10^{o}C$ during 5 h is shown.

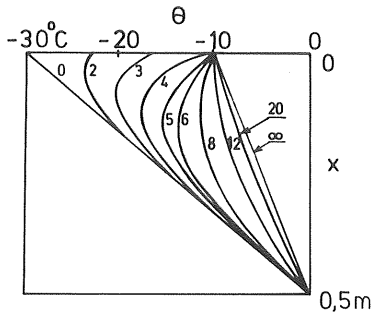

Figure I-8. Temperature profiles in an ice cover at different points of time for initial surface temperature $\theta_o = -30^{o}C$, "double amplitude" of change $2A = 20^{o}C$ and half period 5 h.

I-8 How to Treat Boundary Conditions Analytically

Most authors on thermal ice pressures halt at the problem of giving analytical solutions for realistic boundary conditions. The analytical solutions given above have, for example, been founded on prescribed temperatures at the upper and lower boundary of the ice. A more realistic boundary condition formulated in paragraph I-2 is the condition for forced convection by wind

$$-\lambda \partial\theta/\partial x = -A(\theta - \theta_a); \quad x = 0 \qquad \ldots (I\text{-}49)$$

It is possible to give solutions to the equation of thermal diffusion for such a boundary condition in the form of an expansion in the characteristic functions of the problem:

$$\begin{aligned} &\partial\theta/\partial t = a\,\partial^2\theta/\partial x^2 \\ &\lambda\partial\theta/\partial x = -A\theta; \quad x = 0 \\ &\theta = 0 \qquad\qquad x = h \end{aligned} \qquad \ldots (I\text{-}50)$$

These characteristic functions or eigenfunctions are of the type

$$\theta_n = \exp(-a\beta_n^2 t)\ (\cos \beta_n x - \frac{A}{\lambda\beta_n} \sin \beta_n x) \qquad \ldots (I\text{-}51)$$

where the characteristic values or eigenvalues β_n are the consecutive positive roots of

$$\lambda\beta = +A \tan\beta h \qquad \ldots (I\text{-}52)$$

Solutions would then be of the form

$$\theta = \sum_1^\infty A_n \theta_n \qquad \ldots (I\text{-}53)$$

whose coefficients are chosen to satisfy the initial condition $\theta = f(x)$ for $t = 0$.

Such expansions are given by Monfore and Taylor (1948) for an ice cover as well as by Carslaw and Jaeger (1959). Presently it is more convenient to solve these problems by difference methods, because expansions in (I-51) have rather complicated coefficients A_n.

I-9 Short-Wave Radiation

That part of the solar radiation that has short wave lengths will penetrate into the ice cover where it is absorbed as heat. The absorbed energy per unit of volume and time will correspond to a termperature "release", M, at different depths, x, in the ice cover

$$M(x) = \frac{J_o k}{C_p \rho} e^{-kx} \qquad \ldots (I\text{-}54)$$

where J_o is the intensity of short wave radiation passing the upper surface

k the coefficient of absorption

C_p the specific heat capacity of ice

ρ the density of ice

An instantaneous "release" of temperature $M(\eta)\, d\eta\, d\tau$, at $x = \eta$ and $t = \tau$ in a region initially at zero temperature and bounded by two parallel planes kept at zero temperature will give the temperature distribution

$$\theta = \frac{M(\eta)\, d\eta\, d\tau}{2\sqrt{\pi a(t - \tau)}} \cdot$$

$$\cdot \sum_{n=-\infty}^{\infty} \exp\left(-(x - \eta - 2nh)^2/4a(t-\tau)\right) - \exp\left(-(x+\eta-2nh)^2/4a(t-\tau)\right) \quad \ldots(I\text{-}55)$$

This equation is received by the method of sources and sinks, see for example Carslaw and Jaeger (1959).

By integration of (I-55) over the depth of the ice cover and over time a solution for the temperature distribution is formed that is not very convenient, but alternative solutions expressed in Fourier series or the series (I-53) are not much easier, and actually even this problem is best solved by a difference method. The complexity is partly compensated for by the fact that good accuracy is established by using only a few of the terms or images of the series.

I-10 Conclusions

For every idealized case of heat conduction it is probably possible to find an analytical solution. For the unsteady state cases considered in this dissertation all solutions will, however, be expressed in infinite series or tabulated functions, and it has been shown that especially the boundary conditions and internal procuction of heat will lead to complicated expressions.

Some of the displayed solutions are relevant for the discussion of the temperature transient and comparison with the results of others.

The solution of a real case including surface thermal resistance, condensation, short and long wave radiation, varying temperature etc. will, on the other hand, be best solved by a numerical difference method.

APPENDIX II

FIELD MEASUREMENTS OF TEMPERATURE PROFILES IN AN ICE COVER

CONTENTS OF APPENDIX II

II-1 Introduction

During the winters 69/70 and 70/71 field measurements of the temperatures in the ice cover of a Swedish lake were performed. The lake, Ängsjön, is situated in southern Sweden ($12^{o}48'E$ $59^{o}52'N$) at an altitude of 273 m. Ängsjön is 4 km long in the direction SE-NW and it is 300 m wide. As the ultimate goal of the measurements was to relate the rate of change of temperature to thermal ice pressure, efforts was also done to measure the ice pressure during the winter 69/70.

The field measurements were sponsored by the Swedish Natural Science Research Council and Chalmers Univeristy of Technology.

II-2 Field Measurements

The following parameters were observed

- o temperature at differet depths in the ice
- o horizontal pressure at three depths in the ice (only 1969/70)
- o ice deformation at the surface (only 1969/70)
- o air temperature
- o wind speed
- o ice thickness
- o snow depth

The measurements were performed in different ways the two winters, why measuring arrangements and weather conditions are described for each measuring term separately below. The results and comparison with calculations are, however, reported together in paragraph II-6.

Originally the purpose of the measurements was to verify the whole complicated course of events taking place when an ice-sheet is heated and expands. It proved to be very difficult to measure the deformations of the ice cover. Furthermore, there was very much snow on the ice covers both winters during the measurements, so that only small ice pressures and consequently small deformations could develop. Because of this, the efforts of the second winter were devoted to mapping the course of temperature only.

II-3 The Winter 1969/70

In late January 1970 the experimental site was erected on Ängsjön. On an open peninsula a place was arranged for the measuring of the weather parameters, and out on the ice cover probes for temperature and pressure were placed in the ice.

On the peninsula a standardized thermometer cage was placed. It contained calibrated thermometers for temperature, maximum temperature and minimum temperature. At a small distance to the cage a small mast, 2 m, was placed for measuring the wind speed. Probes for radiation balance and solar irradiation was also placed on masts 1.5 m above ground. The radiation fluxes were insignificant during the observed periods over the snow cover.

At three places on the lake ice cover, probes were placed to measure the temperatures in the ice. The probes were placed in the 35 cm thick columnar ice by gently chiselling pitches 25 cm deep, where the lowest probes were laid on the bottom and covered with a few cm of water. When this water had frozen the next probe was positioned and a new layer of water was poured into the pitch. The vertical distance between the ice surface and the probes were measured.

The probes were thermocomples, and six were placed in each vertical at intervals of 5 to 10 cm.

The pressure probes were placed close to one of the sets of thermocouples in the middle of the lake. They were arranged so that three of them senced the pressure at three depths in W-E-direction and the other three in S-N-direction. On this place also the deformation at the surface was measured with a mechanical deformation meter. The results from these last measurements proved to be very inaccurate. The pressure was insignificant during the periods observed. The results from the pressure and deformation measurements are not reported because of their bad quality.

On February 4, water started to leak up on to the ice cover along its shores, On February 24, after repeated snowfalls, the water had spread all over the lake.

The measurements were, because of the water leaking on to the ice, restricted to the period February 17-23. Only the place situated centrally on the lake was dry at this occasion. The snow had been transported away form the place earlier, but was shovelled back during the measurments. A try to get more values was done in the middle of april, when the snow cover had melted completely. The weather was, however, too mild during this period why the ice rottened fast.

II-4 The Winter 1970/71

On December 21, 1970 six sets of thermocouples with six couples each were placed in the ice cover of Ängsjön. This time 5 cm wide slots were sawn in the ice cover, and the thermocouples were hung in the slots. At this occasion the ice was clean from snow and the temperature approximatedly $-20^{o}C$, why the slots very soon froze over, and already the next day water could be filled to the original ice-surface.

By this means good accuracy was attained in the relative positioning of the thermocouples. However, there was a mild period around new year, why the ice thawed at its upper surface and the distance from the upper surface may have decreased from 5.0 cm to between 3 and 4 cm.

On February 15 the weather station was erected. This time on the ice conveniently close to the thermocouples. The temperature of the air stayed, however, between $+1.3^{o}C$ and $-1.4^{o}C$ up till February 23 when the observations were postponed to March 1.

Between March 1 and 7 the weather was suitable and a thin snow cover covered the places with the thermocouples. The snow was removed from some of the groups of thermocouples, so that comparisons between temperatures in snow covered and bare ice could be done. On March 7 the temperature of the ice was above $0^{o}C$ again.

In early March a new attempt to measure was done, but the weather was above freezing at this occasion, and the ice was covered by 12 cm of snow slush and 12 cm of wet compact snow. The measurements were stopped for the season.

II-5 Computer Programme

A simple Fortran-programme was done for the calculation of the temperatures in an ice cover. The programme used an explicit difference scheme, and took into account the variation of air temperature, wind-speed and the snow cover.

The influence on the temperatures from the growth in thickness of the ice cover was neglected as this influence is very small, see Appendix I. The solar irradiation was insignificant during the periods of measurement. The radiation balance was measured over the snow field and proved to be negligibly small. The radiation balance over the black ice might not have been negligible. In the computer programme the solar irradiation is neglected completely and the long-wave radiation balance is partly included in the coefficient of heat transfer. See paragraph II-6 below.

The degree of concord between the calculated values and the measured values depens not only on a correct weather input and chosen thermal properties but also on the accuracy of the used scheme for calculation. In the computer programme a method with central differences and ice differences dx of 0.04 m were used. The time intervals dt were chosen with the help of the optimum condition $dt = dx^2/(6a)$.

The ice could have been divided into thinner ice differences to increase the accuracy of calculations. The accuracy of the contained parameters and the measured values is, however, not good enough to motivate a greater accuracy.

II-6 Comparison Between Measured and Calculated Values

In Figures II-1 and II-2 calculated and measured temperature profiles are shown. Figure II:1 shows the temperature profile at three consecutive times of measuring at the same place. The air temperature and wind-speed varied from time to time according to the following table.

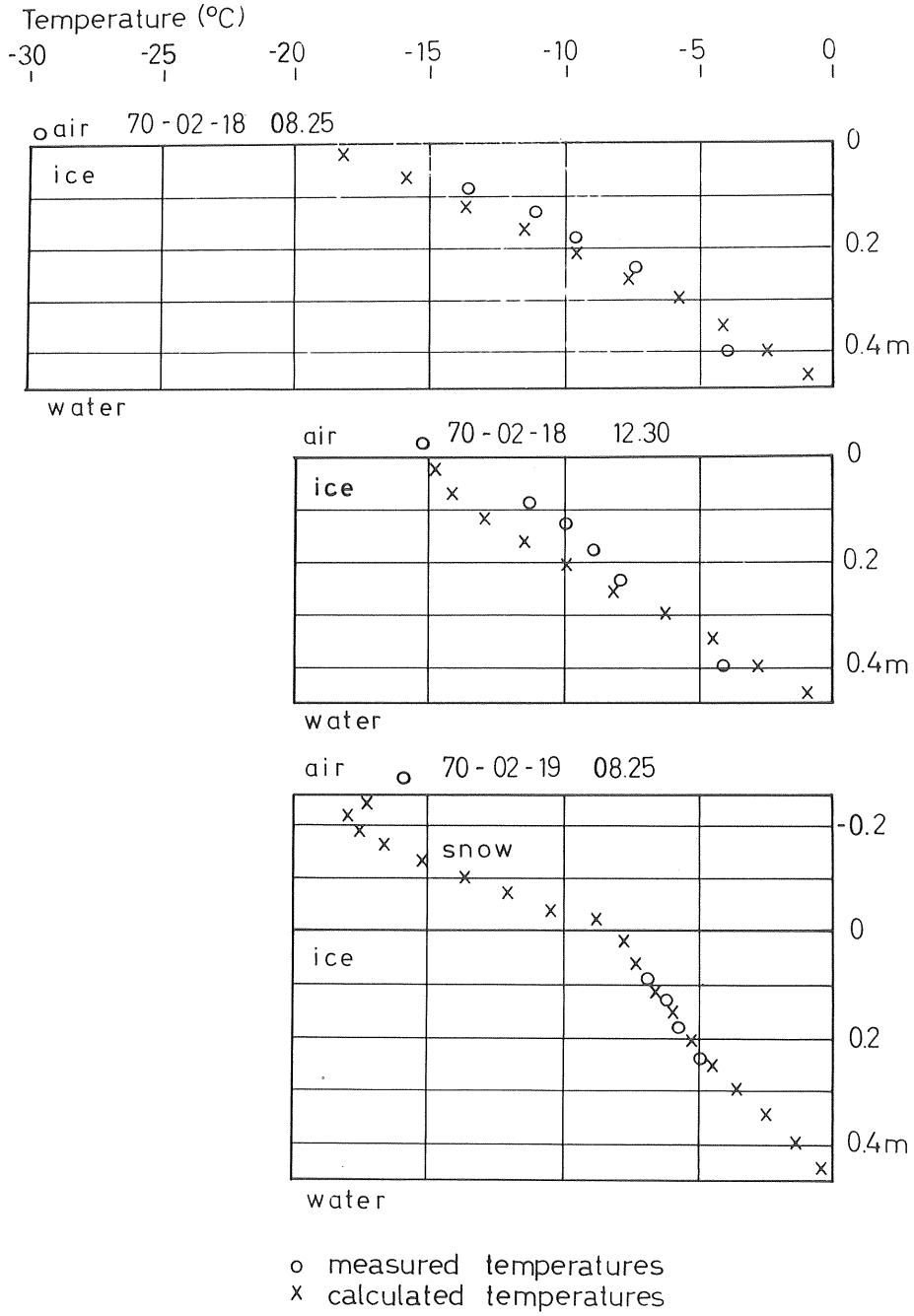

Figure II-1. Temperature profiles in the ice cover of Ängsjön, February 1970. Place first freed from snow then covered with snow, Feb 18, 1970. 17.40.

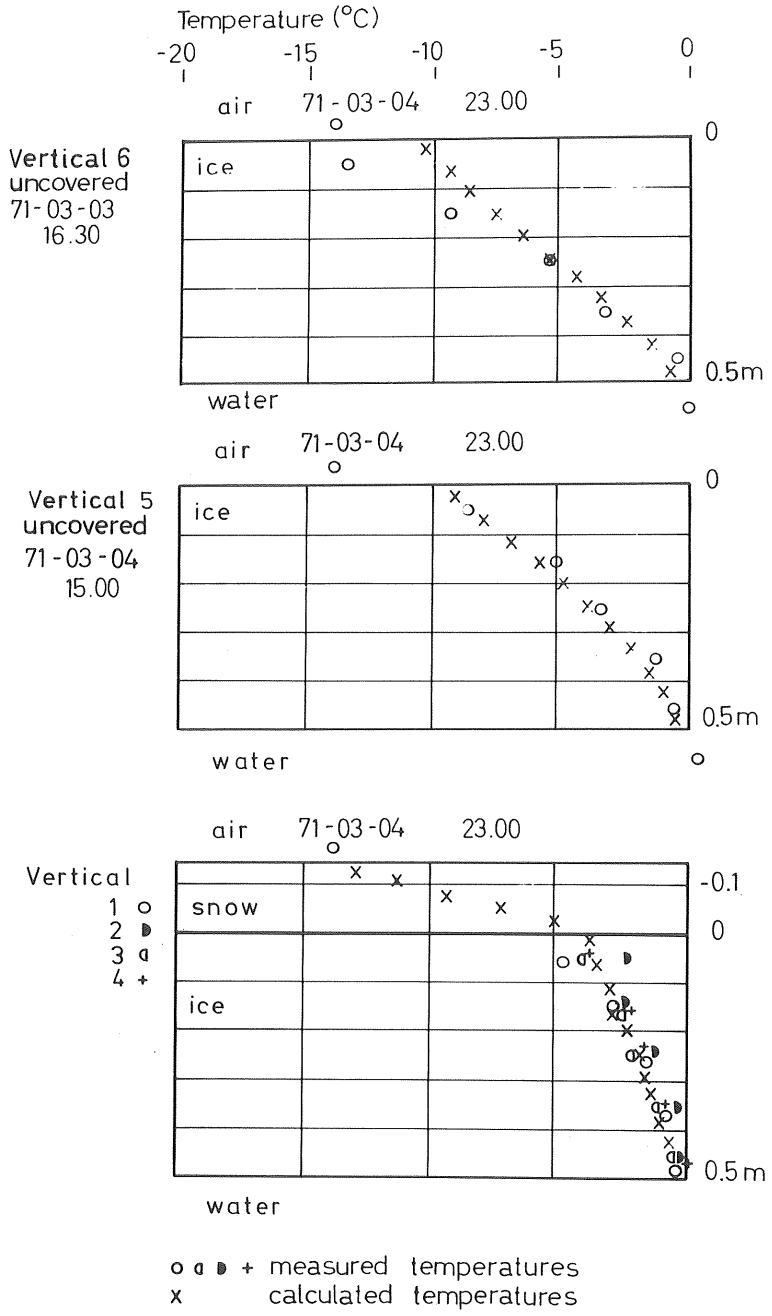

Figure II-2. Temperature profiles in different verticals in the ice cover of Ängsjön at the same occasion, March 4, 1971, 23.00. Places first covered by snow, but freed from snow at different points of time.

Date and Time	Air Temp.	Wind Speed	Comments
70-02-18 08.25	-29.6°C	0 m/s	Sunny
70-02-18 12.30	-15.2°C	0 m/s	Sunny
70-02-19 08.25	-15.8°C	0.3 m/s	Snowing

The rise of temperature in the ice between morning and noon Feb. 18 is due to the rise of air temperature. The rise between noon and morning the next day is however caused by increased insulation by snow. The place was shovelled over with 26 cm of snow at approximately 17.40 the first day.

Figure II-2 shows temperature profiles measured at the same time, 23.00 March 4 1971, but at six places. Four of the places were covered with snow all the time while the other two had been freed from snow two days(vertical 6) and one day (vertical 5) in advance.

Figures II-3 and II-4 shows the calculated and measured positions of the isotherms for -3, -5, and -7°C. Figure II:3 is from the vertical covered manually with snow Feb. 18, 1970. Figure II:4 is taken from a vertical freed from snow March 3, 1970.

From all Figures II:1 through II:4 it can be seen how important a factor the snow insulation is. Actually the 14 cm thick snow cover of March 1971 is enough to prevent the weather variations to influence the ice cover beneath the snow to any significant degree.

In order to get as good an accordance as possible between the calculated and the measured values the programme has been run with a series of values on the coefficient of thermal diffusion of the ice. The runs did not give significant improvements of the concordance.

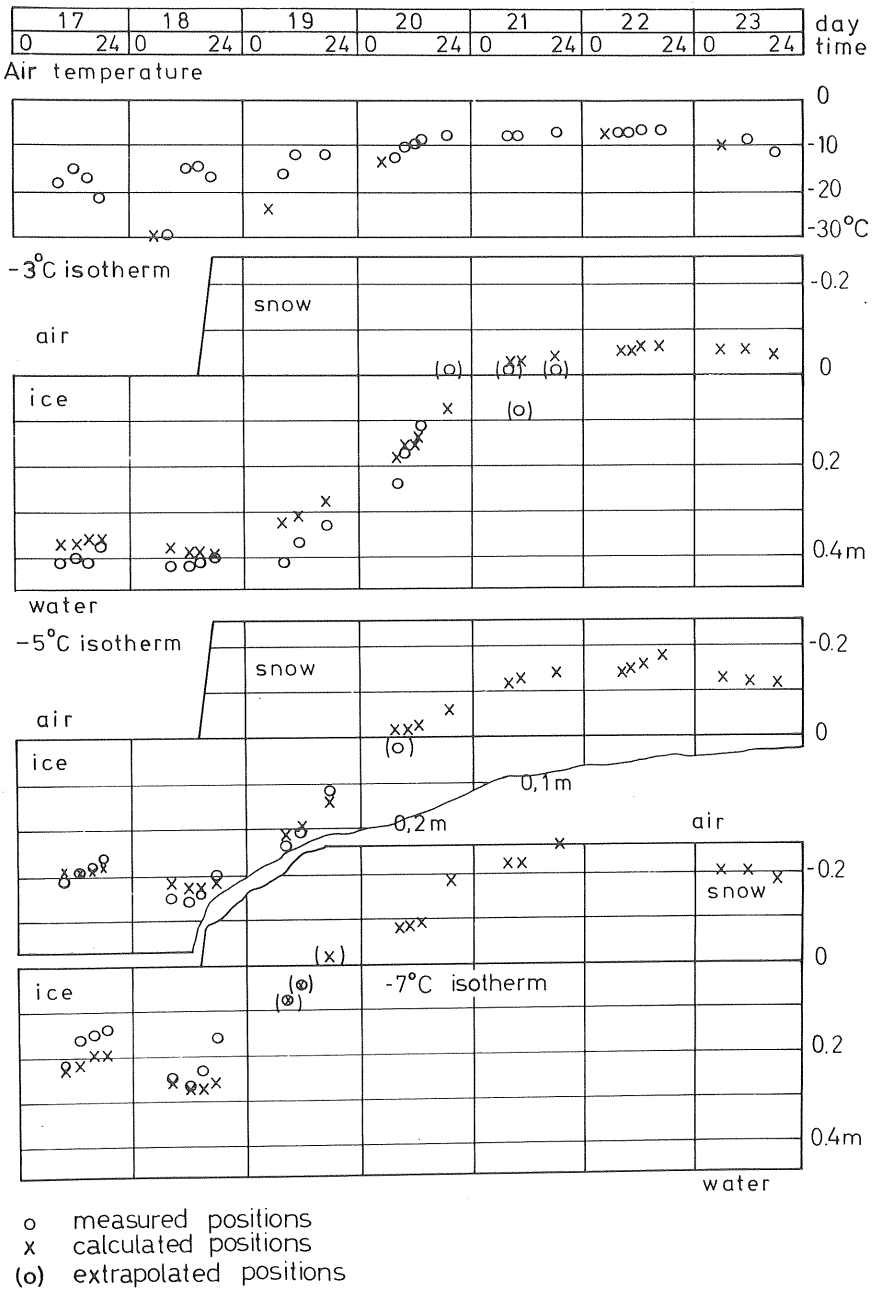

Figure II-3. Positions of measured and calculated isotherms in the ice cover of Ängsjön in February 1970.

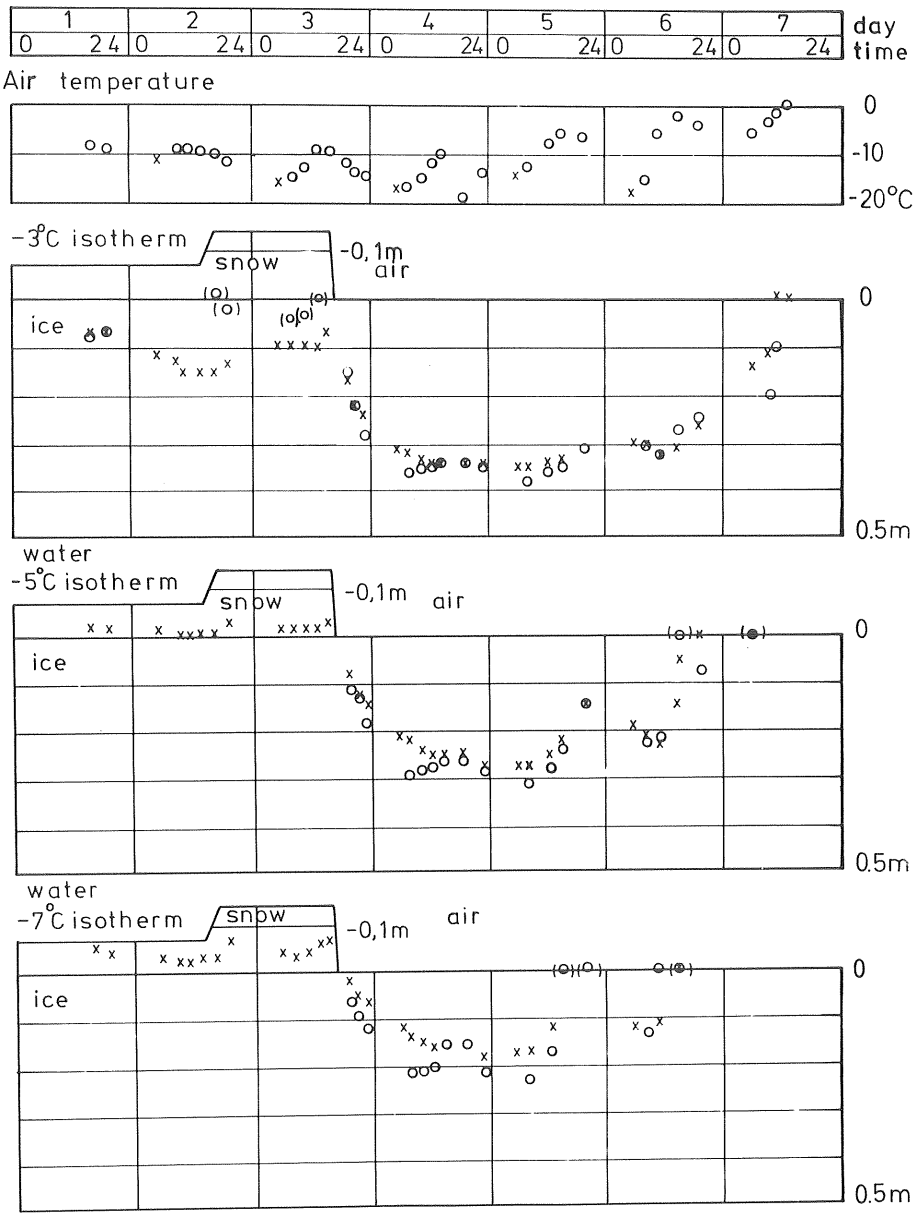

o measured positions
x calculated positions
(o)extrapolated positions

Figure II-4. Positions of measured and calculated isotherms in the ice cover of Ängsjön in March 1971. Vertical No. 6.

Variations of the coefficient of heat transfer between air and ice or air and snow give, however, decisive changes of the temperature profile. The coefficient of heat transfer was finally set to $A = 10.4\ (1 + 0.40\ u)$ W/(m^2 ^oC) for the wind $u < 5$ m/s and $A = 4.2\ (1 + 1.8\ u^{0.78})$ W/(m^2 ^oC) for $u > 5$ m/s. The function includes the effect of condensation and back radiation. The function is originally taken from Bygg I (1961) although 4.2 W/(m^2 ^oC) was added to make a better fit to the measured profiles. For wet road surfaces Magnusson found 16.0 W/(m^2 K) at calm weather ($u = 0$ m/s). See Eq. (3.25).

For a few occasions with almost steady state conditions the coefficient of heat transfer was estimated from the measurements, Table II-1. The heat flux was estimated from the thermal gradient in the ice, the conductivity of which was set to 2.24 W/(m K). Compare Appendix III-5. The arithmetric mean was found to 9.8 W/(m^2 K) and the standard deviation to 2.9 W/(m^2K). Some measurements by Wold (1957) on Maridalsvatn in Norway were used the same way for comparison. They gave 12.0 ± 5.2 W/(m^2K)

Table II-1. Estimated coefficient of heat transfer for some occasions with approximately steady state conditions: Mean 9.8 W/(m^2K), standard deviation 2.9 W/(m^2K).

Date	Hour	Air Temp (^oC)	Wind Speed (m/s)	A (W/(m^2K))
70-02-17	12.50	-14.5	0	11.83
	15.30	-17.1	0	11.83
	17.55	-21.2	0	9.00
70-02-18	8.25	-29.6	0	10.58
	14.25	-14.8	0	14.54
71-03-04	18.50	-19.6	0	5.92
71-03-05	12.30	- 8.1	1.8	5.32
	15.10	- 6.2	0.9	9.85
71-03-06	8.30	-15.6	0	9.58

The total heat flux by radiation, convection, and conduction has thus been calculated as $A \cdot \Delta\theta$ where $\Delta\theta$ is the difference between the temperature of the air at the level 2 m and the temperature of the ice surface. The chosen function give rather good agreement between measured and calculated profiles during the afternoons.

In the diagrams of Figure II-4 the accordance seem to be bad in the mornings. This can be caused by the thermocouples lying closer to the upper surface than estimated. The ice had melted a little beacuse of mild weather. Another reason could be that the back radiation from an ice surface is not negligible although the measurements over the snow gave this result.

For the periods when the ice was covered by snow it has proven impossible to get the calculated profiles to agree with the measured profiles. This is partly due to the fact that the thermal conductivity of the snow varies strongly with packing and structure of the snow. At cold and windy weather the snow depth varies fast at a site as the snow is drifting like dunes over the ice. For the calculations 1969/70 the conductivity of the snow was set to 0.34 and 1970/71 to 0.23 $W/(m^oC)$. The density was set to 350 and 250 kg/m^3 respectively, and therefore the coefficients of thermal diffusion are approximately equal $4.5 \cdot 10^{-7}$ m^2/s.

The places were covered and cleared of snow with a shovel. This could of cause not be done momentarily, why the agreement between calculated and measured values a few hours afterwards should not be expected to be to good.

II-7 Conclusions

The field measurements showed that the influence from the solar irradiation and the long-wave back radiation on the rate of change of temperature in the ice should have been investigated further. The agreement between measured and calculated course of temperature in the ice could be considered good under the circumstances.

It was judged impractical to carry through field measurements of thermal ice pressures and deformations in order to improve the theory. It is difficult to control the conditions for the experiment as to weather, shore lines, ice movements, evenness of ice and snow cover, etc.

In this context my reported field experiments offer the experience that the conditions for thermal ice pressures on Ängsjön, during the winters 1969/70 to 1971/72, were very small. The winter of 1969/70 and 1971/72 the ice was covered very early by insulating snow. In February 1970 and March 1972 the snow cover was so heavy that it pressed the ice under the water and the temperature of the ice was probably around $0^{o}C$ till the breaking-up of the ice. The winter of 1970/71 the ice was bare till mid December. Then it was 0.25 m thick. Before the mild weather arrived soon after new year it had been covered by 5 cm of loose snow. This ought to have been the most suitable occasion for thermal ice pressure during the tree winters.

In order to give a judgement on the probalities of ice pressure of certain magnitudes in a lake, ice observations over several years must be combined with weather records into a model for ice cover expansion.

APPENDIX III

A LABORATORY EXPERIMENT ON THERMAL ICE PRESSURE

CONTENTS OF APPENDIX III

III-1 Introduction

During 1973 and 1974 some few experiments on thermal ice pressure were conducted in the freezing laboratory at the Department of Hydraulics. The aim for the experiments was to verify the whole course of events for the development of thermal ice pressure, why the ice cover was allowed to form in an experimental basin. The ice cover was then subjected to temperature changes and its internal pressure, internal temperature, and expansion was measured.

Two similar experiments have been reported earlier by Löfquist (1954) and by Drouin and Michel (1971). The former grossly verified the course of events. He measured temperature profiles and horizontal pressures in a concrete basin, but did not control the horizontal expansion of the ice, why he could not properly test any stress-strain relationship. Drouin and Michel on the other hand did not succeed in reproducing natural conditions, first because the water did not fill the cracks in the ice, secondly because the walls of their invar basin was not strong enough to resist the horizontal expansion appreciably.

The present experiments did verify the temperature profiles of an ice cover subjected to a variation of the air temperature, the cracking of the ice when the surface temperature decreases, the expansion of the ice when the cracks are filled with water from underneath, and the expansion when the ice cover is heated. The pressures and deformation due to the two types of expansions were measured, but the accuracy should have been better.

The experiments were granted by Chalmers University of Technology and the research basin, a piece of water pipe of prestressed concrete 1.4 m inner diameter, was given by AB Tryckrör, Malmö. The pipe has withstood the internal pressure of 900 kPa at its upper end without any visible damage or leakage.

III-2 Experimental Arrangement

The experiments were performed in a standing circular tube, inner diameter 1.40 m and outer diameter 1.60 m, see Figure III-1 and title page of Appendix. The tube was 1.50 m high and its lower

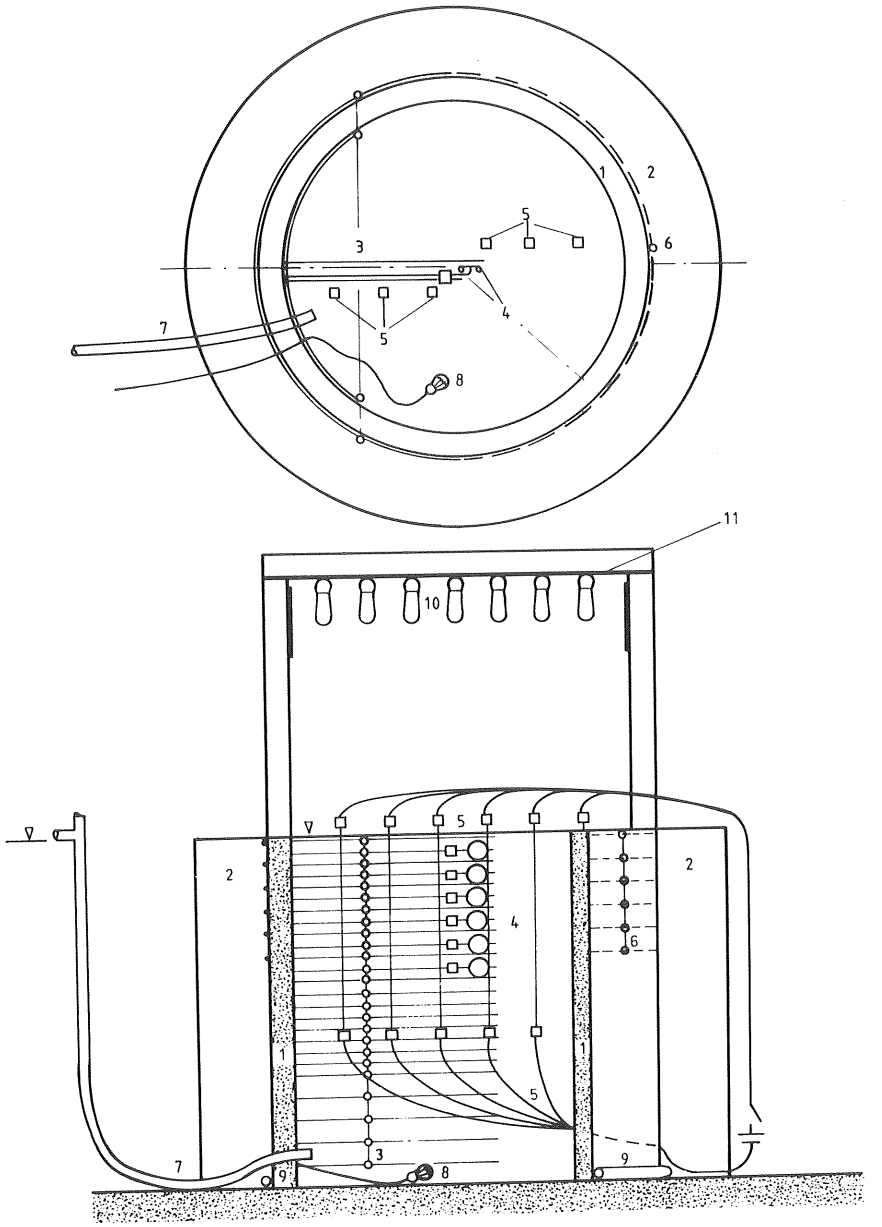

Figure III-1. Experimental arrangement.

1. Prestressed concrete
2. Insulation
3. Thermo couples
4. Pressure probes
5. Thickness meters
6. Strain gauges
7. Outlet hose
8. Lamp
9. Heating hose
10. Sodium lamps 13x270 W
11. Aluminium coated masonite

end was sealed to the floor with a two-component elastic seal so that the floor made the bottom of the basin. The wall of the tube was insulated by 0.40 m of mineral wool in order that the heat flow be mainly vertical. Although the floor of the lab is weakly heated, it proved to be necessary to heat the lower end of the tube by means of a hose with slowly running tap water, otherwise the basin froze from the bottom too. On the bottom of the basin a lamp was placed to make possible a view of the ice cover.

Water Table

The water table in the basin was kept constant by an arrangement with a plastic hose that was led through the wall near the bottom of the basin to a reference level in the control room of the freezing laboratory. There surplus water was allowed to spill over, when the ice cover expanded downwards in the basin. Water was also filled and tapped this way and could be adjusted for the evaporation in the initial stage before the ice covers formed.

Ice Thickness

The thichness of the ice cover was measured at six points along a diameter by wires of constantan hanging through the ice with weights at their lower ends. When one measured, they were heated electrically by 24 V DC so as to melt loose from the ice and it was then possible to lift the weights against the underside of the ice cover and measure the thickness with a carpenter's rule. See figure III-1 and III-2.

Temperature

The temperature was measured in the center of the basin at every 5 cm to the depth of 1 m and then at every 10 cm to the bottom, Figure III-1. On the inside and outside of the wall the temperature was also measured in two diametrical verticals. The outer probes were placed on the strain probes described below, Fig. III-3. The temperature of the air was measured at two points above the basin, and the temperature of the heating hose was measured as well. In all, the temperature was measured at 51 points.

The temperature probes consisted of copper-constantan thermocouples which were made with Quicktip connections and dipped in silicone rubber. The reference temperature was arranged with a mixture of ice and water in a thermos flask which in its turn was placed in an insulated picnic box also filled with a mixture of ice and water. In this way the risk of incorrect temperatures near the walls of the thermos flask was eliminated. The differential voltage was measured with a precision voltmeter which gave a reading accuracy corresponding to ± 0.15°C. The accuracy of the thermocouples were checked to be ± 0.1°C, and the over all accuracy was estimated to around ± 0.2°C. The thermocouples were connected to the volmeter via a double multichannel switch that switched both ends of the circuits of the thermocouples.

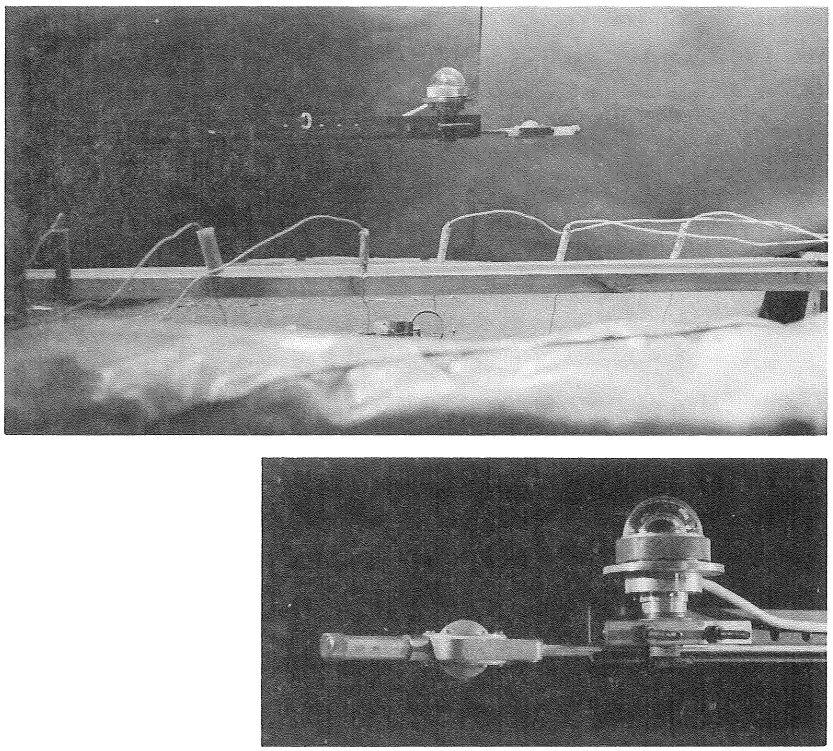

Figure III-2. Radiation-balance meter and solarimeter mounted above the basin. Upper end of ice thickness meters. As soon as the first few cm of ice had formed the board was taken away. The first thermo-couple is seen just below the board, and the second together with the first pressure probe.

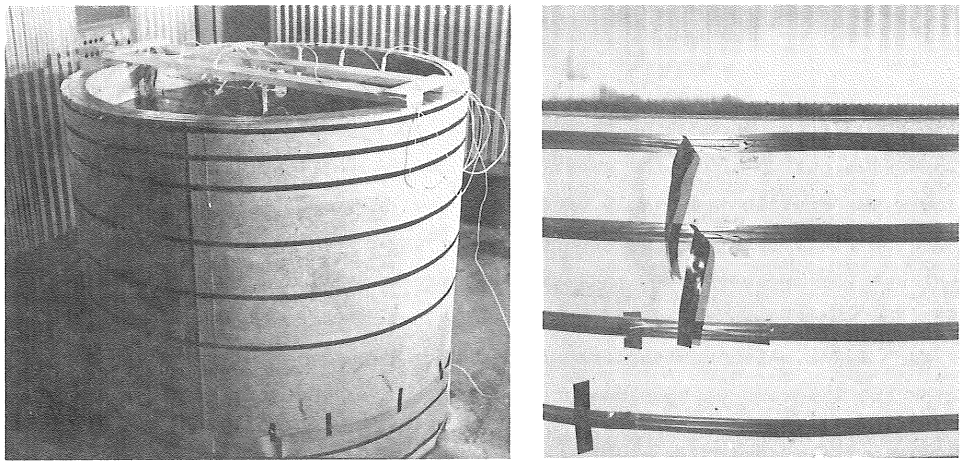

Figure III-3. The basin before insulation. The strain gauges are covered by the plastic tape. The details show the arrangement of the strain wires and thermocouples.

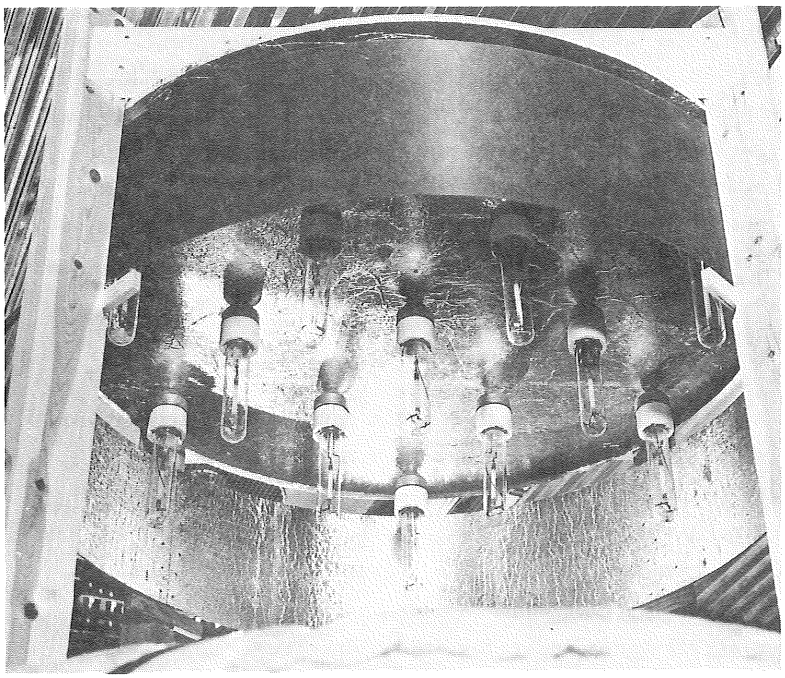

Figure III-4. Arrangement of sodium lamps above the experimental basin. Radiation flux 250 W/m^2.

Short-Wave Radiation

For the purpose of separating the influence of heating by short wave radiation from the heating by conduction, an arrangement of sodium lamps was put up above the experimental basin. Thirteen lamps, each 270 W, was distributed evenly on a board coated with aluminium foil. See the title page of this appendix and Figure III-4. The radiation balance was measured by a radiation balance meter (Ph. Schenk GmbH) and the short-wave irradiction by a solarimeter (Kipp et Zonen). See Figure III-2. Although the transformers for the lamps were placed outside the laboratory the temperature could not be kept constant because of the low capacity of the freezer system. As a consequence the influence of the short-wave radiation could not be calculated properly. Approximately 10% of the electrical input was registered as short-wave radiation directed towards the ice surface.

Deformation

The lateral expansion of the ice cover was estimated indirectly by measuring the expansion of the basin at six levels at a division of 10 cm from the surface of the ice. See Figure III-1 and III-3. The deformation meters consisted of wires of the alloy, nicrothal-1x. They were gently stretched in approximately three rounds at each level on a plastic tape and covered by another tape. On each wire gauge two thermocouples were placed diametrically opposite to each other.

In this way the average deformation at each level could be measured, and expected cracks in the concrete tube could not distort the measured values or destroy strain gauges that happended to be placed across a crack. Each gauge was roughly connected to give a resistance of 120 Ω but was balanced with the help of a shunt resistance of 15 or 33 kΩ which was placed in the control room. The change in resistance was measured with a 5 kHz AC-bridge and the deformation was calculated from given material constants and registered temperatures. The theory for the calculations is given in paragraph III-3.

Pressure

The internal pressure in the ice was measured with Glötzl-probes, that were placed at six levels with 0.10 m intervals and the first one 0.05 m below the uppermost thermo couple, Figure III-1 and III-2. The probes consist of two thin steel membranes that are pressed apart with a hydraulic exchange system to balance the ice pressure when measuring. Pressures below an "opening-pressure" level cannot be measured. The level is different for every probe but around 200 kPa. The accuracy when frozen into the solid ice may be guessed to ± 30 kPa. There was a tendency of falling pressure if the pumping operation was continued for more than half a minute, probably because the ice yielded to the pressure from the membranes.

III-3 Strain Gauge Evaluation

The change of length of the strain gauges is constituted of the thermal expansion $\alpha \cdot d\theta \cdot \ell$ and the strain $d\varepsilon \cdot \ell$, where ℓ is the length of the gauge, α the coefficient of expansion, θ the temperature and ε the strain. The change of length of the gauge is equal to the change of length of the circumference of the basin $d\varepsilon_o \cdot \ell$. This gives

$$d\varepsilon = d\varepsilon_o - \alpha d\theta \qquad \ldots \text{(III-1)}$$

The area of the crossection of the wire, A, increases due to the thermal expansion and decreases because of the contraction by the tension. Consequently

$$dA = A(1+\alpha d\theta)^2 - A + A(1-\nu d\varepsilon)^2 - A \qquad \ldots \text{(III-2)}$$

where ν is Poisson's modulus. If the squares of the small quantities $\alpha d\theta$ and $\nu d\varepsilon$ are neglected the relative change of wire area is received as

$$\frac{dA}{A} = 2(\alpha d\theta - \nu d\varepsilon) \qquad \ldots \text{(III-3)}$$

The electrical resistance, R, of the wire can be written

$$R = c1/A \qquad \ldots \text{(III-4)}$$

where c is the coefficient of resistance of the wire material. Equation III-4 can be written in natural logarithms and be differentiated with respect to temperature, θ, and strain, ε:

$$\ln R = \ln c + \ln l - \ln A \qquad \ldots \text{(III-5)}$$

$$\frac{dR}{R} = \frac{1}{c}\frac{\partial c}{\partial \theta}\, d\theta + \frac{1}{c}\frac{\partial c}{\partial \varepsilon}\, d\varepsilon +$$

$$+ \frac{1}{\ell}\frac{\partial \ell}{\partial \theta}\, d\theta + \frac{1}{\ell}\frac{\partial \ell}{\partial \varepsilon}\, d\varepsilon -$$

$$- \frac{1}{A}\frac{\partial A}{\partial \theta}\, d\theta - \frac{1}{A}\frac{\partial A}{\partial \varepsilon}\, d\varepsilon \qquad \ldots \text{(III-6)}$$

Using the fact that $\partial \ell / \ell \partial \theta = \alpha$, $\partial \ell / \ell\, \partial \varepsilon = 1$ and Eq. (III-3), this is reduced to

$$\frac{dR}{R} = \left(\frac{1}{c}\frac{\partial c}{\partial \theta} - \alpha\right) d\theta + \left(\frac{1}{c}\frac{\partial c}{\partial \varepsilon} + 1 + 2\nu\right) d\varepsilon \qquad \ldots \text{(III-7)}$$

and if finally $d\varepsilon$ is substituted as given by Eq. (III-1) the change of resistance can be written as

$$\frac{dR}{R} = k\, d\theta + g\, d\varepsilon_o \qquad \ldots \text{(III-8)}$$

where the probe factor

$$g = \frac{1}{c}\frac{\partial c}{\partial \varepsilon} + 1 + 2\nu \qquad \ldots \text{(III-9)}$$

was given to 2.4 by the manufacturer, and

$$k = \frac{1}{c}\frac{\partial c}{\partial \theta} - \alpha(1+g) \qquad \ldots \text{(III-10)}$$

According to the manufacturer AB Kanthal $(1/c)\, \partial c/\partial \theta = 5 \cdot 10^{-6}\ {}^{o}C^{-1}$ and $\alpha = 11 \cdot 10^{-6}\ {}^{o}C^{-1}$. Thus k had the value $-32.4 \cdot 10^{-6}\ {}^{o}C^{-1}$. Finally the relative change of geometrical circumference or diameter of the basin was calculated by

$$d\varepsilon_o = \frac{1}{g}\frac{dR}{R} - \frac{k}{g}\, d\theta \qquad \ldots \text{(III-11)}$$

The first term on the right hand side was read directly from the bridge.

III-4 General Observations

The experiments were started by the water being cooled down by the air in the freezing laboratory. When the ice formed at the surface of the basin the temperature in its bottom was still around $+4^{o}C$ which was caused by the warming of its lower edge. Typical temperature profiles are given in Figure III-5 below for approximately steady state conditions.

The ice started to form as a coarse mesh over the surface of the water. Because of the rather strong temperature gradient below the surface the resulting crystals had mostly vertical c-axes. They could be observed to be rather course. Once the hoarfrost pattern on the ice indicated a crystal that covered an area of 200x50 mm. Against the wall of the basin needle-like crystals were formed. The c-axes were probably directed horizontally and parallel to the wall. Near the ice surface there was only a thin layer, the thickness of which grew to about 5 cm at a greater depth in the ice. These deviating crystals were not supposed to influence the over-all deformation of the ice cover. The bulk of the ice consisted of ice type S1: coarse crystals and vertical c-axes.

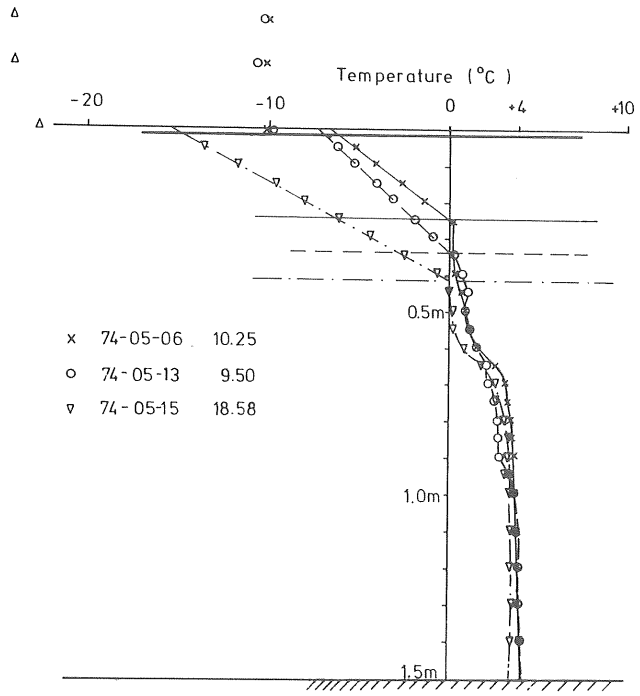

Figure III-5 Measured temperature profiles at three occasions in the same experimental run.

The growth of the ice cover was rather even over the width of the basin. Close to the wall the ice tended to be a little thicker, but within the area where the thickness was measured, that is, from 0.20 m from the wall and inwards the deviations were only ± 1 cm from the mean thickness.

The reinforced concrete wall seemed to be a better conductor of heat than the ice, why its upper end was warmer and its lower end colder than the ice. See Figure III-6. If the temperature deficit in level with the underside of the ice cover had been caused by bad insulation, the brim of the basin should also have been colder than the ice. The thermal conductivity of concrete is given to 1.74 W/(mK) in Bygg I (1961) which is smaller than the value for ice 2.24 W/(mK). Probably the steel in the concrete makes up for this.

When the ice cover increased in thichness cracks developed in its surface. When the temperature in the laboratory was kept at $-10^{o}C$ the cracks were fine and sometimes very little pressure developed when the temperature was raised. When the temperature was kept at $-20^{o}C$ or below, the cracks were wider and pressure always developed when the temperature was raised. Sometimes pressure was read on the pressure meters even before the temperature increase had started. Probably because water was freezing in the cracks. To check this hypothesis an ice cover were formed at $-10^{o}C$ for a considerable time and thereafter the temperature was lowered as fast as possible down below $-20^{o}C$. Then the ice cracked abruptly and water was seen to fill the formed cracks to a great extent. This was followed by a pressure around 300 kPa in the upper part of the ice cover.

When the actual experiment started the thermostat of the laboratory was adjusted manually every hour. For fast rises an electrical heater was put into the room. Unfortunately, the regulating system of the room was only working with a regulating amplitude of ± $1^{o}C$, and when the defrosters of the freezing elements worked the temperature suddenly rose 2-$8^{o}C$ for some minutes. Of course this affected the possibilities to get appropriate measurements.

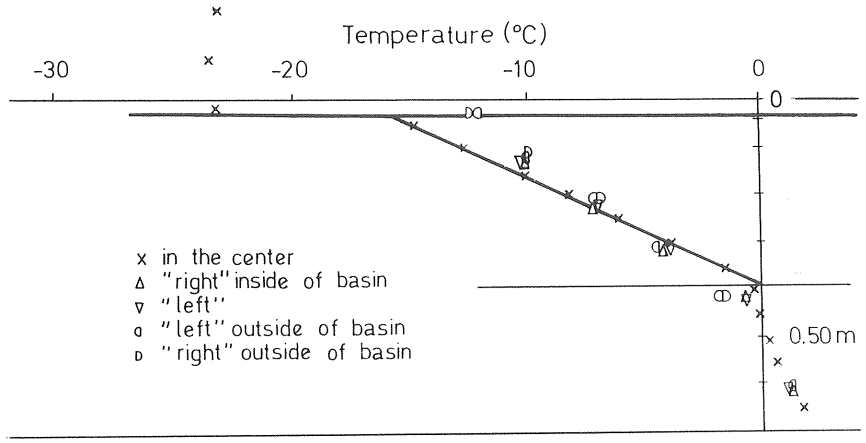

Figure III-6 Temperature profiles in the center of the ice cover and on the inside and outside of the wall of the basin. 1974-05-15 0.05.

As a rough check on the mechanism of the development of thermal pressure the experimental equipment worked out. The experiment is probably too realistic, however, to give correct figures on ice deformation properties or the highest possible pressure for completely stiff walls and completely filled cracks. Perhaps such cases must be calculated from realistic assumptions about ice properties and heat transfer or the technique used by Löfquist (1954), with a manually filled crack, must be used. See Paragraph 2.7.

III-5 Temperature

Coefficient of heat transfer

In the experiments the coefficient of heat transfer was estimated for the ice cover when the temperature of the room had been kept constant for at least 24 hours in advance. The coefficient was evaluated from equating the heat flux in the ice with the flux through the surface. Radiation and evaporation was neglected, that is, they were included in the resulting figures.

$$A\ (\theta_a - \theta_s) = \lambda\theta_s/h \qquad \ldots\ (III\text{-}12)$$

there A = the coefficient of heat transfer

θ_a = air temperature 50 cm above the ice surface

θ_s = temperature of the ice surface, linearly extrapolated from below

λ = 2.24 W/(mK) the conductivity of ice

h = the thickness of the ice cover

The temperature at the ice-water interface is set to 0^{o}C. Values from the laboratory is given in Table III-1 below.

The measured outgoing radiation contributed with 1.3 W/(mK) as an average. The received arithmetic mean 12.3 W/(mK) should then be reduced by 1.3 if the radiation is included in another way. The figure is higher than what is usually used. Magnusson (1977), however, gives 16.0 W/(mK) for wet road surfaces at no wind. This figure is a result of numerous measurements in field. In the field experiments of Appendix II 10.4 W/(mK) was used for no wind.

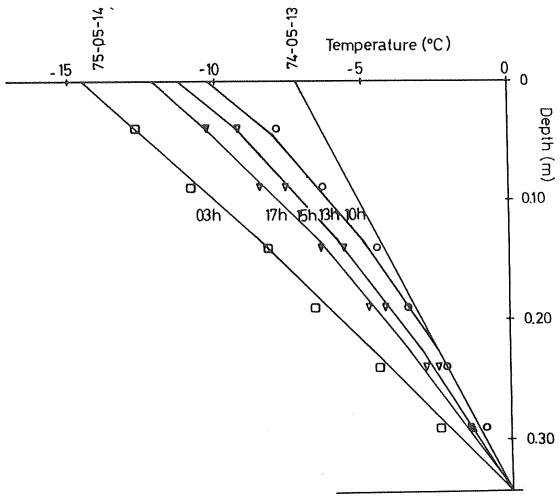

Figure III-7 Ice temperature calculated from the air temperature. Schmidt-graph: Δx = 0.091 m, Δt = 3600 s. a = $1.15 \cdot 10^{-6}$ m^2/s. A = 14 W/mK. Plotted points are measured temperatures. Decreasing temperature. Initial and final air temperature -10.6 and -22.0^{o}C.

Table III-1. Values on the coefficient of heat transfer, A, estimated from the laboratory experiments with Eq. III-12. Arithmetic mean 12.3 $W/(m^2K)$, standard deviation 4.5 $W/(m^2K)$.

Date	Hour	θ_a (°C)	θ_s (°C)	A($W/(m^2K)$	h(m)
73-06-10	8.06	-20.9	-12.4	9.36	0.35
73-06-28	9.01	-20.1	-11.3	9.58	0.30
73-07-01	23.26	-20.0	-13.9	15.28	0.33
73-07-05	10.11	-29.9	-18.4	10.42	0.34
	12.18	-29.3	-18.4	10.58	0.36
	13.13	-29.4	-18.1	9.42	0.38
	15.03	-29.8	-18.5	9.82	0.40
	8.05	-31.2	-20.0	9.51	0.42
73-07-25	13.37	-30.3	-11.1	7.18	0.18
74-05-06	10.25	-10.3	- 6.3	15.1	0.235
	16.35	- 9.5	- 6.4	19.27	0.24
74-05-07	8.25	-10.0	- 6.6	18.12	0.24
	16.43	-11.3	- 6.8	13.54	0.25
74-05-13	11.02	-10.6	- 7.1	13.98	0.325
74-05-15	10.04	-22.9	-16.8	15.82	0.39
74-05-16	08.07	-23.7	-16.3	12.03	0.41
74-06-16	21.07	- 9.5	- 7.3	23.23	0.32
74-06-18	20.00	-27.6	-16.8	10.67	0.36
74-07-10	14.48	-25.1	- 7.8	4.93	0.205
74-07-11	10.03	-25.4	-12.4	7.63	0.28

Thermal Diffusion

Comparisons between the measured temperatures and ice temperatures calculated by the graphic Schmidt method are shown in Figures III-7 and III-8 for decreasing and increasing temperatures. To get a good fit in those examples a coefficient of heat transfer as high as 14 W/(mK) had to be used. Compare Table III-1. With respect to the fact that the pressure depends on the rate of change of temperature over several time steps such a coarse solution is quite satisfactory. In Figure III-9 a comparison with an explicit numerical solution is made for the same case as in Figure III-8.

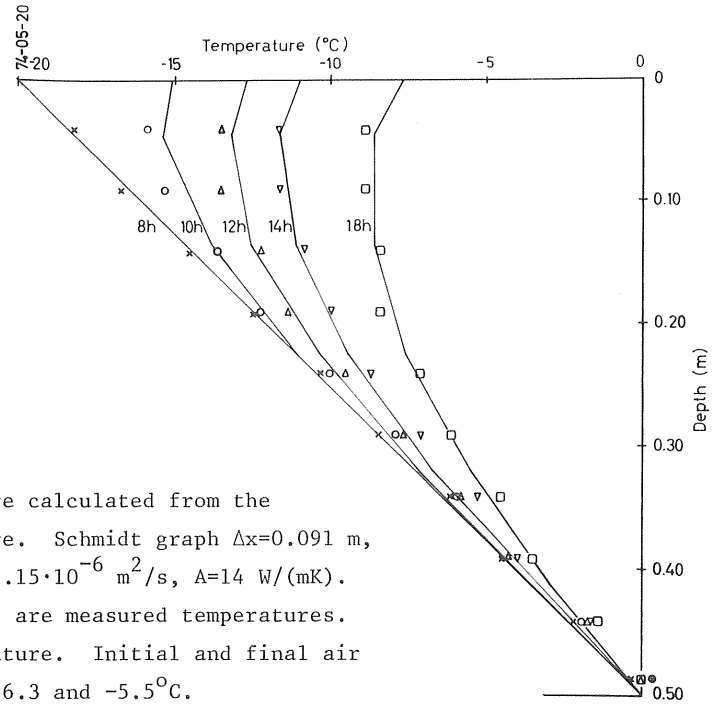

Figure III-8.

Ice temperature calculated from the air temperature. Schmidt graph $\Delta x=0.091$ m, $\Delta t=3600$ s, $a=1.15\cdot10^{-6}$ m^2/s, $A=14$ W/(mK). Plotted points are measured temperatures. Rising temperature. Initial and final air temperature -26.3 and $-5.5^{o}C$.

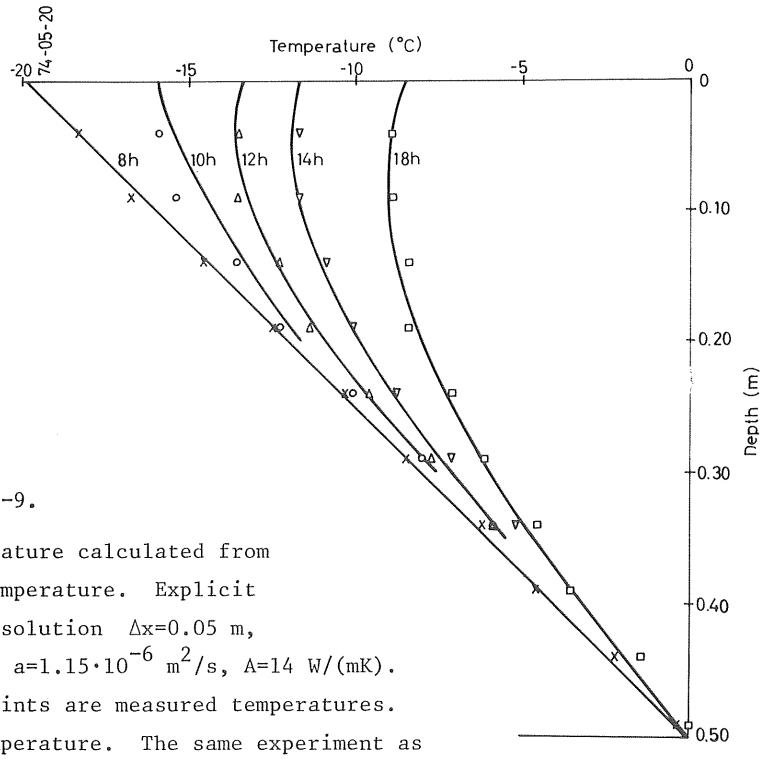

Figure III-9.

Ice temperature calculated from the air temperature. Explicit numerical solution $\Delta x=0.05$ m, $\Delta t=\Delta x^2/6a$, $a=1.15\cdot10^{-6}$ m^2/s, $A=14$ W/(mK). Plotted points are measured temperatures. Rising temperature. The same experiment as in Figure III-8.

Short-Wave Radiation

In Figure III-10 a comparison is made between measured and calculated temperature in an experiment with radiation penetrating into the ice. During the first three hours of the experiment the short-wave irradiation was 132 W/m^2 and the total "balance" 132 W/m^2 thereafter 257 and 252 respectively. If all emitted radiation is supposed to be of frequencies registered by the solarimeter (short waves) this would mean that in the beginning almost all radiation was absorbed in the experimental basin and that as the temperature of the ice cover increased the back radiation increased also. This is mere speculation since the reflected short-wave radiation was not measured separately.

For the calculations it was supposed that all irradiation was short-wave radiation and that the absorption coefficient was 2 m^{-1}. This meant an increase of 0.8, 0.7 and 0.6 $^{o}C/h$ at the depths 0.045, 0.136 and 0.227 m respectively at the later part of the experiment. As can be seen from the figure this is probably too much.

Unfortunately, it proved impossible to hold the temperature in the room at the same level so as to get a steady state. It was also difficult to measure a definite air temperature. In the former experiments the thermocouples in the air and just above the ice surface showed approximately the same temperature. One of the thermo couples above the ice was shielded by a piece of paper. For the shown experiment at the height of 0.30 m the shielded thermocouple showed -19.0 ^{o}C and the bare one -14.5, and the couple just 1 cm above the ice surface showed -15.4 ^{o}C. Under such circumstances its difficult to interpret the measured temperature profiles.

III-6 Pressure

Pressure developed in the ice cover when the temperature was raised in the freezing laboratory due to the expansion of the ice, but sometimes pressure was observed even for constant or decreasing temperatures because of expansion in the cracks when the water fused there.

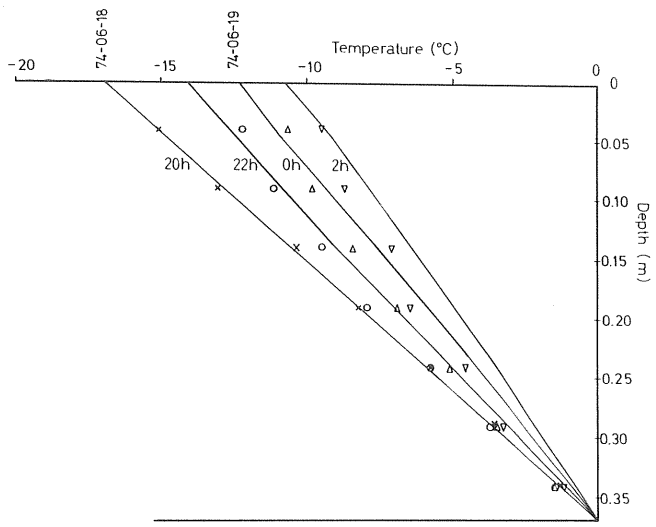

Figure III-10 Ice temperature calculated from the air temperature and short-wave radiation flux. Schmidt graph $\Delta x=0.091$ m, $\Delta t=3600$ s, $a=1.15$ m^2/s, $A=14$ W/(mK). Plotted points are measured temperatures. Initial and final temperature $-24.4^{o}C$ and $-16.4^{o}C$. Short-wave radiation flux 130 W/m^2 to 260 W/m^2. Coefficient of absorption 2 m^{-1}.

Expansion Due to Water Freezing in Cracks

To check what happened when water froze in the cracks special experiments were run. The ice cover was allowed to grow in thickness under a constant temperature in the air. Then the temperature was set down as fast as possible, and the ice cracked distinctly after two or three hours. This was followed by a gradual increase in pressure that sometimes was lower than the opening pressure of the pressure probes. Sometimes it reached a level that could be calculated from an estimated crack width in the following way.

If one assumes that the cracks are widened from the temperature $0^{o}C$ at formation to the actual temperature when the pressure is observed, the restricted expansion must approximately be the product of the difference in thermal contraction and the relative expansion of the water when freezing. Thus the pressure is bounded by

$$\sigma = \theta(\alpha_{ice} - \alpha_{con})\varepsilon_f E \qquad \ldots \text{(III-13)}$$

where θ is the ice temperature

$\alpha_{ice} = 4.82 \cdot 10^{-5}\ {}^{o}C^{-1}$ linear coefficient of expansion for ice

$\alpha_{con} = 1.2 \cdot 10^{-5}\ {}^{o}C^{-1}$ ditto for concrete

ε_f = relative expansion when freezing

E = 6.1 GPa elasticity of ice

If the ice is supposed to expand only laterally because it is fused to the walls of the cracks, ε_f will equal the volume expansion 0.09. Eq. (III-13) then gives for $\theta = -10^{o}C$, σ = 0.2 MPa and for $\theta = -20^{o}C$, σ = = 0.4 MPa. The pressure probes could not measure pressures below 0.1 to 0.2 MPa, but in some of the experiments the pressure rose to between 0.25 and 0.33 MPa. Sometimes the pressure did not run up to expected values, probably because the water table had been too low so that the cracks had healed at the underside of the ice cover. This was not selfregulating as the ice could hang on the rough concrete walls.

Thermal Pressure

For the ordinary experiments the air temperature was kept constant for some days in advance in order to get steady state conditions. Then the temperature of the freezing laboratory was increased manually by changing the thermostat on the wall once an hour at the wanted rate. This caused an increase of the temperatures in the ice, examples of which are shown previously in Figure III-8 and III-9. The ice and basin expanded and pressure was measured by the Glötzl-probes.

The measured pressures were compared to pressures calculated from the measured deformation of the experimental basin. The deformation was measured and calculated according to the description in paragraph III-3. This deformation was assumed to be equal to the total horizontal expan-

sion of the ice cover. If the cracks in the ice were incompletely filled by water at the start of an experiment, this would mean that the ice could expand more than measured, and pressures estimated from the measured total expansion would be greater than the measured ones, especially, at the beginning of the experiments.

The pressure in the ice was then estimated from the equation

$$\dot{\varepsilon} = \dot{\sigma}/E + KD\ \sigma^n \qquad \ldots \text{(III-14)}$$

with $K = 4.40 \cdot 10^{-16}\ m^{-2}\ Pa^{-n}$

$n = 3.651$

$\dot{\sigma} = d\sigma/dt$ the rate of change of stress σ

$\dot{\varepsilon} = d\varepsilon/dt$ " " " " " deformation ε

The elasticity of the ice was calculated by

$$E = (1 - c\theta)\ 6.1\ GPa \qquad \ldots \text{(III-15)}$$

θ = the ice temperature

$c = 0.012\ ^oC^{-1}$

and the diffusion constant

$$D = D_o \cdot \exp(-Q_s/R\ T) \qquad \ldots \text{(III-16)}$$

where $D_o = 9.13 \cdot 10^{-4}\ m^2/s$

$R = 0.31$ J/(mol·K) the universal gas constant

$Q_s = 59.8$ kJ/mol, the activation energy for self diffusion

T = the absolute temperature of the ice

The deformation $d\varepsilon$ of the ice during the time dt was calculated as the difference between the estimated unrestricted deformation of the ice, $\alpha\ d\theta$, and the total deformation of the experimental basin, that is:

$$d\varepsilon = \alpha\ d\theta - d\varepsilon_o \qquad \ldots \text{(III-17)}$$

where $\alpha = 5.1 \cdot 10^{-5}/K$

$d\theta$ = change of ice temperature during dt

$d\varepsilon_o$ = according to Eq. (III-11)

The differentials of Eq. (III-14) were exchanged for their differences and the equation was solved for each time step by the same iterative procedure as described by Bergdahl and Wernersson (1978). Two examples from the experiments are shown in Figures III-11 and III-12 below.

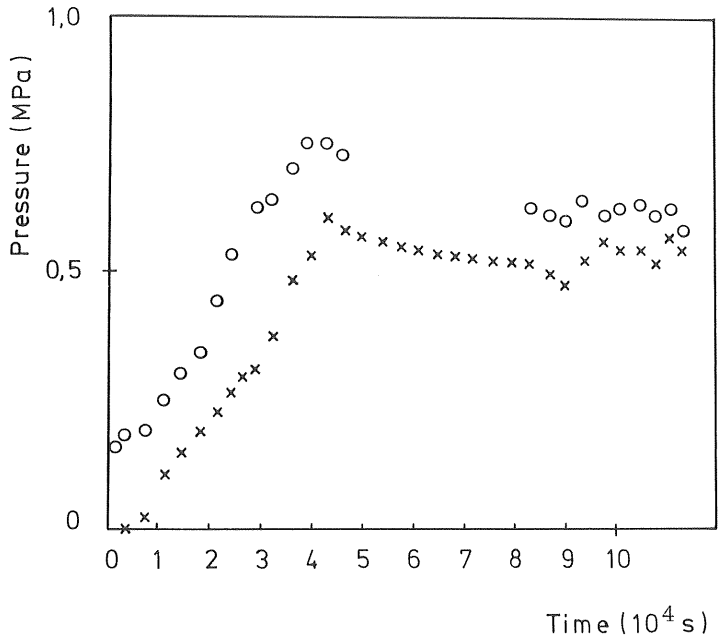

Figure III-11 Measured pressure o and calculated pressure x as functions of time. t= 0 s corresponds to 73-06-10 09.02. At the depth of five cm in the ice cover.

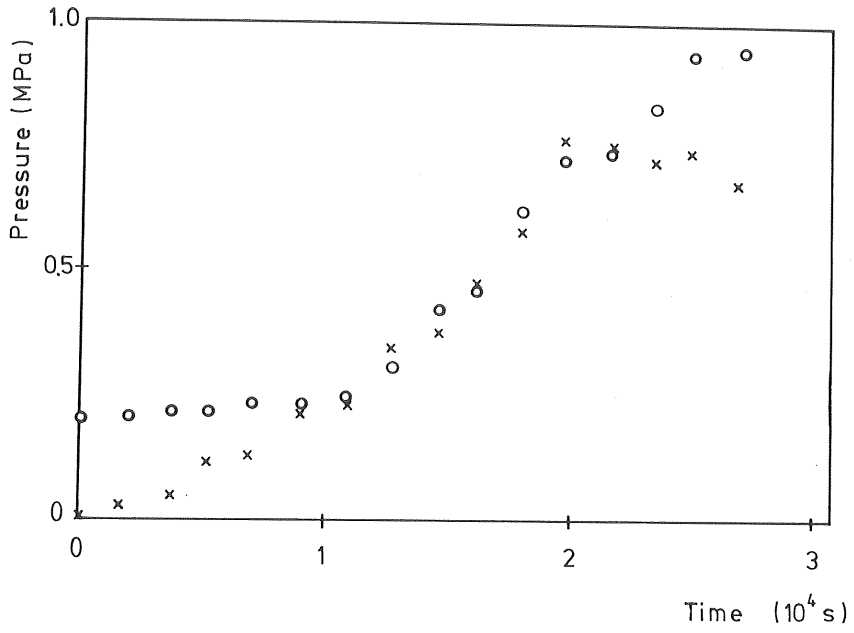

Figure III-12. Measured pressure o and calculated pressure x as functions of time. t = 0 s corresponds to 73-06-28 09.01. At the depth of five cm in the ice cover.

III-7 Conclusions

The thermal conduction in the ice is adequately calculated by using a constant coefficient of diffusion of $1.15 \cdot 10^{-6}$ m^2/s. In the laboratory the use of an ordinary coefficient of heat transfer also seems to be satisfactory. For the conditions in the used freezing laboratory the coefficient was measured to 12.3 ± 4.5 $W/(m^2\ ^oC)$ for stationary conditions, but for non-stationary conditions 14 $W/(m^2\ ^oC)$ gave a better result.

The attempt to measure the influence from the short wave radiation did not succeed because of the insufficient cooling capacity of the laboratory. Such an experiment should be performed.

The used pressure gauges did not work very well. The read values depended to a considerable degree on how the pumping was done when

measuring. A few of them were damaged in the ice of unknown reasons. Better equipment should be used. (See Metge et al. 1975).

The used way of measuring the deformations of the ice cover was sound for a concrete wall, as it was avoided to measure local deformations over cracks or between cracks in the concrete. A drawback was that one could not calibrate them, but had to use the manufacturer´s figures on its properties. A better concept could be to stretch steel bands around the basin and to applicate smaller prefabricated and temperature compensated strain gauges on the bands. Another problem with the used gauges was that, as soon as the temperature reached the melting point, the moisture on the gauges made the resistance drop disastrously.

The most important experience is that it is very difficult to produce thermal pressure in a small diameter basin in the same way as in a vast floating ice cover. Often the developed cracks will not be filled by water. If one wishes to get reproducible results one must arrange this filling in some controlled way, for example by Löfquist´s method with double walls. (See Section 2.7.). Another experience is that the walls must be rather stiff so as to make the development of the pressure possible and so that the pressure profile is correctly reproduced. If the walls deform too much at the surface of the ice cover the expansion on lower levels will not be enough to produce appreciable pressures, before the ice at the surface has crept a considerable time. The pressure for a completely restricted ice cover is not reproduced under such conditions.

APPENDIX IV

TABLES OVER WEATHER OBSERVATIONS PRECEDING
CALCULATED MAXIMUM ICE PRESSURES

Table IV-1

Lake Torne Träsk 68.3°N 19.5°E

Maximum calculated ice pressure 437 kN/m 1970-02-22 22.00
Ice thickness 0.76 m and snow depth 0.05 m

Weather observations:

Date and time	Air temperature °C	Wind speed m/s	Cloudiness eighths	Air vapour pressure Pa
70-02-20 19.00	- 31.2	0	0	40
70-02-21 01.00	- 33.8	0	0	30
07.00	- 36.0	0	4	20
13.00	- 27.0	0	4	60
19.00	- 25.0	1	6	70
70-02-22 01.00	- 26.8	1	4	60
07.00	- 34.4	0	2	30
13.00	- 16.0	4	8	150
19.00	- 13.8	4	8	160
22.00	- 14.5	5.5	8	155

Period concerned 1965 - 1976

Table IV-2

Lake Stora Bygdeträsket 64.3°N 20.5°E

Maximum calculated ice pressure 357 kN/m 1961-03-23 13.00

Ice thickness 0.55 m Snow depth 0 m

Weather observations:

Date and time	Air temperature °C	Wind speed m/s	Cloudiness eighths	Air vapour pressure Pa
61-03-20 19.00	- 10.0	2	0	250
61-03-21 07.00	- 16.2	1	0	150
13.00	- 2.0	2	0	480
19.00	- 6.2	1	0	350
61-03-22 07.00	- 13.2	0	6	190
13.00	- 2.6	1	8	460
19.00	- 3.0	2	8	460
61-03-23 07.00	- 1.9	4	0	460
13.00	+ 4.5	9	5	690

Period concerned 1961 - 1976

Table IV-3

Lake Runn 60.6°N 15.6°E

Maximum calculated ice pressure 318 kN/m 1971-01-07 18.00

Ice thickness 0.39 m and snow depth 0.01 m

Weather observations:

Date and time		Air temperature °C	Wind speed m/s	Cloudiness eighths	Air vapour pressure Pa
71-01-05	07.00	- 16.4	2	0	150
	13.00	- 16.2	0	0	150
	19.00	- 24.4	0	0	70
71-01-06	min.temp. assumed 06.00	- 29.1			
71-01-06	07.00	- 28.0	1	0	50
	13.00	- 24.0	1	1	80
	19.00	- 27.6	1	0	50
71-01-07	min.temp. assumed 06.00	- 28.4			
	07.00	- 16.4	1	8	150
	13.00	- 2.8	7	8	430
	18.00	- 1.97	4.5	8	455

Period concerned 1961 - 1976

Table IV-4

Lake Glan 58.6°N 16.0°E

Maximum calculated ice pressure 282 kN/m 1962-03-08 13.00
Ice thickness 0.42 m and snow depth 0 m.

Weather observations:

Date and time		Air temperature °C	Wind speed m/s	Cloudiness eighths	Air vapour pressure Pa
62-03-05	19.00	- 7.8	0	4	260
62-03-06	07.00	- 19.4	1	7	110
	13.00	- 4.4	4	3	340
	19.00	- 8.2	3	0	240
62-03-07	07.00	- 17.6	2	5	130
	13.00	- 6.4	0	6	350
	19.00	- 5.4	2	8	300
62-03-08	07.00	- 7.0	4	2	310
	13.00	- 3.0	6	1	390

Period concerned 1961 - 1976

Table IV-5

Lake Vidöstern 57.1°N 14.0°E

Maximum calculated ice pressure 256 kN/m 1962-03-08 13.00
Ice thickness 0.34 m and snow depth 0 m.

Weather observations:

Date and time		Air temperature °C	Wind speed m/s	Cloudiness eighths	Air vapour pressure Pa
62-03-04	19.00	- 4.4	4	7	360
62-03-05	07.00	- 22.2	0	0	80
	13.00	- 3.8	1	1	250
	19.00	- 9.1	1	2	270
62-03-06	07.00	- 19.5	0	2	110
	13.00	- 4.0	4	2	300
	19.00	- 7.2	1	1	290
62-03-07	07.00	- 18.4	1	7	110
	13.00	- 2.0	3	7	390
	19.00	- 6.1	1	1	350
62-03-08	07.00	- 1.7	5	7	440
	13.00	+ 0.2	3	2	380

Period concerned 1961 - 1976

LIST OF TABLES

LIST OF FIGURES

LIST OF NOTATIONS

Most notations used in Chapter 2 are not listed. Sometimes the same notation is used, but the units in Chapter 2 may not be SI-units unlike in the rest of the report. Forces in Chapter 2 may for example be given in kgf, kp, tonnes, lbs. This is stated for each case separately.

A	Amplitude of sinusoidal temperature variation	^{o}C
A	tridiagonal matrix	
A	coefficient of heat transfer	$W/(m^2\ ^{o}C)$
A	constants	
A_e	coefficient of heat transfer for equilibrium temperature concept	$W/(m^2\ ^{o}C)$
A_n	Fourier coefficients	
a	coefficient of thermal diffusion	m^2/s
a	constants	
B	Bowen´s ratio	-
B	tridiagonal matrix	
B	constants	
b	Burgers´s vector	m
b	constants	
C	cloud cover	eighths
C	column vector	
C_p	specific heat capacity	$J/(kg\ ^{o}C)$
c	constants	
D	number of a day in a year with D=1 for January 1.	–
D	column vector	
D	coefficient of self diffusion for molecules of ice	m^2/s

D_o	constant	m^2/s
d	differential operator	–
E, E_1, E_2	moduli of elasticity	Pa
E_a	apparent elastic modulus	Pa
E_m	time average elastic modulus	Pa
e	saturation vapour pressure at the ice surface	Pa
e_a	vapour pressure of the air	Pa
f(u)	wind-speed function	m/s
H	solar time of the day	h
h	local solar angle of the day	rad
h	ice cover thickness	m
J	intensity of short-wave radiation	W/m^2
J(t)	compliance function	Pa^{-1}
K	coefficient for viscous deformation	m^{-2} Pa^{-n}
k	absorption coefficient	m^{-1}
k	attenuation factor, wave number	m^{-1}
k	index for point of time	–
L	specific latent heat of fusion	J/kg
L_s	specific heat of sublimation	J/kg
m	exponent for σ in creep law, Drouin	–
n	ditto proposed model	–
n	summation index	–
n_o	initial number of dislocations per unit area	m^{-2}
P_b	buckling load	N/m
p	model parameter	Pa
p	energy source per unit volume and unit time	W/m^3

Q_c	activation energy for creep	J/mol
Q_s	activation energy for self diffusion	J/mol
q	heat flux, energy flux	W/m^2
q_b	emitted long-wave radiation flux	W/m^2
q_C	incident radiation at cloudy weather	W/m^2
q_{CL}	short-wave irradiation from a clear sky	W/m^2
q_c	total convective heat transfer	W/m^2
q_e	latent heat transfer	W/m^2
q_i	incoming energy flux	W/m^2
q_ℓ	absorbed long-wave radiation	W/m^2
$q_{\ell a}$	long-wave atmospheric radiation	W/m^2
$q_{\ell c}$	atmospheric long-wave radiation for cloudy weather	W/m^2
q_m	energy flux used to melting	W/m^2
q_o	outgoing radiation	W/m^2
q_o	constant	W/m^2
q_S	sensible heat transfer	W/m^2
q_s	absorbed short-wave radiation	W/m^2
R	the universal gas constant	J/(mol.K)
r	reflection coefficient	–
T	absolute temperature	K
T_a	absolute temperature of the air	K
T_o	273.15 K, 0^oC	K
T_1, T_2	column vectors of temperatures	^oC
T	period	s
T	time for increase of temperature	s
t	time, duration of load	s
t_o	relaxation time for elastic lag	s
u	wind speed	m/s

x	vertical coordinate	m
α	altitude of the sun	rad
α	coefficient of linear thermal expansion	–
α	constant	
α_1	angle of incidence	rad
β	angle of refraction	rad
β	rate of increase of dislocations	m^{-2}
β	weighting factor	–
γ	the psycrometric constant	$Pa/^oC$
Δ	difference operator	–
δ	declination of the sun	rad
ε	strain, expansion, deformation per unit length	–
ε	emissivity	–
ε_a	emissivity of the atmosphere	–
η, η_1, η_2	viscosity moduli	Ns/m^2
η	integration help variable	
θ	temperature	^oC
θ_a	air temperature	^oC
θ_i	initial temperature	^oC
θ_o	initial surface temperature	^oC
θ_s	ice surface temperature	^oC
λ	thermal conductivity	$W/(m\ ^oC)$
λ_w	thermal conductivity of water	$W/(m\ ^oC)$
ν	Poisson´s modulus	–
ρ	density	kg/m^3
ρ_w	density of water	kg/m^3
σ	Stefan Boltzmann´s constant	$W/(m^2\ K^4)$

σ	stress	Pa
τ	integration help variable	s
φ	latitude	rad
φ	phase lag	rad
ω	angular frequency	rad/s
∂	differential operator	–
$\dot{}$	$\partial/\partial t$ first derivative with respect to time	–
$\ddot{}$	$\partial^2/\partial t^2$ second derivative with respect to time	–

REFERENCES

Abramowitz, M. and Stegun, I.A.(1972): Handbook of Mathematical Functions with Formulas, Graphs and Mathematical Tables. U S Department of Commerce, NBS Applied Mathematics Series No. 55, Washington DC 1972.

Assur, A. (1959): Maximum Lateral Pressure Exerted by Ice Sheets. IAHR VIIIth Congress Paper 22-SI, Montreal 1959.

Bengtsson, L.(1976): Snowmelt Estimated from Energy Budget Studies, Nordic Hydrology 7, 1976, pp 3-18.

Bergdahl, L. (1977): Physics of Ice and Snow as Affects Thermal Pressure. Department of Hydraulics, Chalmers University of Technology, Report Series A:1.

Bergdahl, L. and Wernersson, L.(1978a): Calculated and Expected Thermal Ice Pressures in Five Swedish Lakes. Department of Hydraulics, Chalmers University of Technology, Report Series B:7.

Bergdahl, L. and Wernersson, L. (1978b): Probabilities of Thermal Ice Pressures in Five Swedish Lakes. IAHR Symposium on Ice Problems, Luleå, Aug. 7-9, 1978.

Brown, E. and Clarke, G.C. (1932): Ice Thrust in Connection with Hydro-Electric Plant Design. With Special Reference to the Plant at Island Falls on the Churchill River. The Engineering Journal p.18-25, Jan. 1932.

Bygg I (1961): Handbook for civil engineers (in Swedish) Paragraph 143:712, AB Byggmästarens förlag, Stockholm 1961.

Carslaw and Jaeger (1959): Conduction of Heat in Solids, Oxford University Press 1959.

Drouin, M. (1967): Amortissement d´un cycle de température à l´intérieur d´un champ de glace. Comptes rendues. XII ème Congres de l´Association Internationale de Recherches Hydrauliques. 11-14 Septembre 1967.

Drouin, M. (1970): State of research on ice thermal thrust. IAHR Ice Symposium Reykjavik 1970.

Drouin, M. et Michel, B. (1971): Les poussées d´origine thermique exercées par les couverts de glace sur les structures hydrauliques. Rapport S-23 Génie Civil, Université Laval, Quebec 1971.

Drouin, M. (1972): Laboratory Investigation on Ice Thermal Pressures. IAHR Ice and its Action on Hydraulic Structures. Leningrad USSR 1972.

Flügge, W. (1975): Viscoelasticity, Springer-Verlag, New York 1975.

Glen, J.W., Stephens, RWB (1958): The Mechanical Properties of Ice. The Plastic Properties of Ice. Advances in Physics. Vol. VII No. 25-28, London 1958.

Gold, L.W. (1958): Some Observations on the Dependence of Strain on Stress for Ice. Canadian Journal of Physics, Vol. 36 No. 10, Oct. 1958.

Hildebrand, F.B. (1962): Advanced Calculus for Applications. Prentice Hall, Englewood Cliffs 1962.

Janson, L-E. (1963): Frost Penetration in Sandy Soil. Elanders Boktryckeri AB, Göteborg, 1963.

Jumppanen, Pauli (1973): Ice Thermal Loads against Walls of Water Reservoirs. 2:nd Int. Conf. on Port and Ocean Engineering under Arctic Conditions. Reykjavik 1973.

Kjeldgaard, J.H. (1977): Thermal Ice Forces on Hydraulic Structures. River and Harbour Laboratory at the Norwegian Institute of Technology, Trondheim 1977.

Korzhavin, K.N. (1962): Action of ice on engineering structures. Novosibirsk, Akademij Nauk SSSR 1962, Translation TL 260 from CRREL Hanover, New Hampshire, 1971.

Korzhavin, K.N. (1972): General Research Results Obtained in the USSR on Ice-Thermal Conditions in the Vicinity of Hydraulic Structures. IAHR Symposium Ice and Its Action on Hydraulic Structures, Leningrad 1972.

Lindgren, Sune (1968): Istryck vid temperaturhöjningar. Dept. of Hydraulics, Royal Technical University, Stockholm 1968. (Ice pressure at increases of temperature).

Lindgren, Sune (1970): Thermal Ice Pressure. IAHR Ice Symposium, Reykjavik 1970.

Löfquist, Bertil (1954): Studies of the effects of temperature variations. ASCE Paper No. 2656. Ice pressure against dams, a symposium.

Lyons, J.B. and Stoiber, R.E. (1959): The Absorptivity of Ice, A critical Review, Dartmouth College, Hanover, New Hampshire, Scientific Report No. 3, Contract AF 19(604) 2159.

Monfore, G.E. (1949): Ice Pressure Measurements at Eleven Mile Canon Reservoir During January 1949. US Bureau of Reclamation, Branch of Design and Construction, Denver, Colorado 1949.

Monfore, G.E. (1951): Laboratory Investigation of Ice Pressure, USBR, Structural Research Laboratory, Report SP-31.

Monfore, G.E. (1954): Experimental Investigations by the Bureau of Reclamation. ASCE Paper No. 2656. Ice pressure against dams, a symposium.

Monfore, G.E. and Taylor, F.W. (1948): The Problem of an Expanding Ice Sheet, US Department of the Interior Bureau of Reclamation. Branch of Design and Construction, Denver, Colorado 1948.

Magnusson, R. (1977): Uppvärmning av vägar (Heating of roads). Chalmers University of Technology, Dept. of Road Construction, Report 29, Göteborg 1977.

Metge, M., Strilchuk, A., Trofimenkoff, P.: On recording stresses in ice. IAHR 3rd International Symposium on Ice Problems, Hanover NH Aug. 18-21, 1975.

Paily, P.P., Macagno, E.O., Kennedy, J.F. (1974): Winter-Regime Surface Heat Loss from Heated Streams. IIHR Report No. 155, Institute of Hydraulic Research, University of Iowa, Iowa City, Iowa March 1974.

Peschanskii, I.S. (1963): Ledovedenie i ledotekhnika, (Ice science and ice technology), Morskoi Transport, Leningrad 1963.

Pounder, E.R. (1965): The Physics of Ice. Pergamon Press 1965.

Proskourickov (1967): Pression statique de la glace sur les ouvrages hydraulique lors de sa dilatation thermique. Proceedings IAHR XII Congress 1967.

Ramseier, R.O. (1967 a): Self-Diffusion of Tritium in Natural and Synthetic Ice Monocrystals. Journal of Applied Physics, Vol.38 No 6, USA 1967.

Ramseier, R.O. (1967 b): Self-Diffusion in Ice Monocrystals CRREL Research Report 232, Hanover, New Hampshire 1967.

Ramseier, R.O. (1971): Mechanical Properties of Snow Ice. Proceedings the First International Conference on Port and Ocean Engineering under Arctic Conditions. NTH, Trondheim Aug. 23-30 1971.

Ramseier, R.O., Dickins, D.F. (1972): A New Approach to Field and Laboratory Tests of Tensile Compressive and Flexural Strength of Polycrystalline Fresh Water Ice. IAHR Ice and its Action on Hydraulic Structures, Leningrad 1972.

Reeh, N. (1970): Thermal Stress in a Visco-Elastic Plate in Simple Extension. The Danish Center for Applied Mathematics and Mechanics, Report No. 7, 1970.

Rose, E. (1947): Thrust Exerted by Expanding Ice Sheet. ASCE Transactions No 2314, 1947.

Royen, N. (1922): Istryck vid temperaturhöjningar. Hyllningsskrift tillägnad F. Vilh. Hansen, AB G.Tisells förlag, Stockholm 1922. Translated as "Ice pressure with increasing temperatures", SIPRE bibliography project, Translation 45, 1955.

Sweers, H.E. (1976): A Nomogram to Estimate the Heat-Exchange Coefficient at the Air-Water Interface as a Function of Wind Speed and Temperature; A critical survey of some literature. Journal of Hydrology 30:375-401.

Veinberg, B.P. (1940): Led. Gostekhteoretizdat, Moscow-Leningrad 1940. (Ice).

Voitkovsky, K.F., Golubev, V.N. (1972): Dependence of Mechanical Properties of Ice on its Structure. IAHR Ice and its action on hydraulic structures. Leningrad USSR 1972.

Wold, K. (1957): Temperaturforhold i snö og is og beregning av varmeledningsevnen i og varme-transporten gjennom isen (Temperature conditions in snow and ice and calculation of the thermal conductivity of the ice and the heat flux through it). Norges Vassdrags- og Elektrisitetsvesen, Oslo 1957.

Yakovlev, G.N. (1971): Studies in Ice Physics and Ice Engineering. Arctic and Antarctic Scientific Research Institute, Proceedings Vol.300, Leningrad 1971. Israel Program for Scientific Translations, Jerusalem 1973.

Institutionen för Vattenbyggnad

CHALMERS TEKNISKA HÖGSKOLA

Meddelanden

78. Cederwall, K.: Havet som recipient. Hydrodynamiska synpunkter.
Föredrag vid Sv. Havsforskningsföreningens årsmöte i Stockholm, mars 1975.

79. Sellgren, A.: Hydraulisk transport av fasta material i rör. 1975.

80. Andreasson, L. och Cederwall, K.: Rubbningar av grundvattenbalansen i urbana områden.
Hydrologisk konferens, Sarpsborg, 1975.

81. Cederwall, K.: Bräddning av avloppsvatten och effekten av utjämningsbassänger. "Världen, Vattnet och vi", Elmia 1975.

82. Cederwall, K.: Gross Parameter Solutions of Jets and Plumes. ASCE, HY5, May 1975.

83. Larsson, Sören och Lindquist, Per: Kalkning av försurade sjöar. Del I: Problembeskrivning samt utvärdering av kalkningen av Östra Nedsjön. Ex.arb. 1974:5.

84. Cederwall, K. och Svensson, T.: "Sediment flusing after dredging in tidal bays". 1975.

85. Göransson, C-G. och Svensson, T.: Strömkorsmätningar. Datorprogram för utvärdering inkl. korrektion för avdrift. Mars 1976.

86. Rahm, L. och Häggström, S.: Oskarshamns Kärnkraftverk. Modellstudier avseende kylvattenspridning vid framtida utbyggnad. Maj 1976. Del I Huvudrapport. Del II Bilagedel.

87. Sjöberg, A.: Beräkning av icke stationära flödesförlopp i reglerade vattendrag och dagvattensystem. Aug. 1976.

Slut på Meddelande-serien.

Institutionen för Vattenbyggnad

CHALMERS TEKNISKA HÖGSKOLA

Report Series A

A:1 Bergdahl, L.: Physics of Ice and Snow as Affects Thermal Pressure. 1977.

A:2 Bergdahl, L.: Thermal Ice Pressure in Lake Ice Covers. 1978.

A:3 Häggström, S.: Surface Discharge of Cooling Water. Effects of Distortion in Model Investigations. 1978.

Report Series B

B:1 Bergdahl, L.: Beräkning av vågkrafter. 1977.

B:2 Arnell, V.: Studier av amerikansk dagvattenteknik. 1977.

B:3 Sellgren, A.: Hydraulic Hoisting of Crushed Ores. A feasibility study and pilot-plant investigation on coarse iron ore transportation by centrifugal pumps. 1977.

B:4 Ringesten, B.: Energi ur havsströmmar. 1977.

B:5 Sjöberg, A. och Asp, T.: Brukar-anvisning för ROUTE-S. En matematisk modell för beräkning av icke-stationära flöden i floder och kanaler vid strömmande tillstånd. 1977.

B:6 Annual Report 76/77.

B:7 Bergdahl, L. och Wernersson, L.: Calculated and Expected Thermal Ice Pressure in Five Swedish Lakes. 1978.

B:8 Göransson, C-G. och Svensson, T.: Drogue Tracking-Measuring Principles and Data Handling. 1977.

B:9 Göransson, C-G.: Mathematical Model of Sewage Discharge into Confined, Stratified Basins - Especially Fjords. 1977.

B:10 Arnell, V. och Lyngfelt, S.: Beräkning av dagvatten-avrinning från urbana områden. 1978.

B:11 Arnell, V.: Analysis of Rainfall Data for Use in Design of Storm Sewer Systems. 1978.

B:12 Sjöberg, A.: On Models to be used in Sweden for Detailed Design and Analysis of Storm Drainage Systems. 1978.